UC Merced
UC Merced Electronic Theses and Dissertations

Title
Ignition behavior of Wildland Grassy Fuels by Heated Metal Particles and Wind Influence.

Permalink
https://escholarship.org/uc/item/6kv0j34g

ISBN
9798297603523

Author
Saha, Shusmita

Publication Date
2025-08-06

Peer reviewed|Thesis/dissertation

eScholarship.org Powered by the California Digital Library
University of California

UNIVERSITY OF CALIFORNIA, MERCED

Ignition behavior of Wildland Grassy Fuels by Heated Metal Particles and Wind Influence.

by

Shusmita Saha

Ph.D. thesis

in

Mechanical Engineering

Committee in charge:

Professor Venkattraman Ayyaswamy (Chair)

Professor Jeanette Cobian-Iñiguez (Advisor)

Professor Ashlie Martini

Professor Min Hwan Lee

Professor Gerardo Diaz

2025

© Shusmita Saha, 2025
All rights reserved.

This Ph.D. thesis of Shusmita Saha is approved, and it is acceptable in quality and form for publication on microfilm and electronically:

Venkattraman Ayyaswamy (Chair)

Jeanette Cobian-Iñiguez (Advisor)

Ashlie Martini

Min Hwan Lee

Gerardo Diaz

University of California Merced

2025

To my family, Mrittunjoy and my parents,

to my lab mates, and to my dearest well wishers,

whose unwavering belief in me made this journey possible.

ACKNOWLEDGMENTS

First, I must express my most sincere appreciation to my Professor, Dr. Jeanette Cobian-Iñiguez for giving me the opportunity to be a part of his research group, the Cobian-Iñiguez Fire Lab. I am grateful to her for all his valuable training, suggestions, comments, and the funding support throughout my ongoing graduate studies at UC Merced.

I am grateful to all my lab friends for helping me with my research. I would also like to thank our undergraduate lab mates for always helping me to conduct the research. Without whom it would not be possible to continue the experiments effectively. I would also like to thank my committee members for their valuable time and support for my qualification examination.

Last but not least, my husband, Mrittunjoy Sarker, for always being with me, believe in me and for his incessant support from the very first day I started my graduate research.

.

ABSTRACT

Wildfires continue to pose increasing risks to ecological systems, human safety, and infrastructure, particularly in fire prone regions such as California. A substantial fraction of wildland and wildland-urban interface (WUI) fires are directly linked to human activities, including construction operations like welding and grinding, which generate hot metal particles capable of igniting dry vegetation. This dissertation systematically investigates the ignition behavior of grassy wildland fuels subjected to heated metal particles under varying fuel structures, particle properties, and wind conditions, including both steady and gusty flows. Through a combination of controlled bench-scale experiments, thermogravimetric analysis (TGA), and parametric studies, the research presents a unified understanding of the factors governing ignition, smoldering flaming (StF) transitions, ignition behavior and fire spread dynamics across different ignition regimes.

Initial experiments focused on the fundamental ignition behavior of wildland grasses such as Bromus, Avena wildoats, and Tall Wheatgrass-when exposed to stainless steel particles of varying size, carbon content, and quantity. Key findings indicate that increasing the number and diameter of particles significantly reduces the ignition temperature required for both flaming and smoldering ignitions. Furthermore, the carbon content of the particles was found to inversely correlate with ignition sensitivity: lower carbon stainless steel (e.g., 304C) induced ignition at lower temperatures due to superior thermal conductivity and faster heat transfer to the fuels. Among the fuels tested, Bromus exhibited the lowest ignition threshold (~320°C), supporting primarily flaming ignition, while Avena and Wheatgrass supported mostly smoldering ignition and required higher temperatures (380–400°C). The lignin content emerged as a key determinant: higher lignin in wheatgrass (20–22%) increased ignition temperature, reduced spread efficiency, and favored smoldering. This relationship between chemical composition specifically lignin and protein content and ignition behavior and the fuel characteristics were further supported by TGA data analysis.

Building on the earlier findings, a follow-up study investigated the impact of fuel structure natural, shredded, and powdered form, on ignition behavior using the same species. Experimental results demonstrated that

powdered fuels ignited at the lowest temperatures and exhibited the shortest burnout times due to enhanced surface area and heat transfer efficiency. Conversely, natural fuels showed greater variability in ignition behavior, supporting all ignition types including sustained smoldering and StF transitions.

This work showed that fuel structure modulates combustion intensity and ignition pathway. Powdered fuels, while igniting easily, did not support prolonged smoldering due to compactness and limited oxygen penetration. Shredded fuels presented intermediate behavior. TGA further validated these differences, revealing distinct degradation profiles, with bromus undergoing mass loss at lower temperatures (~180–200°C), while wheatgrass decomposed above 270°C with higher DTG peaks, indicating greater thermal stability.

Recognizing that real-world ignitions rarely occur in still air, a third set of experiments introduced controlled wind speeds (0.5–2.0 m/s) to assess their effect on ignition dynamics. As wind speed increased, time required for ignition, transition and burnout times decreased across all fuels, while peak ignition temperatures and heat release rates rose sharply. For example, in excelsior fuel, flaming ignition temperature increased from ~330°C to ~500°C between 0.5 and 2.0 m/s, while the HRR surged from ~3000 J/s to ~5200 J/s. The wind's dual role was evident: it enhanced oxygen availability and convective heat transfer but also caused rapid burnout by accelerating combustion kinetics. In fuels like avena and wheatgrass, higher wind speeds facilitated earlier StF transitions by raising pyrolysis rates and supporting faster oxidation. Rate of spread (ROS) was significantly influenced, with values reaching up to 1.2 cm/s in excelsior at 2.0 m/s wind.

To simulate realistic, transient wildfire scenarios, the study introduced wind gusts (frequencies of 0.03–0.07 Hz) over constant wind speeds. Results showed that higher gust frequencies led to faster ignition, shorter transition times, and higher HRR. For instance, in wheatgrass, StF transition times dropped from 135 to 70 seconds and HRR rose from ~2000 J/s to ~2600 J/s as gust frequency increased from 0.03 to 0.07 Hz. Gusts enhanced combustion intensity by disturbing boundary layers, improving airflow penetration, and re-igniting partially extinguished smoldering fuels. The combined effect was a substantial reduction in ignition time and burnout variability. These results stress the importance of accounting for wind transience in fire prediction models, especially in WUI zones where fuel continuity and gusty conditions amplify ignition potential.

This thesis presents a multi-dimensional view of ignition behavior in wildland fuels, highlighting how ignition is governed by an interplay between fuel chemistry, morphology, heat source characteristics, and environmental conditions. The combined results lead to several critical insights:

Hot Particle Properties: Larger, low-carbon particles promote more efficient ignition via greater thermal mass and conductivity.
Fuel Structure: Powdered fuels ignite at lower temperatures but offer limited combustion duration; natural fuels provide a fuller range of ignition types.
Fuel Chemistry: Fuels with higher lignin and protein contents (e.g., wheatgrass) are more resistant to ignition due to higher activation energy requirements and reduced char reactivity.
Wind and Gusts: Both steady wind and gusts accelerate ignition and transition dynamics, alter fire spread rates, and significantly influence HRR and combustion stability.

This comprehensive body of work enhances predictive understanding of fire initiation from anthropogenic sources like construction sparks and provides valuable input for fire mitigation policies. It supports the development of safer operational guidelines for equipment usage near wildlands, improved fire spread models, and early-warning systems in WUI regions.

TABLE OF CONTENTS

LIST OF FIGURES

LIST OF TABLES

Chapter 1
INTRODUCTION

1.1 Background and Motivation

Wildfires are natural disasters that pose significant threats to ecosystems, causing extensive damage to infrastructure and human life, including fatalities [1]. Wildfires are becoming more frequent and severe each year. Driving these increases are various factors including climate change, fire exclusion (suppression) and land use changes, which have contributed to the escalating threat to ecosystems, property, and humans due to wildfires [2], [3]. The rising temperatures and prolonged dry conditions create ideal conditions for these fires to spread rapidly and cause greater devastation. Thus, with global warming, wildfire and Wildland-Urban Interface (WUI) fire problem is expected to intensify [4]–[6]. On average, nearly 70,000 wildfires have occurred annually in the U.S. since 1983, with early records possibly indicating even higher counts. In recent decades, wildfire impacts have escalated dramatically, with post-2004 events peaking (e.g., an average of 1.8 million acres burned in July from 2003 to 2021), and between 5 – 22 % of burned lands classified as severely damaged (https://www.epa.gov/climate-indicators/climate-change-indicators-wildfires). The National Fire Protection Association (NFPA) reported that US fire departments responded to an average of 346 800 home structure fires annually from 2014 to 2018, slightly decreasing to around 338 000 by 2021(https://www.nfpa.org/education-and-research/research/nfpa-research/fire-statistical-reports/home-structure-fires) [7] . Despite this decline, home fires remain a serious threat in US, causing over $21.9 billion in property damage and 3500 civilian deaths annually [8]. In recent years, California for instance has caused major fire disasters in the state including the Dixie fire in 2021 caused by Electrical grid infrastructure failures (source: www.nifc.gov/fire-information/statistics) [7]. It is one of the largest wildfires in the state's history, causing extensive damage to landscapes and communities. The fire primarily affected the northern Sierra Nevada region, including parts of Plumas and Butte Counties. Dixie fire burned over 900,000 acres and destroyed over 1329 structures. The Dixie Fire burned over 900,000 acres and destroyed over 1,329 structures, with recorded suppression costs exceeding $500 million. Similarly, the Thomas Fire in 2017, which burned 281,700 acres and destroyed thousands of structures (source: https://www.fire.ca.gov/), serves as another significant example of fires caused by powerline infrastructure. making it the largest wildfire in the state at that time in terms of acreage [9]. Firefighters and emergency responders worked tirelessly to control the blaze, and it took weeks to fully contain the fire. The impact of the Thomas Fire extended beyond immediate destruction, affecting air quality in the region and causing long-term environmental consequences. The fire was determined to be caused by human activity and electrical grid infrastructure failures. In the United States, the growth of the wildland-urban interface has coincided with the rise in uncontrolled wildfire activity, driven by climate change and contemporary shifts in land management practices [10]. One outcome of relocating people closer to the wildland is increased risk of human-caused ignitions. In fact, human caused ignitions are the leading cause of wildfires across the United States and the globe [3], [11]. The impacts of wildland and WUI fires are severe, resulting in extensive environmental devastation, atmospheric combustion emissions, significant property losses, biomass depletion, and considerable human casualties [12], [13].

Figure 1.1. The Dixie Fire burns in the hills on August 17, 2021, near Milford, California (Photo by Justin Sullivan/Getty Images).

Even outside the U.S., some wildfires are large-scale events with significant ecological and human impacts. Major effects include damage to property and infrastructure, as well as severe casualties among civilians and firefighters. A significant, recent example is the 2019–2020 Black Summer bushfires in Australia, which burned an estimated 18.6 million hectares, resulted in fatalities, caused hundreds of injuries, and destroyed over 3,500 structures – making it one of the most devastating fire seasons in the country's history [14]. Other recent devastating incidents include: the 2017 Pedrógão Grande wildfire in Portugal, which claimed lives, injured over 200 people, and destroyed 458 structures; the 2016 Fort McMurray wildfires in Canada, which scorched approximately 590,000 hectares and led to the largest evacuation in Canadian history; and the 2015 Indonesian peatland fires, which burned millions of hectares and had profound impacts on communities and infrastructure [15]–[17].

Numerous instances worldwide have been reported where wildfires were sparked by hot metal particles from clashing power lines, sparks generated by machinery and engines, or grinding and welding sparks [18], [19]. In fact, human caused ignitions are the leading cause of wildfires across the United States and the globe [3], [11]. Among these, human caused ignitions are those due to infrastructure and equipment. Electrical grid infrastructure failures in California, for instance, have resulted in major fire disasters in the state. Fires caused by powerline failures are produced by a process called spot fire ignition in which hot particles produced by electrical failure or arcing are lofted by the wind, transported to nearby wildland fuels such as dry grass, duff, litter, and other materials and then subsequently transferring their thermal energy to the fuel bed and produce an ignition [20]–[25]. Fires caused by mechanical equipment follow a similar ignition phenomenon as machine operations such as cutting or grinding can produce a flux of small, heated metal particles that may act as ignition sources when landing on wildland fuels [20], [21], [24]. Various hot work activities have been implicated in numerous other noteworthy incidents [26].

Indeed, it is estimated that power lines, equipment, and railroads contribute to approximately 28,000 natural fuel fires annually in the United States [27], [28]. Numerous instances in New Zealand, Australia, and Southern Europe illustrate wildfires initiated by metal particles. In New Zealand, for instance, it has been reported that between 2005 and 2010, 275 fires were sparked by flying brands [29]. In Australia, sparks were responsible for some of the devastating wildfires in Sydney in 1994 and the Black Saturday event of February 2009 [14], [30], [31]. Many similar fires exist without reference due to litigation involvement or challenges in determining the fire's origin.

Clearly, the ignition of wildland fuels, such as grasses, debris, litter by hot metal particles is a significant pathway for initiating wildfires and Wildland-Urban Interface (WUI) fires. The existing literature explores various potential particle sources beyond those mentioned earlier, including metal components friction, overheated brakes, and vehicle exhaust systems [32], [33].

It can be stated that the ignition of wildland fuels by hot metal particles is a complex multi-step process governed by the dynamics of ignition particle generation [18], [20]–[22], [34]. Because the heated particles may be at a range of temperatures, understanding how even a low temperature particle may initiate a low temperature ignition known as smoldering ignition and eventually lead to a dangerous uncontrollable fire is a critical step for better risk assessments of any related fire disasters. A high temperature particle, for instance, may ignite a flaming fire upon landing on a fuel bed; once ignited the fire may quickly spread through the landscape given favorable fuel conditions. Both smoldering and flaming events are observed in both residential and wildland fires, and each can transition into the other [18], [35], [36]. Smoldering combustion is the prolonged, low-temperature, flameless burning of porous fuels, representing one of the most enduring combustion phenomena [34], [35], [37], [38]. The smoldering to flaming (StF) transition involves a rapid initiation of homogeneous gas-phase combustion following smoldering fire. This transition poses a threat due to the sudden rise in spread rate, power, and associated hazards [39], [40]. StF is particularly hazardous because smoldering can be ignited by relatively low heat flux providing an alternative pathway to flaming [35], [41]. Smoldering can remain undetected for a long period of time (up to hours) and becomes visible only after the transition to flaming has occurred [42], [43]. Upon transition, the fire may rapidly and erratically grow, placing firefighters and civilians at risk.

The overall chemical pathways of solid fuel combustion are represented by Eqs. (1)– (3). Equation (1) depicts pyrolysis, a common reaction mechanism of solid fuel that produces solid char and gaseous pyrolyzate [39]. Pyrolysis is an endothermic reaction requiring heat to progress. Smoldering combustion occurs when the dominant combustion reaction is the oxidation of char (Eq. (2)), while flaming combustion takes place if the dominant reaction is the oxidation of pyrolyzate (Eq. (3)). Both char and pyrolyzate oxidations are exothermic reactions that generate heat to sustain the chain reactions.

The StF transition occurs when solid burning initially involves smoldering (Eq. (2)) but is then followed by a sudden ignition of pyrolyzate (Eq. (3)). This ignition is triggered by the fulfillment of conditions necessary for the onset of flaming combustion, such as the required concentration of the pyrolyzate-O_2 mixture and its corresponding temperature (the lower flammability limit).

Pyrolysis:

$$Fuel\ (solid) + Heat \rightarrow Pyrolyzate\ (gas) + Char\ (solid) \quad \ldots\ldots\ldots\ldots\ldots\ldots\ldots \ (1)$$

Smouldering combustion:

$$Char\ (solid) + O_2\ (gas) \rightarrow Heat + CO_2 + H_2O + other\ gases + Ash\ (solid) \quad .. \ (2)$$

Flaming combustion:

$$Pyrolyzate\,(gas) + O_2\,(gas) \rightarrow Heat + CO_2 + H_2O + other\ gases \ldots\ldots\ldots\ldots \quad (3)$$

Clearly seen that, seemingly less dangerous, low temperature particles may produce a weak ignition in the form of a smoldering fire which can transition to flaming fire upon encountering the right conditions called smoldering-to-flaming [35], [44], [45]. Depending on what are the thermal properties of a particle, what are the physical and chemical properties of a fuel bed, how the heated particles land on it, the particle may produce a smoldering ignition, a smoldering to flaming transition ignition or a flaming ignition, potentially developing into a spot fire [24], [46], [47].

The issue of igniting spot fires with hot particles can be dissected into three distinct processes: (1) metal particles / spark generation (arcing, friction), (2) metal particles lofted and transported by wind and (3) characteristics of the particles at landing. The following subsections provide concise summaries of the research undertaken in each of these domains, along with an overview of work conducted on alternative forms of hot particle ignition. It is essential to highlight that, although the ensuing discussion centers around hot particles, numerous phenomena exist with the potential to initiate spot fires.

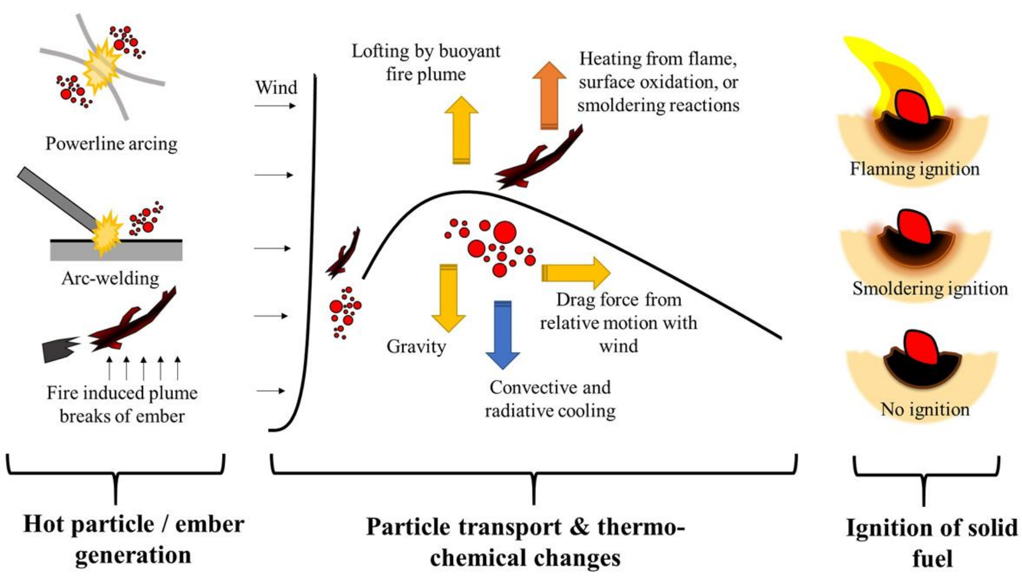

Figure 1.2. Steps in the development of spot wildfires [18].

1.2 Spot fire ignition process by hot particles

The assessment of particle generation, even from a single process, presents challenges. However, numerous experimental studies have delved into particle generation from diverse sources. In the 1970s, responding to bush fires, the State Electric Commission of Victoria (SECV) commissioned studies on the ignition potential of particles resulting from aluminum conductor clashing [24], [48], [49]. Regrettably, the results are housed in unpublished internal reports, creating contradictory evidence.

According to Coldham's literature review, a subsequent SECV-commissioned study by Joynt utilized high-speed photography to measure particle temperature and ejection velocity from copper conductor clashing [50]. Coldham reports a maximum ejection velocity of 20 m/s, with produced particles reaching up to 1.3 mm in diameter. Maximum temperatures observed reached as high as 2240°C, but due to particle cooling during flight, temperatures ranged between 1100 and 1500°C upon impact [50]. However, Coldham notes uncertainty as this study followed earlier SECV studies, leaving ambiguity about whether the data is based on separate copper conductor experiments or restated from potentially inaccurate work on aluminum conductors [50].

In another study, Ramljak et al. explored the statistical distribution of particle sizes resulting from low-voltage aluminum power line clashing [51]. They examined various power system protection scenarios, finding a mean particle size of around 1 mm in both live network and laboratory tests, with a Dagum distribution best characterizing the size distribution. The study also referenced prior investigations on particle production due to clashing [51].

Another recent study by Mikkelsen investigated particles generated by various forms of hot work, including welding, abrasive, and thermal cutting [26]. The focus was on determining the spatial distribution of particles created by these processes and estimating safe working clearances. The study identified welding processes as posing a higher risk of igniting material close to the workpiece, while cutting and grinding processes could eject particles over longer distances. Although the size of individual particles was not characterized, study images illustrated that various processes could produce large globules of hot material. It was also observed that particle oxidization significantly affects impact temperature, and different materials exhibit distinct oxidation characteristics (i.e., higher or lower impact temperatures). Mikkelsen's work encompasses a comprehensive literature review of past studies on ignition by industrial hot work processes [26].

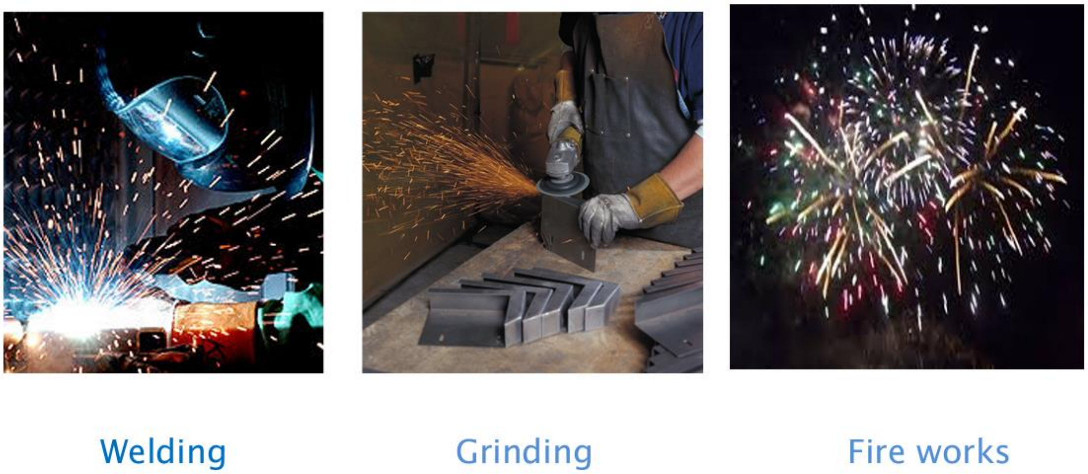

Figure 1.3. Common hot particles sources of ignition [18].

In wildland fires, firebrand transport is one of the largest factors when it comes to wildfire spreading. The transportation phase in the spot fire formation process has been extensively studied, primarily through computational models. While these models have mainly focused on particles generated by power line interaction, their consideration of the kinematics, cooling, and oxidation of ejected particles makes them applicable to various particle sources. In some instances, these models are even relevant to the transport of firebrands [49].

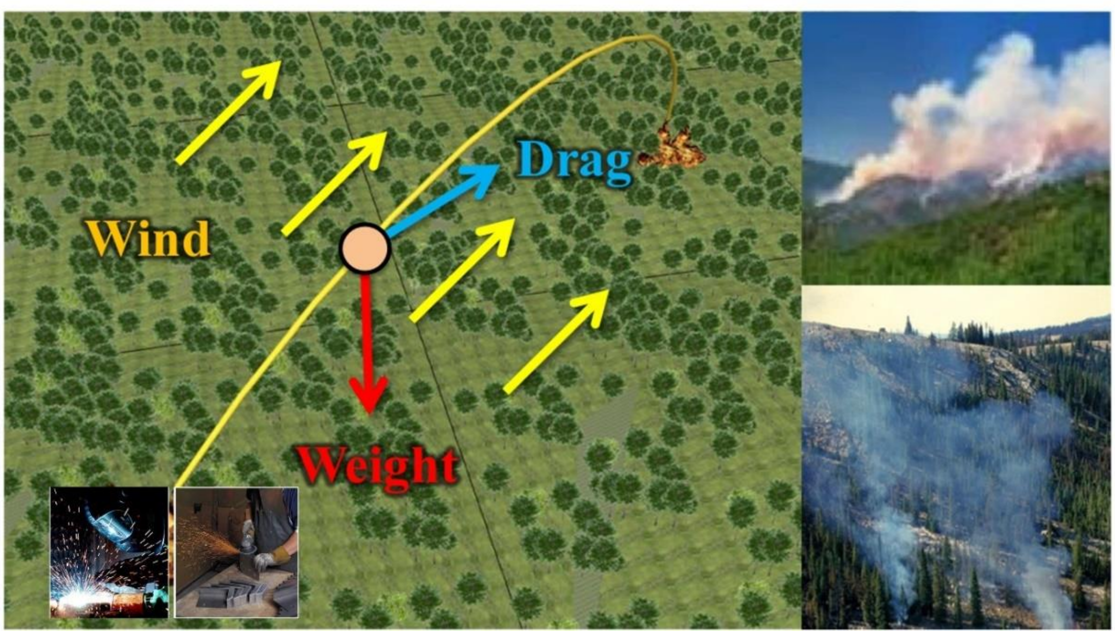

Figure 1.4. Particles ejected and transported by wind [18].

One of the most interesting studies was done by Fernandez-Pello formulated an extensive model, employing it to examine the transport, combustion, and ignition risk associated with aluminum and copper particles, as well as firebrands generated by conductor interaction during high winds [49]. They solved the coupled ballistic equations in three dimensions, considering a wind velocity profile typical of grassy terrain. Additionally, they incorporated experimental data for aluminum combustion in air to address particle burning in their model. Remarkably, their model yielded reasonable results without requiring an effective particle diameter. The study revealed that aluminum particles could both combust and travel farther than their heavier, non-combusting copper counterparts. Despite this, the higher volumetric heat capacity and constant mass of copper particles still resulted in impactful thermal energy upon impact.

One study found that firebrands can be transported several kilometers ahead of the fire front, potentially creating new fires [52]. In this study, a mathematical model developed for firebrands' transportation by wind. The study results that spherical and disc-shaped particles have best transportation ability. The result also concludes that the transfer coefficient does not exceed one within the air flow velocity of 1-10 m/s [52]. Another study which used the Hierarchical Bayesian approach was used to develop probabilistic models [53]. Hierarchical Bayesian models (HBMs) were used to estimate probabilistic distributions for the size and transport distance of firebrands. It showed that existing probabilistic models underestimated the dispersal range of firebrands.

1.3 Effects of Fuel Properties and Morphologies in Wildland Ignition Behavior

Fuel structure and species composition are another critical factors governing the ignition behavior of grassy fuels, particularly in fire prone wildland-urban interface (WUI) regions [20], [40]. Among surface fuels, grassy vegetation plays a disproportionately critical role as it forms the first layer of ignition and can facilitate rapid fire spread once ignited [54]. So, small sizes surface fuels can initiate the sparks for fires and transfer them to larger sizes of branches, trees etc [19], [55], [56]. Which refers to understanding the influence of fuel bed properties and morphologies such as powdered, shredded, and solid (natural) forms is essential for accurately predicting ignition behavior and fire spread in wildland environments [57]. These structural configurations directly affect the surface area, bulk density, porosity, and airflow dynamics within the fuel bed, all of which play a critical role in heat transfer, oxygen availability, and combustion sustainability [24], [57], [58]. For example, powdered fuels have a high surface-area-to-volume ratio and compact structure, leading to rapid heat absorption and lower ignition temperatures, but they may also extinguish quickly due to limited oxygen penetration. In contrast, natural (solid) fuels, with their larger voids and discontinuities, may support sustained smoldering and flaming transitions but require higher energy input to initiate ignition due to reduced thermal contact. Shredded fuels, occupying an intermediate position, provide valuable insight into how partial fragmentation affects combustion kinetics. By systematically comparing these morphologies, researchers can better understand how real-world disturbances such as mowing, trampling, or drying alter fuel bed behavior and ignition risk [57], [58].

Very little research has been conducted to explore the effect of the fuel bed properties, fuel chemistry, and morphology in the ignition process and mechanism for natural fuels and combustible materials [23], [34], [47], [48]. Additionally, while prefabricated and biomass fuels have received little attention, work examining wildland fuels is even more limited. This knowledge gap is crucial for developing accurate fire spread models, designing fuel management strategies, and informing safety regulations in wildland-urban interface (WUI) zones.

1.4 Critical Role of Wind in Wildfire Ignition

Wildfire, though a natural event, is a complex phenomenon shaped by the burning process, weather conditions, and various environmental and social factors that dictate its growth and determine whether it overcomes initial containment efforts to become a large-scale disaster [59], [60]. Among weather and environmental factors, the key influences on wildfire behavior include wind and gusts, dry conditions, high temperatures, prolonged droughts, and terrain and topography [60]–[62]. In particular, wind is pivotal and one of the most influential factors, as it rapidly spreads flames and carries embers over long distances, often igniting new areas [60], [62]–[64].

Wildfire behavior is governed by the intricate interplay of three principal factors: terrain, weather, and fuels. While each of these factors can independently influence the progression and intensity of wildfire, their combined effects often result in more complex and dynamic fire behavior. Among these environmental influences, wind stands out as one of the most dominant and multifaceted factors. It plays a central role in shaping ignition potential, combustion intensity, and the directional spread of fire [65]. Even under moderate conditions, wind can rapidly escalate a wildfire by supplying fresh oxygen, tilting flames toward unburned fuel, and lofting embers far beyond the main fire front frequently initiating spot fires well ahead of the burn zone.

Although wildfire is a natural phenomenon, its behavior is shaped not only by combustion physics but also by weather conditions and a wide array of environmental and social drivers [59], [60]. Among these, wind and gusts, dry weather, elevated temperatures, prolonged droughts, and topographical features are particularly influential [60]–[62].

Wind directly influences key fire parameters for fire ignition behavior [66]–[69]. Both the direction and magnitude of wind determine not only the velocity of fire spread but also its predictability and stability [67], [69]. Rapid wind-driven increases in heat transfer to nearby unburned fuels further amplify the energy release rate, making wind a critical enabler of sudden fire intensification, especially in wildland and WUI zones [46], [70], [71].

Moreover, wind frequently interacts with other meteorological variables, such as ambient temperature and relative humidity, compounding its effect on fire behavior [72]. Numerous studies have demonstrated that higher wind velocities intensify combustion by increasing convective heat transfer and enhancing oxygen availability at the flame front [73], [74]. These factors collectively make fire containment more difficult and often demand swift tactical adaptations by fire suppression teams. In summary, wind is not merely a background variable in wildfire dynamics, it is a primary driver that governs ignition success, flame propagation, and overall fire severity. Its variable and unpredictable nature underscores the need to incorporate wind effects in laboratory-scale studies, predictive simulation models, and community-level risk mitigation strategies.

Wind velocity affects the rate of fire spread by modifying the rate of heat transfer from active flames and burned materials to adjacent unburned fuel [75]–[79]. The relationship between wind speed and fire spread is further shaped by the buoyant motion of the fire plume and the inertial forces imparted by wind [80]. Ongoing climate change and widespread deforestation are altering these relationships, leading to increasingly erratic fire behaviors [81]. Additionally, heterogeneity in vegetation and fuel density introduces turbulence and localized variations in wind flow, which further complicate spread predictions [82]. Understanding and accounting for these wind-driven dynamics are essential to forecasting fire evolution and improving mitigation strategies in fire-prone regions.

1.5 Gusty wind effects in ignition behavior process

Wildfires continue to pose an escalating threat to ecosystems, infrastructure, and public safety particularly in regions prone to prolonged dry conditions and complex wind patterns [83], [84]. Among the multitude of environmental drivers influencing wildfire behavior, gusty winds emerge as a particularly potent and unpredictable force. Unlike steady winds, gusts are characterized by short-term, rapid fluctuations in speed and direction, which dramatically amplify fire behavior [85]. These transient wind surges not only accelerate the spread of flames but can also influence the initial ignition of fuels, especially in the Wildland-Urban Interface (WUI) where vegetative and structural fuels co-exist in close proximity [46], [86].

Gusty winds have been repeatedly implicated in some of the most destructive wildfire events globally. For instance, during the 2009 Black Saturday fires in Victoria, Australia, wind gusts exceeding 100 km/h facilitated the rapid spread of flames across approximately 450,000 hectares, resulting in 173 fatalities the deadliest wildfire in Australian history [14]. Similarly, in Portugal, intense downward wind gusts on June 17, 2017, propelled embers well ahead of the fire front during the Pedrógão Grande fire, igniting new fires that consumed over 45,000 hectares and caused 66 deaths within hours [87]. The United States has seen comparable tragedies linked to high wind events. The Marshall Fire in Colorado (December 30, 2021) began during an intense windstorm with gusts reaching 185 km/h (115 mph), destroying over 1,000 homes in less than eight hours [88]. Likewise, California's infamous Camp Fire (2018) was propelled by 52 mph winds, rapidly engulfing over 153,000 acres and more than 19,000 structures, incurring $16.5 billion in damages [89]. Statistical records support the correlation between gust intensity and wildfire severity. In 2024, a year marked by stronger winds, the U.S. experienced 64,897 fires that burned 8.9 million acres—more than triple the area burned in 2023, which had milder wind conditions [61], [90], [91]. In California, Santa Ana and Diablo winds—characteristically hot, dry easterly winds—are strongly linked to large-scale fire disasters. A USGS study analyzing 643 Santa Ana events from 1948 to 2018 found that stronger winds not only increased fire starts but significantly expanded the total area burned. During high-wind years, the average number of homes destroyed rose from about 500 (1950–2000) to 2,700 (2000–2018), largely due to wind-driven embers igniting structures at the wildland edge [91], [92]. Recent events such as the Pacific Palisades Fire (January 2025), which burned 12,000 acres and over 1,000 buildings in a single day, and historic cases like the 1991 Oakland/Tunnel Fire ($1.5 billion in damage and 3,500 homes lost) further reinforce the critical role of wind gusts [93], [94]. The Wine Country Fires of October 2017 devastated northern California, destroying 9,000 structures and causing over $10 billion in insured losses [95]. The Thomas Fire (2017), briefly California's largest, was fueled by gusts of 60–79 mph, pushing flames across mountainous terrain. In 2019, the Getty Fire followed the same pattern, as gusts exceeding 50 mph enabled the fire to jump containment lines and roadways, igniting homes in dense neighborhoods [91], [95].

These field-scale observations clearly demonstrate that gusty winds do not simply intensify existing fires, they can decisively determine whether a small ignition develops into a catastrophic wildfire. Given the unpredictable and highly variable nature of wind gusts, there is an urgent need for detailed laboratory investigations that can isolate and systematically evaluate their influence. Parameters such as gust duration, frequency, amplitude, and wind-fuel interactions must be carefully studied to improve predictive fire models and develop more effective mitigation strategies.

However, capturing the effects of gusty winds in controlled settings remains a significant research challenge. Most laboratory fire studies have focused on steady-state wind conditions, which while reproducible fail to reflect the chaotic and intermittent nature of real-world wildfire scenarios. Gusts create dynamic oxygen supply regimes and shifting convective heat transfer patterns, which can influence ignition thresholds and flame development in unpredictable ways. These unsteady flow conditions may be the determining factor in whether a fire ignites, sustains combustion, or transitions from smoldering to flaming.

Understanding how gusty wind dynamics shape ignition behavior is therefore essential for wildfire risk forecasting, emergency planning, and WUI fire safety. Without this knowledge, both predictive tools and firefighting tactics remain incomplete in the face of nature's most variable and dangerous fire-driving mechanism.

1.6 Research objectives

1.6.1 Objective for Spot Ignition project (Chapter 3)

There are still experimental studies related to the generation of heated metal particles and the study of spot fire ignition, particularly in wildland fuels. Most investigations into ignition behavior, such as ignition temperature and ignition time, have been conducted by using metal particles on prefabricated controlled fuels (excelsior, insulation foam) to circumvent the complexities arising from the physical and chemical properties during combustion ignition [24], [48]. Consequently, the question of studying ignition behavior in wildland fuels remains unanswered. While metal particles have been widely investigated as ignition sources, most studies have focused on single-particle scenarios [23], [48], [57], [58]. In contrast, the behavior of multiple metal particles remains relatively underexplored. Although some research has examined multiple firebrands, primarily wooden ones, very few studies have utilized metal particle firebrands in such investigations [18], [25], [55], [96].

To answer the research questions, this study aims to investigate the effect of the properties of multiple stainless-steel ignition particles and wildland fuel beds in shaping ignition behavior. Unique to this work is the examination of stainless-steel particles of different grades, corresponding to varying carbon contents, along with the modeling of fuel beds using real wildland fuels. By including wildland fuels, the study integrates the effects of physical and chemical composition of fuel species on ignition behavior. The goal is to contribute to a fundamental understanding of the key ignition particle and fuel characteristics that govern favorable ignition conditions in wildland fires and to offer practical fire safety guidance for the use of machining equipment near wildland areas. This guidance may serve as a foundation for management and policy recommendations related to fire safety practices in construction and other machining operations that generate heated metal fragments. The research questions addressed in this study are as follows:

(1) How do the size and number of hot metal particles affect the ignition behavior (ignition temperature and time) of wildland fuels for both smoldering and flaming ignition?

(2) Does the carbon content in hot metal particles influence the smoldering and flaming ignition time and temperature of wildland fuels?

(3) Do the properties and morphologies of wildland fuels significantly impact smoldering and flaming ignition behavior (ignition temperature and time)?

1.6.2 Objective for Fuel Properties project (Chapter 4)

Numerous instances worldwide have been reported where wildfires were sparked by hot metal particles from clashing power lines, sparks generated by machinery and engines, or grinding and welding sparks[18], [19] . The fires can initiate when hot particles land on fuels such as dry grass, duff, litter, and other materials. A good amount of literature has already described the process of the ignition of combustible materials, grass, litter, and shrubs by heated metal particles[18], [21], [47], [57]. However, the physical and chemical properties of wildland fuels during ignition remain less well understood. This knowledge is needed to uncover how these properties influence ignition thresholds and fire spread in diverse wildland fuel types. Very little research has been conducted to explore the effect of the fuel bed properties, fuel chemistry, and morphology in the ignition process and mechanism for natural fuels and combustible materials [23], [34], [47], [48]. Additionally, while prefabricated and biomass fuels have received little attention, work examining wildland fuels is even more limited. Upon analysis, we found that most prior studies focused on comparing ignition behavior within a single fuel bed, specifically natural fuel bed structures, with only a few works addressing multiple structures [20], [57]. Furthermore, most studies have examined flaming ignition cases, while very few have comprehensively analyzed all ignition types, including single smoldering, or moldering to flaming transition ignition behaviors.

Thus, our study builds on this previous knowledge by investigating a range of wildland fuels with different fuel bed structures, including natural, shredded, and powdered fuel beds, and providing a detailed analysis of ignition behavior. Additionally, to support the analysis of ignition behavior and to better understand how the chemical composition of grassy fuels influences the ignition and combustion processes, thermogravimetric (TG) testing was incorporated. This technique was used to evaluate the temperature of maximum degradation, which serves better understanding on the degradation process in multiple degradation process of chemical contents such as lignin, protein. Which concludes, this comprehensive experimental approach, combined with TG analysis, aims to address gaps in existing research on different fuel structures and ignition types.

1.6.3 Objective for Wind Effects project (Chapter 5)

Wildfire is a complex natural phenomenon shaped by combustion dynamics, weather patterns, and environmental conditions [59], [60]. Among weather and environmental factors, the key influences on wildfire behavior include wind and gusts, dry conditions, high temperatures, prolonged droughts, and terrain and topography [60]–[62]. In particular, wind is pivotal and one of the most influential factors, as it rapidly spreads flames and carries embers over long distances, often igniting new areas [60], [62]–[64]. To better understand fire dynamics, researchers have used both field and lab experiments to study ignition behavior and its relationship to atmospheric conditions and fuel properties and fire spread [66]–[69], [97]–[99]. However, several significant parameters have been overlooked or inadequately studied, such as different ignition modes and the performance of different wildland fuel species under various wind conditions. In particular, most studies have focused exclusively on flaming ignition when evaluating ignition parameters, with little attention given to smoldering or the transition from smoldering to flaming [37], [66]–[69]. Consequently, there is a notable shortage of laboratory experiments that provide comprehensive datasets to explain the ignition behaviors across various ignition types, particularly for wildland fuel species. To address existing research gaps, this study aims to investigate the relationship between wind speed and wildfire behavior during the ignition of wildland fuels across various ignition types. To clarify our objectives, we have formulated the following research questions:

(1) How does wind speed affect ignition behavior, including ignition time and ignition temperature, of wildland fuels across various ignition types?

(2) How does wind speed influence fire spread behavior, including fire spread rate, mass loss rate, and heat release rate, of wildland fuels across different ignition types?

(3) How do fuel properties influence ignition behavior under varying wind conditions?

1.6.4 Objective for Gusty Wind project (Chapter 6)

Gusty winds play a critical role in the initiation and escalation of wildfires, especially in wildland urban interface (WUI) regions where unsteady airflow can convert low risk smoldering ignitions into fast-moving flaming fires [46], [86]. While steady wind effects on wildfire spread are relatively well studied, the influence of transient gusts on ignition behavior remains poorly understood, particularly on the bench scale.

This study aims to fill that knowledge gap by investigating how wind gust frequency and speed modulate ignition dynamics in wildland fuels exposed to hot metal particles. Using a controlled wind tunnel setup, the research examines three common fuel types motivated from our previous studies under varying gust frequencies and wind speeds. The specific research questions guiding this work are:

(1) How do wind gust frequencies influence ignition parameters such as ignition time, temperature, and mode (smoldering, flaming, or StF transition) across different wildland fuel types? (2) What is the relationship between gust frequency and combustion intensity, as measured by burnout time and HRR, for each ignition mode? (3) How do different wildland fuels interact with transient wind conditions to affect the likelihood and timing of smoldering-to-flaming transitions?

By addressing these questions, the study provides fundamental insights for improving fire behavior prediction models, informing fire suppression strategies, and guiding fuel management practices in gust-prone environments.

Chapter 2
LITERATURE REVIEW

The literature review is organized into four systematic sections; each aligned with the objectives and development of Projects 1 through 4. The first section reviews studies related to the effects of heated metal particles on fuel ignition behavior, with particular emphasis on how particle properties (e.g., size, material) and fuel characteristics influence ignition dynamics. These insights directly informed the foundation of Project 1, which analyzed the combined influence of particle and fuel properties on ignition outcomes. Building on these findings, the second section focuses on fuel properties and morphology, aiming to explore why these characteristics play a critical role in ignition behavior. Project 2 was designed in response, using a two-pronged approach: first, by examining ignition in fuels with different structural forms (natural, shredded, and powdered); and second, by applying thermogravimetric analysis (TGA) to understand the thermal degradation and chemical behavior of each fuel type. The third section shifts attention to another key environmental driver of wildfires, wind speed. Motivated by gaps in previous research, Project 3 investigated how low, steady wind speeds influence ignition parameters, even in otherwise controlled conditions. Finally, the fourth section explores the influence of wind gust frequency, a relatively understudied but potentially critical factor in wildfire ignition. Project 4 assessed this by introducing three controlled gust frequencies, the maximum achievable within our experimental setup, to evaluate their impact on ignition time, transition behavior, and combustion intensity.

2.1 Effect of metal particles on ignition behavior

Even though wildfires are increasing globally each year, controlling them is challenging due to their unpredictable nature. Limited in number and mostly focused on non-wildland fuels, several studies have examined the mechanisms governing the ignition of natural fuel beds by heated metal particles [18], [21], [23], [24], [34], [35]. Findings from these studies indicate that particle properties and fuel composition determine ignition behavior.

During the previous studies, steel, aluminum, and copper received great attention due to their common use in day-to-day activities. Copper, aluminum, and steel are commonly used as conductor materials in electrical power systems. Steel is often used to construct power line towers (pylons) because of its strength. Hadden et al. investigated the ignition of cellulose fuel beds by heated steel particles [23]. Their experiments showed a correlation between particle size and fuel bed ignition temperature and indicated that the ignition temperature was higher for smaller particles than for larger particles. This relationship between ignition temperature and steel particle size was also observed in experiments conducted with cellulose fuel beds in Zak et al. [58]. Zak et al. 2014 has tested different types of particles, with varying size and temperature to determine the effect of particle properties on the ignition limit of cellulosic fuel beds [24], [34], [58]. The study has investigated varying diameter from 2-11 mm of metal particles composed of Stainless Steel 302, Aluminum 1100, Brass 260, and Copper 110 were heated using a tube furnace and dropped onto a fuel bed seated inside the test section of a bench-scale wind tunnel. The temperature of the particles varied from 550-1100°C with a tube furnace. The results showed that no ignition has been observed for the particle temperature range up to 575°C. Also, ignition probability was found to be less than 5% for 2mm stainless-steel particles and 95% for 6-11 mm of stainless-steel particles. In addition, for particle temperature ranges of 900-1100°C and particle sizes of 6-10 mm the flaming ignition probability was found 100% for all types of particles. So, the study suggests that the particles size and temperature influence ignition probability of cellulose fuel bed. This relationship between hot particle temperature and particle size was also observed in experiments conducted with pine needle fuel beds by Wang et al. [22]. Similarly, in work by Wang, Chen, and Liu et al. and Wang et al investigating the ignition of expandable polystyrene foam by heated steel particles it was found that increases in particle size decreased the temperature required for ignition, thus approximating results from the natural fuel studies mentioned above [22], [100].

In terms of fuel bed properties, fuel chemistry and morphology are known to shape ignition behavior [101], [102]. Therefore, numerous studies have focused on examining how these factors affect ignition in wildland fuels. For instance, in a study employing metal particles as ignition sources, Urban, Zak, and Fenandez-Pello et al. examined ignition trends in several wildland fuels and found that fuels with higher alpha-cellulose content typically ignited at lower temperatures than fuels with lower alpha-cellulose content [57], [96]. To investigate the role of alpha-cellulose, they isolated this component and found only marginal influences on ignition behavior. They therefore hypothesized that lignin and protein rather than alpha-cellulose play a major role in shaping ignition behavior in wildland fuels. This is further supported by findings by [102], [103]. In addition, lignin along with cellulose content has been found to affect ignition delay time [104]–[107]. Moreover, the presence of other chemical components such as essential oils has been shown to increase fuel flammability and accelerate the ignition time (Guerrero et al. 2021; Murray, Hardstaff, and Phillips 2013).

In addition to fuel bed properties, the properties of the particles used as ignition sources may play an essential role in shaping the ignition behavior of wildland fuels. Among the various metals used in daily life, stainless steel plays a critical role, particularly due to its extensive utilization in construction and household materials and widely adopted for its significant anti-corrosive quality and durability, it is highly valued in the construction industry. Due to its significant contribution and applications in machining, stainless steel has attracted attention for studying its role as a hot metal particle in wildland fuel ignition [18], [21], [22]. Previous works investigating the ignition behavior of powdered cellulose fuel beds using heated stainless steel as ignition sources have observed ignition probability and boundaries based on ignition particle size and temperature [21], [34], [57]. Similarly, Wang et al. evaluated the ignition behavior of pine needles when stainless steel particles of varying sizes and temperatures were used as ignition sources. The study by Wang et al observed that for similar particle temperatures, larger particles have a higher ignition probability, and a lower ignition delay time compared to smaller particles, both in direct flaming and in smoldering to flaming transition [22]. Grade 304 stainless steel is commonly used in architecture for both interior and exterior purposes, such as kitchen equipment and chemical containers. On the other hand, 440C stainless steel finds extensive use in construction for cutting tools, bearings, and fasteners, thanks to its exceptional hardness and wear resistance. It has been found that for stainless steel, increasing the amount of carbon content in its material properties decreases the thermal conductivity, which in turn affects its ability to effectively conduct and transfer heat when acting as an ignition source [108]. Stainless steel is integrated into construction projects, it is typically cut or grinded, causing sparks that, when landing on ignitable material, may produce a fire. In the case of new housing developments expanding toward undeveloped areas, the prevalence of grassy wildland fuels may yield a significant fire hazard [108].

This study aims to investigate the effect of the properties of stainless-steel particles and wildland fuel beds on ignition behavior. Unique to this study is the examination of stainless- steel particles of different grades corresponding to varying carbon contents and the modeling of fuel beds using real wildland fuels. By including wildland fuels, we aim to integrate the effects of the physical and chemical composition of grassy fuels on ignition behavior. The goal of this work is to contribute to a fundamental understanding of the key parameters governing the ignition of grassy wildland fuels by metal particles. In addition, results from this study can offer the first steps toward management and policy recommendations for fire safety practices in construction and other machining operations that produce heated metal fragments during use.

2.2 Fuel bed properties and morphologies: insights from Thermogravimetric Analysis

Numerous instances worldwide have been reported where wildfires were sparked by hot metal particles from clashing power lines, sparks generated by machinery and engines, or grinding and welding sparks [18], [19]. The fires can initiate when hot particles land on fuels such as dry grass, duff, litter, and other materials. Previous studies have provided critical insight into the mechanisms leading to the ignition of combustible materials including grass, litter, and shrubs by heated metal particles [18], [21], [47], [57]. However, the physical and chemical properties of wildland fuels during ignition remain less well understood. This knowledge is needed to uncover how these properties influence ignition thresholds and fire spread in diverse wildland fuel types. Very little research has been conducted to explore the effect of the fuel bed properties, fuel chemistry, and morphology in the ignition process and mechanism for natural fuels and combustible materials [23], [34], [47], [48]. For instance, studies by Fernández et al. (2017) and Urban et al. (2018) examined the effects of fuel morphologies, such as varying structures, on ignition behavior, though these investigations were limited to prefabricated fuels [18], [24]

Comparing wildland fuels, additional experiments and investigations have been conducted on biomass fuels to explore their effects on the ignition process, such as ignition temperature and ignition time due to their physical and chemical properties [26], [51], [101]–[103]. In addition to chemical properties, several studies have focused on physical properties, such as fuel particle size and bulk density, to understand their effects on ignition characteristics, such as mass loss, ignition time, burning rate, and total burnout time [109]–[113]. Additionally, while prefabricated and biomass fuels have received little attention, work examining wildland fuels is even more limited. For more clarification a table is provided below with few prior research:

Table 2.1. Details of few prior research

Author list	Fuel bed properties	Ignition Source	Observation, Findings and Contributions
Zak et al 2013 [57]	Dry alpha cellulose powder	Heated stainless steel and brass particles with 1.59 – 12.7 mm in diameter.	Ignition temperature analysis for flaming, possible flaming and no ignition.
Urban et al 2018 [24]	Alpha-cellulose, a grass blend of fuels in shredded and powdered structures.	Heated 2-8 mm diameter aluminum particles	Flaming ignition temperature and probability for all fuels (barley/wheat, and dead pine needles)
Urban et al 2017 [34]	Natural powdered grass blend	Heated steel and aluminum particles with 1.6 - 8 mm in diameter.	Flaming and smoldering ignition temperature and propensity of powdered grass blend.
Urban et al 2015 [114]	Cellulose powder	Heated aluminum, steel, copper, brass particles with 2-11 mm in diameter.	Flaming ignition temperature and probability of cellulose powder
Hadden et al 2011 [23]	Dry alpha-cellulose powder	Heated steel particles with 0.8-19.1 mm in diameter	Theoretical and experimental studies of no ignition, smoldering and flaming ignition.
Supan Wang et al 2019 [22]	Dead natural pine needle	Hot Steel Sphere particle (6-14 mm) diameter	Flaming ignition time, ignition temperature and ignition
Baranovskiy et al 2015 [115]	Forest fuel pine needle litter	Hot Steel sphere single particle	Flaming ignition time and temperature
Fang et al 2020 [116]	Dead and dry natural pine needle	Heated steel particles with 8, 10 and 12 mm diameter	Flame radiation ignition temperature, time, probablity
Saha et al 2024 [20]	Dry natural Bromus, Avena and Wheatgrass	Heated different steel particles of 12-30 mm diameter	Smoldering and flaming ignition temperature
Shi et al 2023 [117]	Coal dust layer	Heated steel, aluminum, cooper particles with 5-10 mm in diameter.	Flaming ignition temperature, ignition time

Upon analysis, we found that most prior studies focused on comparing ignition behavior within a single fuel bed, specifically natural fuel bed structures, with only a few works addressing multiple structures. Furthermore, most studies have examined flaming ignition cases, while very few have comprehensively analyzed all ignition types, including single smoldering, or smoldering to flaming transition ignition behaviors. Thus, our study builds on this previous knowledge by investigating a range of wildland fuels with different fuel bed structures, including natural, shredded, and powdered fuel beds, and providing a detailed analysis of ignition behavior. Additionally, to support the ignition behavior analysis, we incorporated thermogravimetric (TG) testing to evaluate the temperature of maximum degradation, representing the ignition temperatures. This comprehensive experimental approach, combined with TG analysis, aims to address gaps in existing research on different fuel structures and ignition types.

2.3 Wind-Driven Ignition Behavior of Wildland Fuels

Wildfire, though a natural event, is a complex phenomenon shaped by the burning process, weather conditions, and various environmental and social factors that dictate its growth and determine whether it overcomes initial containment efforts to become a large-scale disaster [59], [60]. Among weather and environmental factors, the key influences on wildfire behavior include wind and gusts, dry conditions, high temperatures, prolonged droughts, and terrain and topography [60]–[62]. In particular, wind is pivotal and one of the most influential factors, as it rapidly spreads flames and carries embers over long distances, often igniting new areas [60], [62]–[64]. Wind directly impacts wildfire behavior, affecting factors such as ignition time, burning rates, and fire spread [66]–[69]. Irrespective of wind direction and boundary conditions, higher wind speeds significantly reduce the time required for ignition [67], [69]. Researchers attribute this to the fact that stronger winds boost the fuel's burning rate, which in turn accelerates the rise in hot gas temperatures [66], [67], [69]. Moreover, while it is well established that fire spread rates increase with wind speed, the specific interplay among the physical processes is also influenced by wind speed, thereby affecting overall fire behavior [66], [68]. Several studies suggest that under constant flow conditions, increasing wind speeds result in a linear increase in fire rate of spread, a finding that aligns with other laboratory-based models [67], [97]. For instance, Albini's study of wind-driven grass fires in Australia revealed significant variations in fire speed times, ranging from approximately 6 minutes under low wind conditions to over 45 minutes in stronger winds, with the fire front width playing a key role [118]. In contrast, a wind tunnel study by Curry and Fons involving experiments with shallow (8 cm deep) pine needle and excelsior beds demonstrated that equilibrium was reached within just a few minutes, largely unaffected by wind speed [119]. Their point-ignition tests in pine needle litter also showed that while wind speed influenced the fire speed, it also increased the time to equilibrium and affected the final spread rate. In addition to the experimental study, numerical analysis also revealed an increased fire spread rate in response to stronger wind conditions [120].

Besides ignition characteristics (ignition time, ignition intensity), fire spread behavior and heat release is another crucial component of wildfire behavior, as it represents the energy emitted by burning materials that can be transferred back to the fuel, creating a feedback loop that accelerates fire growth and spread (Cobian-Iñiguez et al. 2022; Madrigal et al. 2011; Park 2020). The heat release rate is calculated by multiplying the fuel burning rate (i.e., the mass of fuel consumed per unit time) by the heat of reaction (i.e., the energy released per unit mass of fuel burned) (Cobian-Iñiguez et al. 2022). However, the heat of reaction varies depending on the fuel type and the fuel-to-air mixture ratio (Park 2020). Studies have demonstrated that the relationship between wind speed and heat transfer rate is highly interdependent, influencing overall fire dynamics (Cobian-Iñiguez et al. 2022; Madrigal et al. 2011; Park 2020). A study by Cobian-Iñiguez et al. found a marked increase in heat release rates in wind-driven fires compared to non-wind-driven fires, noting that the addition of wind increased the heat release rate from 328 kW to 526 kW for a crown base height of 0.60 m, and from 243 kW to 503 kW for a crown base height of 0.70 m (Cobian-Iñiguez et al. 2022). Similarly, another study investigated the heat release rate (HRR) under different wind conditions for a Pinus pinaster dead fuel bed and found that wind speed significantly impacted HRR – the peak HRR was approximately 2.3 kW at 2 m/s, compared to about 1.7 kW at 1 m/s. Additionally, a study by Carmignani et al. examined poplar dowels and found that increasing wind speeds also increased the mass loss rate of the dowels (Carmignani et al. 2024).

Besides ignition characteristics – such as ignition time, ignition intensity, and fire spread rate – heat release is another crucial component of wildfire behavior, as it represents the energy emitted by burning materials that can be transferred back to the fuel, creating a feedback loop that accelerates fire growth and spread [71], [121], [122]. The heat release rate is calculated by multiplying the fuel mass loss rate (i.e., the mass of fuel consumed per unit time) by the heat of reaction/combustion (i.e., the energy released per unit mass of fuel burned) [122]. However, the heat of reaction varies depending on the fuel type and the fuel-to-air mixture ratio [121]. Studies have demonstrated that the relationship between wind speed and heat transfer rate is highly interdependent, influencing overall fire dynamics [71], [121], [122]. A study by Cobian-Iñiguez et al. found a marked increase in heat release rates in wind-driven fires compared to non-wind-driven fires, noting that the addition of wind increased the heat release rate from 328 kW to 526 kW for a crown base height of 0.60 m, and from 243 kW to 503 kW for a crown base height of 0.70 m [122]. Similarly, another study investigated the heat release rate (HRR) under different wind conditions for a *Pinus pinaster* dead fuel bed and found that wind speed significantly impacted HRR – the peak HRR was approximately 2.3 kW at 2 m/s, compared to about 1.7 kW at 1 m/s. Additionally, a study by Carmignani et al. examined poplar dowels and found that increasing wind speeds also increased the mass loss rate of the dowels [37].

Since understanding fire behavior is crucial, researchers have also analyzed large-scale fire data to compare with laboratory experiments. To capture real-world dynamics, they have conducted field experiments to gather data on the overall behavior of wildland fires and how it relates to average atmospheric conditions and fuel properties [98], [99], [123].
However, several significant parameters have been overlooked or inadequately studied, such as ignition temperatures and the performance of different wildland fuel species under various wind conditions. In fact, ignition temperature is a crucial parameter in the study of ignition behavior, as demonstrated by previous experimental literature [24], [26], [47].

Furthermore, most studies have focused exclusively on flaming ignition when evaluating ignition parameters, with little attention given to smoldering or the transition from smoldering to flaming [37]. Consequently, there is a notable shortage of laboratory experiments that provide comprehensive datasets to explain the ignition behaviors across various ignition types, particularly for wildland fuel species.

To address existing research gaps, this study aims to investigate the relationship between wind speed and wildfire behavior during the ignition of wildland fuels across various ignition types. To achieve this aim, experiments were conducted in a laboratory-based wind tunnel to monitor both flaming ignition and the transition from smoldering to flaming ignition in different wildland grasses under varying wind conditions.

2.4 Role of Wind Gusts in Modulating Ignition behavior

The destructive potential of wildfires is significantly amplified by wind, especially under gusty conditions, which not only facilitate the rapid spread of flames but also influence the initial ignition of fuels in the wildlands and wildland-urban interface (WUI)[86]. Among the numerous environmental factors affecting wildfire dynamics, gusty winds stand out as a dominant and highly variable force, capable of initiating spot fires, modifying combustion modes, and triggering ignition in seemingly low-risk zones [46] . Numerous incidents around the world have already demonstrated how wind gusts can dramatically influence wildfire behavior and impact. During Black Saturday in Victoria, Australia (February 7, 2009), strong wind gusts over 100 km/h helped the fire spread quickly across about 450,000 hectares and caused 173 deaths the deadliest wildfire in Australian history [124]. A similar situation happened in Portugal, strong intense downward winds on June 17, 2017, helped the Pedrógão Grande fire throw burning embers ahead of the flames, which killed 66 people and burned about 45,000 hectares in just a few hours [87]. In the United States, many of the fastest and most destructive fires have happened during high-wind events. For example, Colorado's Marshall Fire (December 30, 2021) started during a powerful windstorm with gusts reaching 185 km/h (115 mph), which led to the loss of 1,084 homes in less than eight hours [88]. California's Camp Fire (November 8, 2018) began during 52 mph winds in a narrow mountain pass and went on to burn over 153,000 acres, destroy more than 19,000 buildings, and cause $16.5 billion in damages [89]. U.S. fire records reflect how wind makes fire seasons worse: in 2024, which had stronger winds, there were 64,897 fires that burned 8.9 million acres compared to just 2.7 million acres burned by 56,580 fires in the less windy year of 2023. In California, the worst wildfires are usually linked to strong dry winds from the east, like Santa Ana or Diablo winds. A study by USGS of 643 Santa Ana wind events from 1948 to 2018 showed that stronger wind and more fire starts led to much more land being burned. While most Santa Ana days didn't have fires, if one started during those winds, it usually became very large. On average, the number of homes destroyed per year jumped from about 500 (1950–2000) to about 2,700 (2000–2018), mostly because wind-blown embers reached houses at the edge of wildland areas [90], [92]. A recent example is the Pacific Palisades Fire (January 2025), where Santa Ana winds over 100 mph pushed the fire through about 12,000 acres and over 1,000 buildings in a single day, setting a new record for damage in Los Angeles [93]. Past events show the same pattern as the 1991 Oakland/Tunnel Fire, where strong winds destroyed around 3,500 homes and caused $1.5 billion in damage[94]. Another devastating case occurred on October 8, 2017, when wildfires swept through north-central California, burning roughly 250,000 acres near Santa Rosa and Napa [86]. These "Wine Country" fires destroyed about 9,000 structures, caused over $10 billion in insured losses, led to 44 deaths, and exposed millions to harmful smoke. One striking example is the Thomas Fire in 2017, which briefly became the largest wildfire in California's modern history. It was strongly driven by Santa Ana winds, with gusts reaching 60–79 mph (97–127 km/h), allowing the fire to spread rapidly across mountainous terrain and into nearby communities [91], [95]. The 2019 Getty Fire followed a similar path, with winds over 50 mph helping flames jump across fire lines and roads into residential areas [125].

These real-life examples show that strong, dry winds not only help fires grow but often decide whether a small fire turns into a major disaster. These field-scale observations highlight the need for detailed laboratory investigations that can systematically decouple the effects of wind speed, gust duration, and fuel type on ignition metrics. That's why it's important to study wind effects more closely in the lab so we can better understand how wind speed, gust length, and fuel type affect fire starting and fire growth. However, translating field observations to controlled laboratory data remains a challenge. Most existing fire behavior studies in laboratory settings have emphasized steady wind conditions, often overlooking the real-world complexity of wind variability or wind gusts. While steady-state wind tunnels provide reproducible data on flame spread and combustion, they fail to replicate the transient nature of wind gusts observed during extreme fire events. Gusts, characterized by short-term fluctuations in wind speed and direction, can create rapid changes in local oxygen availability and convective heat transfer, directly impacting the thermal environment around potential ignition zones. These unsteady dynamics may play a critical role in determining whether a fire ignites, what form that ignition takes, and how it evolves.

To address this, our study employs a bench-scale wind tunnel capable of generating repeatable wind gusts to simulate conditions similar to those found in gust-prone fire environments. By controlling gust parameters such as peak velocity, duration, and frequency, we aim to create a repeatable experimental platform for analyzing ignition behavior. Our study is motivated by the need to bridge the knowledge gap by focusing on the bench-scale investigation of ignition dynamics under gusty wind conditions. The aim is to isolate and quantify how controlled wind gusts affect ignition time, ignition temperature, and the mode of ignition (e.g., flaming, smoldering, and smoldering-to-flaming transitions) for three different fuel types: prefabricated excelsior, avena (wild oat), and wheatgrass. Understanding these ignition modes is essential, as smoldering can be more difficult to detect and extinguish yet still result in dangerous flare-ups under subsequent gusty conditions. The transition from smoldering to flaming, in particular, is a critical phase that may be strongly influenced by the transient airflow patterns of gusts. Besides ignition behavior this study also aims to investigate the fire spread and heat release rate mechanisms in different wind gusts frequencies.

Chapter 3

Experimental Study on the Ignition Behavior of Wildland Fuels Ignited by Heated Stainless-Steel Particles

Hot metal particles from activities like machining, grinding, and welding are significant ignition sources for wildland fuels. Thus, this study examines the effects of stainless-steel particle geometries and wildland fuel beds on wildfire ignition behavior. To this purpose, experiments have been conducted to investigate the impact of particle type, composition, diameter, number, and wildland fuel bed species on ignition behavior. Three common California wildland grass fuel species were studied: Bromus (Bromus diandrus), Tall Wheatgrass (Thinopyrum ponticum), and Avena Wildoats (Avena fatua). Various stainless-steel grades were tested as ignition particles. The findings from this study support prior research and indicate that increasing the quantity and diameter of ignition particles reduces ignition temperature and affects the type of ignition (flaming, smoldering, or none). This increase in particle size or quantity enhances the area of heat transfer within the fuel bed, leading to faster ignition at lower temperatures. Furthermore, this increase in heat transfer area serves to boost thermal mass though simultaneously increasing heat loss to the surroundings. Moreover, it has been noticed that increasing the carbon content of the steel raises the ignition temperature, likely due to the decrease in thermal conductivity. Consequently, the ability of the metal particles to transfer heat to the surrounding grass decreases, leading to a higher ignition temperature, as it takes longer for the grass to reach its ignition point. Moreover, increasing the carbon content in the metal particles increases their specific heat capacity, enabling them to retain more heat before transferring it to the fuel bed. This heat absorption by the carbon-enriched metal particles contributes to a higher ignition temperature of the surrounding fuel bed. In addition, wildland fuel species influenced ignition type and temperature. This work asserts that species-specific fuel morphology, chemical, and thermal properties affect the flammability of grassy fuels when these are ignited by metal particles and observes that in addition to particle geometry, the chemical properties of ignition particles, such as carbon content, may also play a key role in shaping ignition behavior.

As already mentioned, and explained, the ignition behavior analysis of wildland fuels has been ignored or less explained. So, the aim of this study is to investigate the effect of the properties of stainless-steel ignition particles and wildland fuel beds in shaping ignition behavior. Unique to this study is the examination of stainless-steel particles of different grades corresponding to varying carbon contents and the variations of fuel beds using real wildland fuels. By including wildland fuels, we planned to integrate the effect of physical and chemical composition of fuel species on ignition behavior. To aim the research goal, an experimental setup has been designed to analyze the effects of the heated stainless steel on the fuel bed in the laboratory study which practically portrayed the effects of heated particles generated from the machining works to the natural wildland grasses or forests. The experimental procedures and analysis have been explained below. This work was done without the effects of any other additional influence parameters. So, the work accomplished in no wind condition and avoiding the effects of moisture in the fuels and environment.

3.1 Experimental Methods

3.1.1 Experimental apparatus and procedure

A photograph of the experimental apparatus is shown in Figure 3.1. After preparing the fuel bed the heated metal particles are dropped to the fuel bed to examine the ignition behavior. A steel spoon is used to hold metal particles. The spoon (holder) is 34 cm in length and 8.2 cm in bowl diameter. The metal particles are heated by using a propane torch. The particles are heated for 90 sec for each experiment and dropped from 18-20 cm height in the fuel bed. The heating time is designed to be 90 seconds so that the particles get heated but do not melt to the spoon. If the particles are heated up for more than 90 sec, then it starts breaking and reaches its melting point. Besides, the molten steel particles may stick to the spoon. Thermocouples and the infrared camera (IR) are placed into the fuel bed to measure the ignition temperature during the experiments. Four pairs of K-type thermocouples were attached to the steel pan and were placed on the fuel bed to obtain the initial particle temperature and ignition temperatures of the fuel bed. The initial temperature is the temperature of the heated particles at the time they touch the fuel beds. Data acquisition and recording from thermocouples was conducted through a NI-9425 DAQ system. The IR camera model is FLIR-E5-XT and is used to obtain the fuel temperature at ignition. The IR camera temperature sensor point is positioned to the center of the fuel bed where the particle dropped from the spoon to the fuel bed. A stopwatch is used for measuring the ignition time and later verified with video recording. A digital camera is used for recording experiments.

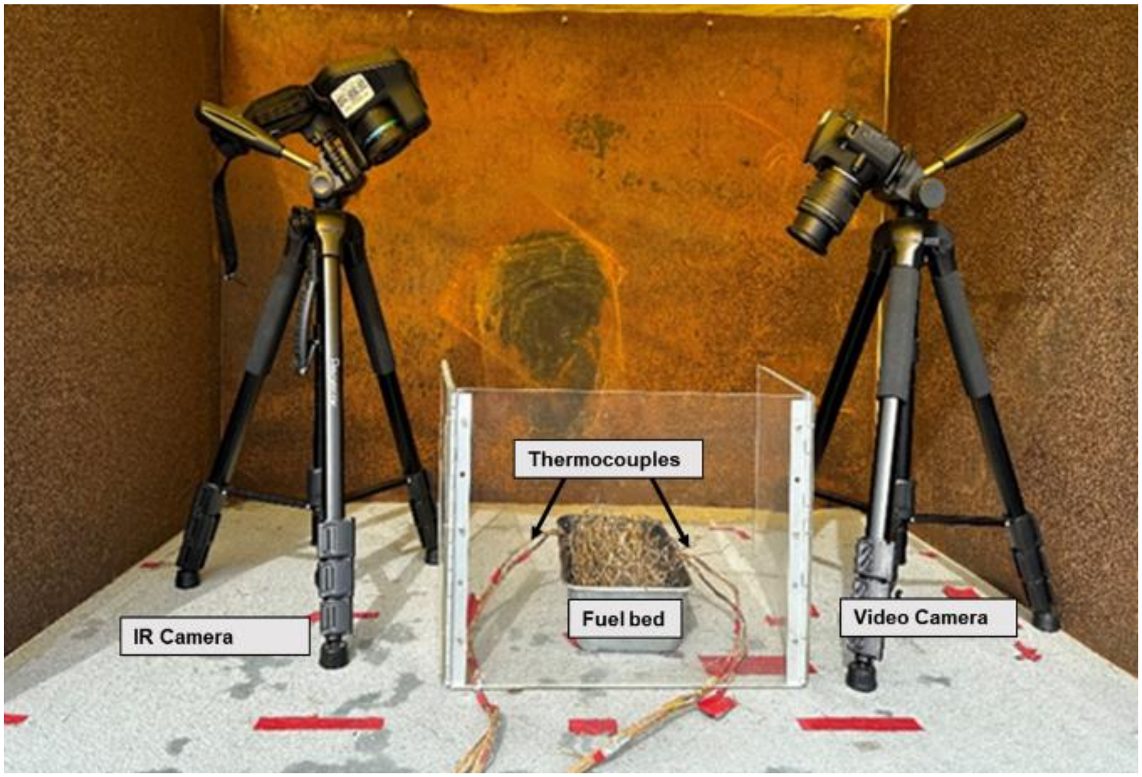

Figure 3.1. Schematic of experimental apparatus and procedure.

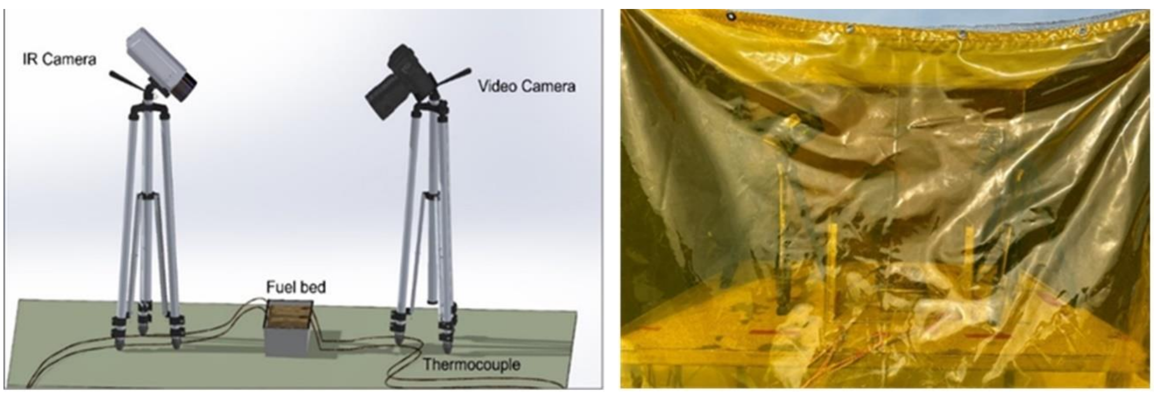

Figure 3.2. Photograph of Experimental setup (left one is without wind protected curtain and the right one is with the wind protected curtain).

This work consists of finding two major queries: the effects of various properties of metal particles on ignition behavior, and the influence of the physical and chemical composition of different wildland fuels on their ignition characteristics. To achieve the objective, the parameters used in the study are presented in the experimental matrix below in Table 3.1. Three types of experimental sets or combinations were conducted, in the first set, only the size and number of heated particles are varied where the type of fuel and particles were constant. In the second set, the type and number of metal particles were varied where size of metal particles and type of fuels are constant. In the third set, the only varied parameter is the type of fuels.

Table 3.1. Experimental Matrix

Fuel	Particles material	Particle size	Number of Particles
Mix Bromus	304 C Stainless Steel	3 mm	10 to 35
Avena Wild Oat	420 C Stainless Steel	4 mm	
Wheatgrass	440 C Stainless Steel	5 mm	

3.1.2 Fuel bed and ignition particle properties

The ignition behavior of wildland fuels is examined in our study using three different fuel types: Bromus (mix of bromus tectorum and bromus diandrus), Wild oat (avena fatua), and Wheatgrass (thinopyrum ponticum). These fuels were chosen for their wide availability and significance to wildfire regions in California. Various wildland fuels are targeted to overcome the difficulties and make a compatible analysis of fuel properties with fuels in forests. The chemical compositions of the different fuels are shown in Table 3.2. The fuels were collected from the UC Merced campus grounds and dried in an oven to control their moisture content. To ensure a lower moisture content, the dried fuels were tested using a moisture analyzer to verify that it is below 3%. For each experiment, 18 g of fuel was evenly distributed in a rectangular steel tray measuring 28.5 cm in length, 14.6 cm in width, and 7.62 cm in height.

Table 3.2. Composition of fuel beds.

Grass Fuel Species	Chemical Composition
Bromus	Protein (8%), Fat (1.5) %, Fiber (31.3%), Lignin (8.4%), Ash (8.1%) [68]
Wild Oat	Protein (15.4%), Fat (6.4) %, Fiber (15.0%), Starch (35.9%), Ash (3.8%), lignin (13-20%) [69]– [71]
Wheatgrass	Protein (25.40), Starch (51.617), Fiber (9.500), Ash (5.200) and Fat (1.740), lignin (20-22%) [72], [73]

The following metals were used for ignition particles, 304 C stainless steel, 440 C stainless steel, 420 C stainless steel. Integrating different grades of stainless steel in the experiments allowed us to examine the effect of carbon content on ignition behavior. The relevant thermal and material properties are shown below in Table 3. We used particles ranging in size from 3-5 mm in diameter and 12-30 in number to study the effect of varying size and number on ignition behavior. The metals used for the ignition particles were 304 C stainless steel, with 15 particles, each having a diameter of 4 mm. In selecting particle size for this study, our starting point was previous studies focusing on investigating the effects of heated particles effects on spot fire ignitions [23][19][14]. The metal particles were employed only once in each experiment, indicating that they were not reused for subsequent tests following each ignition test. The sample size was kept at a minimum of 5 and at a maximum of 12 for each type of configuration. The relevant thermal and material properties are shown below in Table 3.3 (properties taken from matweb (https://www.matweb.com/index.aspx)).

Table 3.3. Properties of materials used in the experiment (taken from [74]).

Material	Yield Tensile Strength (MPa)	Ultimate Tensile Strength (MPa)	Brinell Hardness	Carbon content (%)	Melting range (°C)	Specific Heat capacity (J/kgK)	Thermal conductivity (W/mK)
440 C SS	445	745	285	1-1.2	1483	460	24.2
420 C SS	345	345	241	0.42-0.50	1454-1510	460	24.9
304 C SS	215	215	123	≤ .08	1400-1420	500	21.5

3.1.3 Ignition behavior analysis protocol

The metrics of ignition behavior used in this study are the type of ignition (flaming or smoldering), ignition temperature, and time to ignition. The criteria used to determine the success of an ignition were as follows: for flaming ignitions, a successful ignition was defined as a flame igniting the fuel and remaining for at least 10 seconds; for smoldering ignitions, a successful ignition was determined visually by the ignition of fuels in the smoldering regime, with the smolder spread lasting for more than 15 seconds. The waiting time for successful ignition is longer in cases of smoldering ignition due to the extended time required for smoldering ignition compared to flaming ignition. If no ignition was observed during a five-minute period with undisturbed fuels, the experiment was classified as 'no ignition' and considered unsuccessful. Ignition time was measured by analyzing experiment videos, with the initial time (t = 0) set at the moment when the heated particles first made contact with the fuel bed. The ignition time (t = ignition time) was designated as the time when ignition was first observed. K-type thermocouples and an infrared camera were employed for the purpose of measuring the ignition temperature. The thermocouples were placed in pairs within the fuel bed, with a total of four pairs positioned. Four sets of thermocouple pairs have been positioned within the fuel bed, with each individual pair containing two thermocouples. The thermocouples are positioned at the center of the fuel bed, as heated particles are introduced to the central area. This allows us to utilize the thermocouple temperatures for assessing the ignition temperatures of the fuel beds. The IR camera continuously captured the temperatures of the centrally heated area, which were considered as the ignition temperature, and they have been used to verify the ignition temperatures obtained from the thermocouples. To ensure reliable results and minimize the effects of uncontrolled parameters on the experiments, at least five tests were conducted for each material at a specific diameter and number of particles. Common uncontrolled parameters included variations in the placement of heated particles, scattering particles upon falling into the bed, unexpected penetration into the fuel bed, and direct sinking of particles to the bed bottom. By conducting multiple tests and accounting for these factors, the researchers aimed to achieve a comprehensive quantitative analysis and reduce the impact of uncontrollable variables.

3.2 Results and Discussions

The study conducted two sets of experiments to examine the effect of fuel species and the impact of carbon content in heated metal particles on ignition behavior. The first set of experiments focused on investigating the influence of fuel species across various ignition particle sizes and quantities. The second set aimed to understand how the variation in carbon content of heated metal particles affects the ignition behavior of fuel species. To explore this, various kinds of stainless steel with differing carbon content were utilized as ignition sources during the experiments. Representative results are presented in the following section in Figure and Figure . Afterward, detailed results and analysis for the two sets of experiments are presented.

3.2.1 Representative Results

Representative results from flaming and smoldering experiments including ignition temperature curves, IR and visual images are presented in Figure 3.3 and Figure 3.4, respectively. The individual frames from the video and IR camera recordings are processed separately to extract relevant information concerning the drop point, ignition point time, and temperature. Thermocouples have been placed on the fuel bed in such a way that they lie at the point where particles were dropped to obtain the ignition temperature. The obtained ignition temperature has been verified with the IR camera's temperature readings to ensure accuracy. The representative figures (Figure and Figure 3.4) show the details of temperature reading during the drooping time of metal particles and ignition time obtained from thermocouple and IR video camera. In the representative figure, the thermocouple temperatures during the drop time are much lower because it is positioned within the fuel bed and presents the fuel bed temperature while the particles are dropped. In contrast, the drop temperature captured by the IR camera is significantly higher, as it targets the hot spot during the drop time and accounts for the temperatures of heated metal particles.

Figure 3.3 presents the flaming ignition temperatures when 304 C stainless steels as ignition particles on bromus fuel beds. In the experiment presented, 24 particles with a diameter of 3 mm were used. In Figure 3.3, the drop point is recorded at 114.5 seconds, and the ignition point occurs at 115.2 seconds. By examining the thermocouple data, it was observed that ignition time had a lag for nearly 10 seconds compared to the time captured in the video and IR images which is the preheat delay time for thermocouples. The 10-second lag observed in the thermocouple data indicates the time it takes for the thermocouples to reach steady-state conditions after the heated particles drop onto the fuel bed. When the particles initially make contact, the thermocouples, which are at atmospheric temperature, require this time to accurately measure the rise in temperature due to the ignition. This delay is expected due to the thermocouples' response time, which was determined through calibration and assessment. It does not necessarily indicate that the thermocouples are too large or improperly placed but rather reflects the inherent response time of the sensors to stabilize at the new temperature conditions. The results indicate that both the IR camera and the thermocouple detected ignition temperatures at approximately 322°C. The trend of flaming ignition demonstrates that it occurs in all cases within seconds of dropping the heated particles.

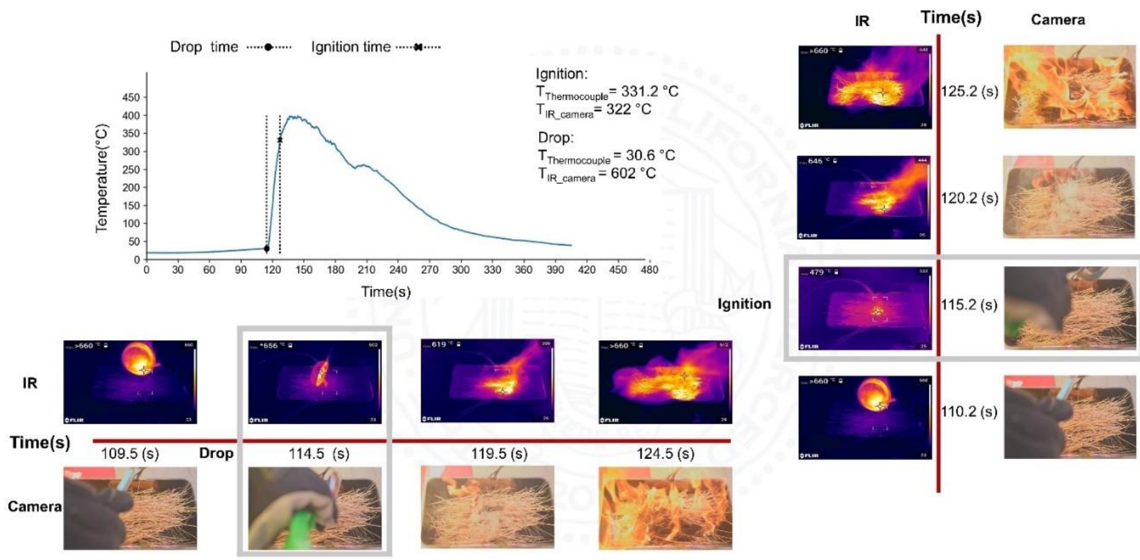

Figure 3.3. The estimated flaming ignition temperature over time. In the figure $T_{Thermocouple}$ and $T_{IR\ Camera}$ represent the temperatures obtained from the thermocouple and IR video, respectively. The experiment was conducted on bromus fuel using 3mm diameter, 24 number of 304 stainless steel heated metal particles.

Figure 3.4 presents the smoldering ignition temperatures for wheatgrass fuel using 12 of 304 C stainless steel 3mm particles. In Figure 3.4, the drop point is recorded at 127 seconds, and the ignition point occurs at 147 seconds. The results indicate that both the IR camera and the thermocouple detected ignition temperatures at approximately 161°C. The smoldering ignition trend indicates that, in all cases, the ignition temperature is lower than the flaming ignition temperatures. Furthermore, smoldering ignition consistently occurs a few seconds after dropping the heated particles onto the fuel bed, which takes longer compared to flaming cases.

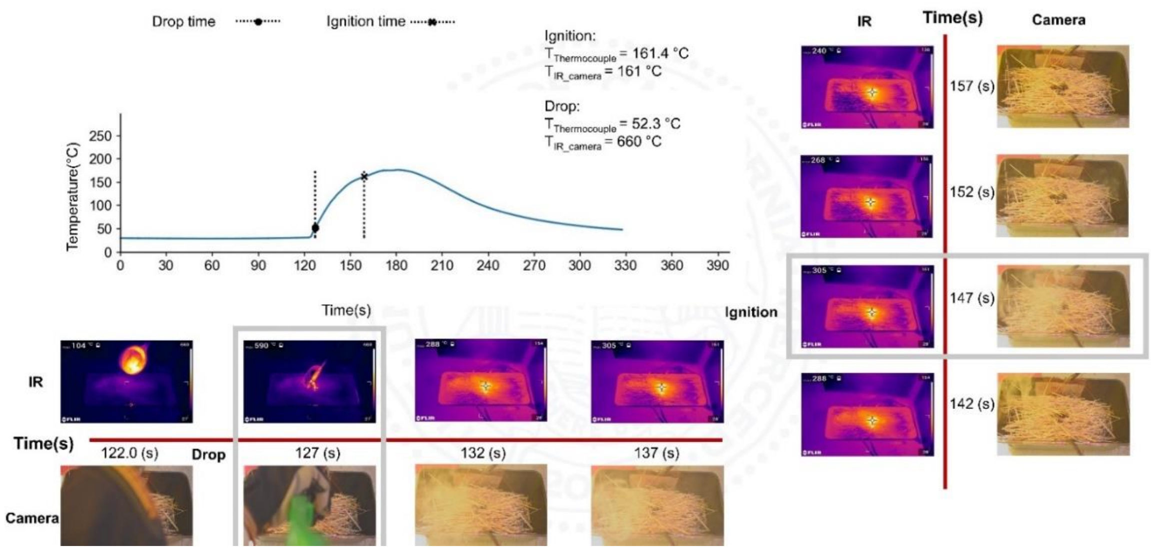

Figure 3.4. The estimated smoldering ignition temperature over time. On the figure $T_{Thermocouple}$ and T_{IR_camera} represent the temperatures obtained from the thermocouple and IR video, respectively. The experiment was conducted on wheatgrass fuel using 3mm diameter, 12 number of 304 stainless steel heated metal particles.

3.2.2 Effects of metal particle and fuel bed properties on ignition

To examine the effect of particle size on the ignition behavior in each of the fuel species examined in this study, we first focused on varying the ignition particle diameter. The particle diameters tested were 3 mm, 4 mm and 5 mm of metal spheres. For all particle diameters considered, the number of particles remained constant for each type of ignition tested. For flaming ignitions, 24 particles were selected since this was the smallest number that led to a flaming ignition. For smoldering ignitions, 18 particles were selected as this was the smallest number that led to the maximum number of smoldering ignitions for all kinds of fuels.

Results from experiments testing the potential of particles of various sizes to ignite each of the fuel species considered are presented in Figure . There, it can be seen that the ignition temperature decreased linearly with increasing particle diameter for flaming ignitions. To illustrate this trend, we summarize our observations for one particular case, ignitions of Bromus fuel beds using 304 stainless steels (see Figure 3.5 a) where ignition temperature averages at 336°C for 3 mm particles, dropping to 317°C for 4 mm particles, and further to 277°C for 5 mm particles. Similarly, in avena and wheatgrass fuel beds, the experiments consistently exhibit a similar trend of decreasing ignition temperature with increasing particle sizes. The trend was also observed for smoldering ignition cases, which has been followed by 3 mm of 18 particles of 304 C and 420 C stainless steel particles. Only flaming ignition was observed for the 18 particles with the other diameters, and as a result, smoldering ignition cases could not be presented. Next, regardless of the particle size or particle number considered, wheatgrass fuel beds always ignited at the highest temperature followed by avena then bromus fuel beds. Similarly, wheatgrass fuels exhibited the highest ignition temperature trend compared to avena and bromus fuels while varying the number of ignition particles. A discussion of this result is provided later in this section.

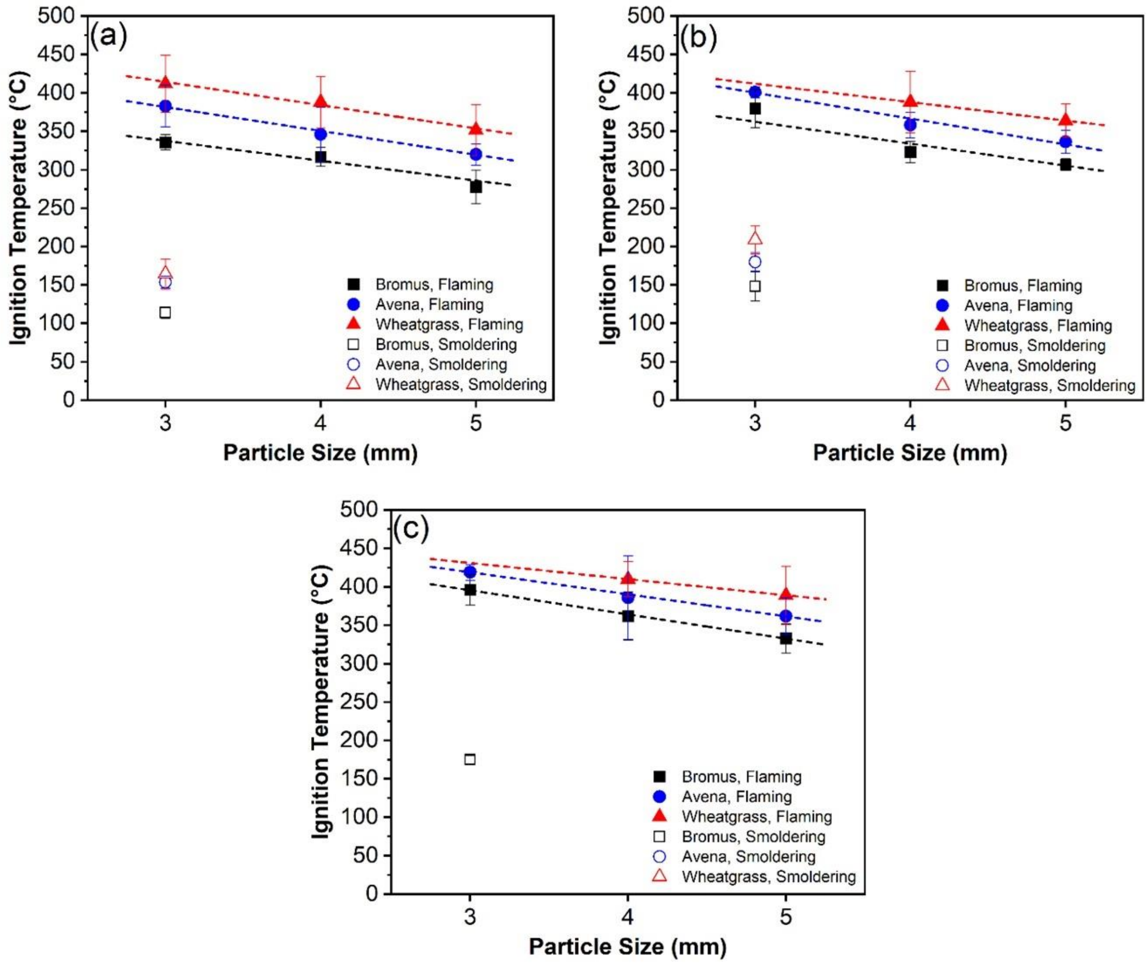

Figure 3.5. Flaming and smoldering ignition temperature by using 24 number and 18 number of heated metal particles respectively for (a) 304 c (b) 420 c and (c) 440 c stainless steel (from left to right).

As previously stated, the experiments explored both the influence of heated particle size and number of ignition particles. The number of particles used as ignition sources varied from 12 to 30 particles. The particle diameter was maintained at a constant 3 mm. This number was chosen since it resulted in the maximum number of smoldering ignitions for all particle types, enabling us to compare the results across particle types. The results are presented in Figure 3.6.

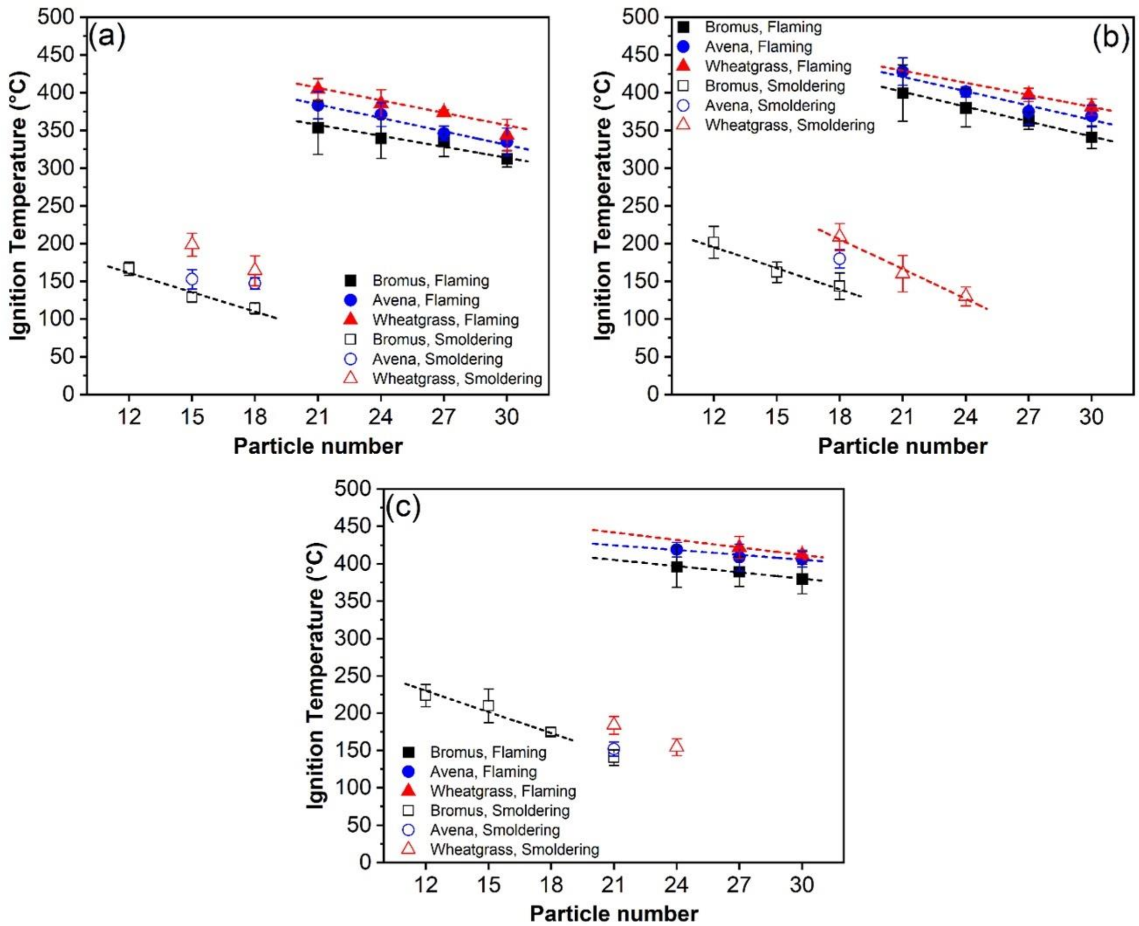

Figure 3.6. Flaming and smoldering ignition temperature for (a) 304 c (b) 420 c and (c) 440 c stainless steel (from left to right). Ignition particles for all experiments had a diameter of 3mm.

The trend of flaming and smoldering ignition behavior is depicted in Figure 3.6, showing that the ignition temperature decreases with an increasing number of particles for both types of ignition cases. To illustrate this trend we describe one case, ignitions of bromus fuel beds using 304 C stainless steel particles (Figure 3.6 a). There it can be observed that in bromus fuel beds, ignition occurred at an average temperature of 353.6°C with 24 particles. Using 24 particles lowered the ignition temperature to 339.8°C and increasing to 30 particles further reduced it to 312°C. Similar trend has been observed for the avena and wheatgrass fuel experiment results. Figure 3.6 demonstrates that it follows a similar relationship between the fuel species as follows in Figure . Wheatgrass fuel beds always ignited at the highest temperature followed by avena then bromus fuel beds, which exhibited the lowest ignition temperature. The smoldering ignition temperature threshold is 100 ± 17°C for bromus fuels, whereas the threshold is 150 ± 25°C for avena and wheatgrass fuels. The smoldering ignition temperature thresholds of wheatgrass and avena differ from bromus grass likely due to their distinct physical and chemical characteristics. Thus, our results point to a relationship between wildland fuel species and ignition behavior. We argue that this relationship is likely governed by the chemical and physical properties of the fuels. Specifically, lignin has been found to affect ignition behavior in a variety of biomass fuels. For example, Urban et al observed that biomass fuels containing ligno-cellulosic materials required higher ignition temperatures than fuels lacking this component [24]. Our findings align with this trend: wildland fuels with higher lignin and protein content ignited at higher temperatures. For instance, wheatgrass, which exhibited the highest ignition temperature across all experiments, contains the greatest amount of lignin (20% – 22%) and protein (25.40%). This is followed by Avena (wild oats), which had the second-highest lignin content (13% – 20%) and protein content (15.4%). Bromus fuels supported ignition at the lowest temperature and contained the lowest lignin content (8.4%) and protein content (8%). Similar trends were reported by Wang et al. and Yan et al. who observed that biomass and feedstock ignition behavior was primarily affected by lignin content rather than other chemical components like cellulose, hemicellulose, and carbohydrates [107], [126], [127]. In their work, the peak temperatures were always higher during lignin combustion than cellulose or hemicellulose combustion. These findings are further supported by studies on natural fibers[128], [129]. Overall, the mechanisms governing the lignin effect on ignition behavior are likely related to the fact that lignin contributes to a higher thick-walled char yield in the biomass cell, which leads to higher activation energy requirements for combustion. Here, the activation energy refers to the energy required for the initiation of the pyrolysis process [105]. In our study, the higher activation energy needs translated to higher ignition temperature requirements. Besides lignin content, protein also has been shown to have a significant effect on the pyrolysis process. For instance, studies have shown that higher activation energy is required for the combustion process for protein compared to other components like carbohydrates [126].

3.2.3 Effects of particle properties and carbon content on ignition

To examine the effect of stainless-steel grade corresponding to various amounts of carbon content, three types of metal particles have been considered, varying the carbon content from 0.08% to 0.1% (Table 3.3). As can be seen from Figure 3.7, 304 C stainless steel carries the lowest amount of carbon content, and 440 C stainless steel carries the highest.

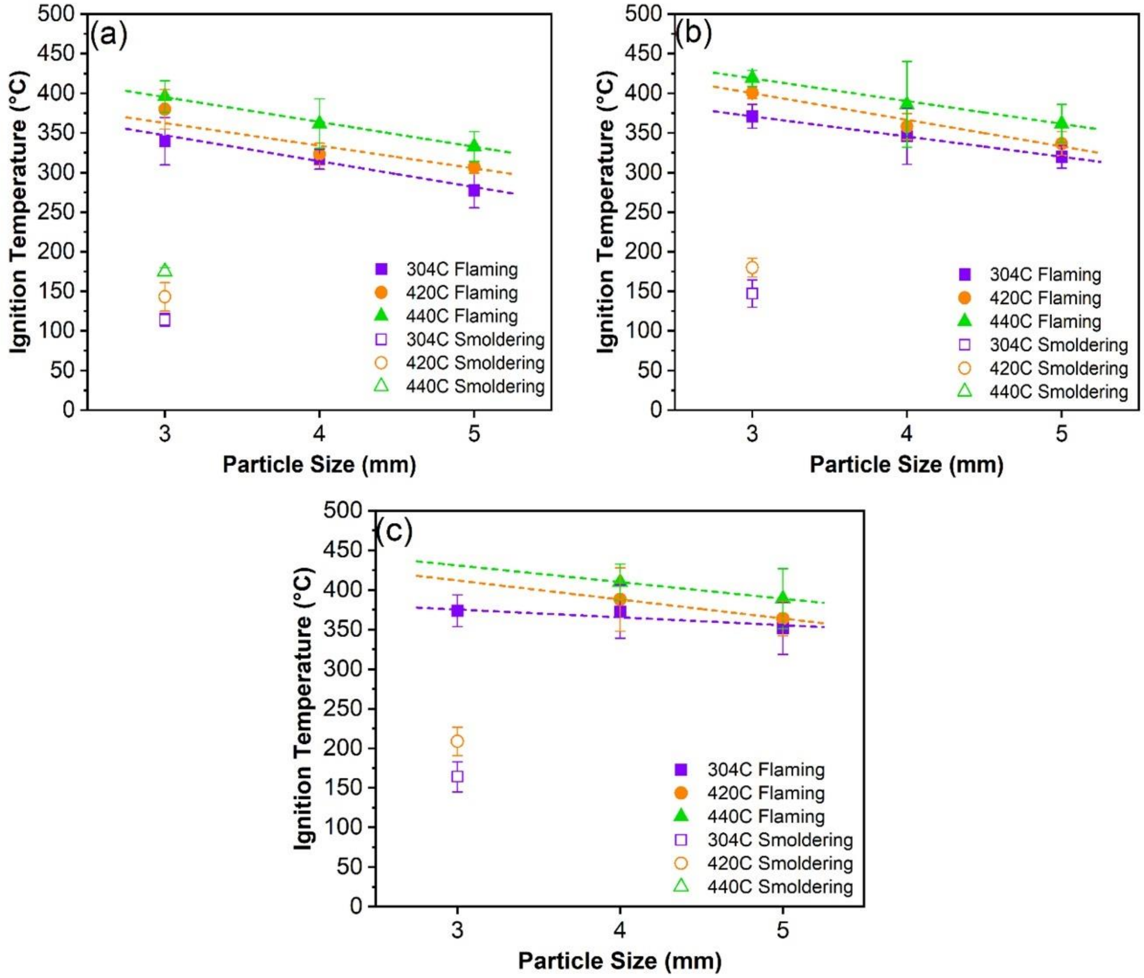

Figure 3.7. Flaming and smoldering ignition temperature using 24 and 18 number of metal particles respectively for (a) bromus (b) avena and (c) wheatgrass fuels (from left to right).

Focusing on results presented in Figure , it is shown that using 18 and 24 numbers of 3 mm metal particles, the 304 C stainless steel always ignites at lower temperatures compared to 420 C and 440 C stainless steel heated particles. While undergoing flaming ignition, the 3 mm particles consisting of 24 of 304 c stainless steel ignite bromus fuel at an average ignition temperature of 339.8°C, rising to 380.6°C for 420 C stainless steel particles, and further to 396.4°C for 440 C stainless steel particles. Similarly, in avena and wheatgrass fuel beds, the experiments consistently exhibit a similar trend of increasing the ignition temperature with increasing the amount of carbon content in heated metal particles (Figure 3.7 b-Figure c).

Furthermore, the effect of metal particle properties like carbon content in the ignition behavior was also analyzed. It has been observed that variation of carbon content in the heated metal particles affect the ignition temperature during the ignition mechanism. While comparing the smoldering ignition temperatures for 3 mm of 12 metal particles it has been shown that on average 304 C stainless steel ignites at lower temperature (167°C) compared to the 420 C (202°C) and 440 C (224°C) stainless steel. Moving on from smoldering to flaming ignition, for all the numbers from 24 to 30 metal particles, 440 C always exhibits ignition at higher temperatures compared to 420 C sand 304 C stainless steel. For 21 particles, 440 C stainless steel never shows flaming ignition for any kind of fuel (Figure 3.8). The flaming ignition for 440 C stainless steel starts with 24 particles in bromus and avena fuels and requires at least 27 particles to achieve flaming in wheatgrass fuels. In contrast, 304 C stainless steel shows flaming ignitions for all types of fuels with only 21 particles.

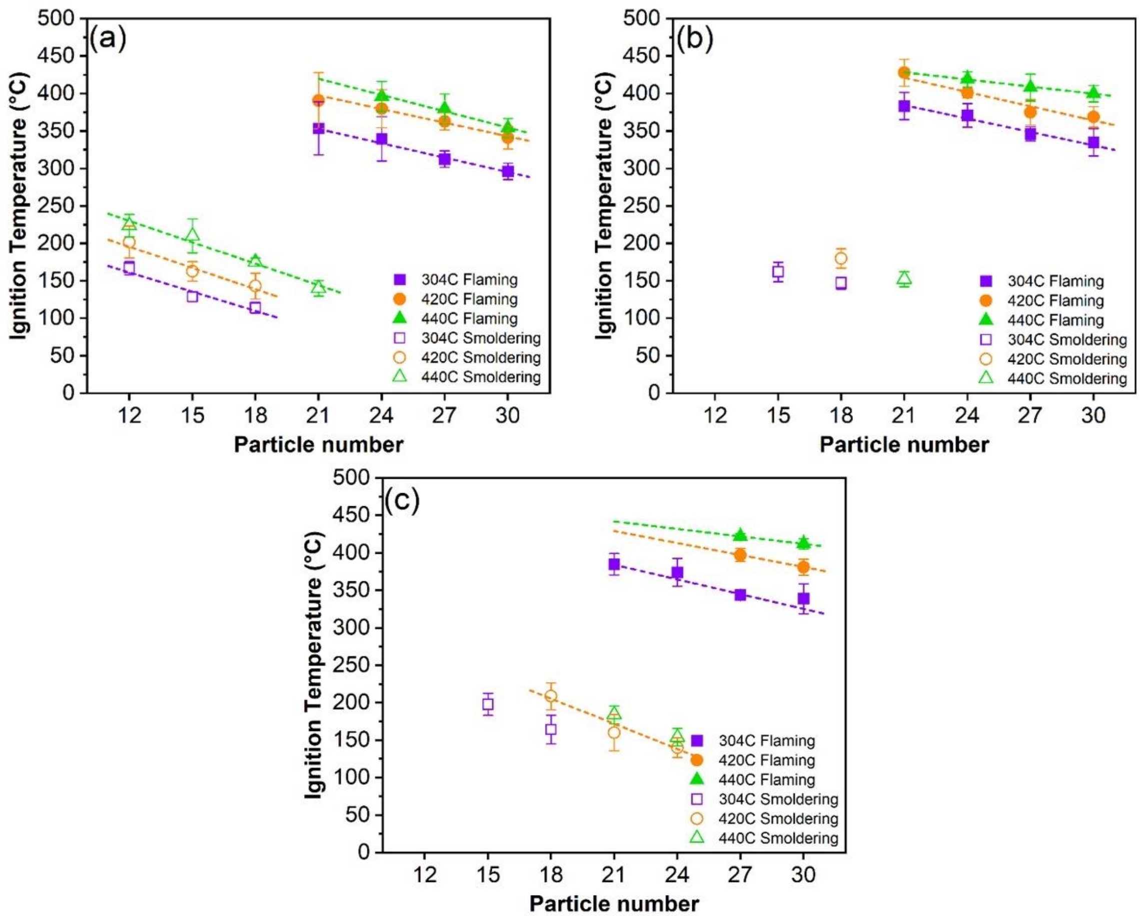

Figure 3.8. Flaming and smoldering ignition temperature using 3 mm of metal particles for (a) bromus (b) avena and (c) wheatgrass fuel beds (from left to right).

Thus, our results indicate a relationship between the size, number, and type of heated metal particles, and ignition behavior for all experimental configurations. Regarding particle sizes and quantities, some details are presented in Figures (3.5–3.8). All the results can be summarized as follows: increasing the size and quantity of heated metal particles decreases the ignition temperature. This increase in particle size or quantity enhances the area of heat transfer within the fuel bed, leading to faster ignition at lower temperatures. Furthermore, this increase in heat transfer area serves to boost thermal mass while simultaneously increasing heat loss to the surroundings.

Furthermore, in this work, three types of heated metal particles corresponding to varying grades of stainless steel were used, 440 C, 420 C, and 304 C. The stainless-steel grades differed in their material and thermal properties which we argue led to alterations to their behavior as ignition sources. For instance, 440 C and 420 C stainless steel consistently exhibited higher temperatures at ignition than 304 C. This can be explained by the higher thermal conductivity of 440C and 420 C, which likely resulted in a decrease in thermal flux to the fuel bed. However, it is difficult to explain the observed trends based solely on thermal conductivity. For instance, 440 C has a marginally lower thermal conductivity than 420 C stainless steel, yet it consistently requires higher temperatures to ignite fuel beds. Therefore, it is worthwhile to consider additional material properties in the analysis. Among the various properties, carbon content is the feature that best aligns with the observed trend in ignition temperature behavior. That is, the metal with the highest carbon content, 420 C, required the highest temperature to ignite the fuel beds, whereas the metal with the lowest carbon content, 304 C, required the lowest temperature. Therefore, the answer to the original question posed at the onset of this work, "How does carbon content affect ignition behavior?" is that, in our study, metals with higher carbon content required higher temperatures to reach ignition of the fuel beds than metals with lower contents. Thus, carbon content increased the temperature at ignition. These results are promising, as prior works have argued that carbon content may alter thermal properties in stainless steel. We caution, however, that greater study is required to understand the mechanisms causing this behavior. This is because although some have found that carbon content can alter the thermal behavior of stainless steel by way of changes to thermal conductivity, this trend was indeed not consistent with our results, as thermal conductivity was not directly correlated to the carbon content [108]. Furthermore, careful examination of other components of stainless steel could provide important insights. Thus, future studies could focus on isolating the effects of carbon and other components on the thermal properties of stainless steel and work to connect these to these metals' behavior as an ignition source. In this regard, results from the current study could therefore serve as valuable input data for modeling studies focusing on such analysis.

3.3 Summary

This study investigated the effect of fuel bed species and ignition particle characteristics on fuel bed ignition behavior. To understand ignition trends in wildland fuels, fuel beds were constructed from grass species commonly found in California: bromus, avena, and wheatgrass. The results showed that wheatgrass fuels required higher temperatures to ignite than avena and bromus fuel beds. We hypothesize that this is due to the higher amount of lignin and protein content in wheatgrass and avena fuels. This is because lignin content may deter ignition by increasing the activation energy required for pyrolysis during ignition. Additionally, consistent with previous studies, thicker fuels exhibited higher ignition temperatures. Among the three fuels, wheatgrass stands out as the thickest, followed by avena and bromus.

In addition to evaluating various fuel bed properties, the study investigated the impact of metal particles on ignition behavior. To answer the first research question, we posed: "How do the size and number of hot metal particles affect the ignition behavior (ignition temperature and time) of wildland fuels?" To answer this question, we observe that our results aligned with similar research on the ignition of fuels by hot metal particles, in that we found that larger particles could initiate ignition at lower temperatures, while smaller particles necessitate higher temperatures to produce ignition. In addition, the study explained the effects of ignition particle composition on ignition temperature. The results showed that 304 C stainless steel metal particles ignited fuel beds at lower temperatures, likely due to their lower thermal conductivity compared to other metal particles. Furthermore, although in our evaluation of one of the research questions posed in this study: "How does carbon content affect ignition behavior?" our results seem to indicate a correlation between higher carbon content and higher temperatures at ignition, we argue that further work is required to establish the mechanisms through which carbon influences the ignition behavior. Overall, results from this study can contribute to a greater fundamental understanding of the mechanisms leading to successful ignitions of wildland fuels by heated metal particles and the development of safer machining operations near the wildland. Future work will examine ignition behavior under wind-driven conditions and the effect of fuel bulk density on ignition trends. Additionally, we suggest that future studies could integrate results from our experimental findings in numerical modeling simulations using the Fire Dynamics Simulator (FDS) to better understand the ignition process. This modeling approach will allow us to simulate various scenarios and conditions, providing deeper insights into the underlying mechanisms governing ignition phenomena. Moreover, integrating numerical simulations will enable us to explore complex interactions and dynamics that may not be fully captured through experimental methods alone.

Acknowledgement

I thank Cobian-Iñiguez Fire Lab for their support in the research work. My special thanks go to the undergraduate students - Nicholas Maldonado, *Arturo Juarez, Arturo Baza, Jovannie Ruiz, Jazmin Claros, and Brian Arroyo - for their invaluable assistance in conducting experiments. This research is supported through startup funding from the University of California, Merced, School of Engineering.*

Chapter 4

Experimental Study on the Ignition Behavior of Wildland Fuels Ignited by Heated Stainless-Steel Particles

Grassy vegetation represents a significant fuel source in multiple fire-prone regions around the globe. These fuels are a major component of surface fuel beds and are therefore typically the first layer of the wildland fuel strata that ignites. Thus, understanding the drivers of successful grassy fuel ignition is key to developing a comprehensive description of the process leading to fire spread. In the wildland-urban interface, hot metal particles produced by powerline failures or mechanical equipment operations are a leading ignition source for these types of fuels. After hot metal particles are deposited onto the fuel beds, the ignition and spread behavior largely depend on the properties of the fuels. These properties determine whether ignitions will minimum, result in weak and short-lived combustion, or lead to intense, sustained fire spread with significant impact. The goal of this study is to develop improved understanding of the role of fuel species and physical characteristics on the ignition behavior of grass fuels when exposed to hot metal particles. Three common California wildland grass species and one prefabricated excelsior fuels were studied in their natural configuration as well as in configurations in which fuel particles have been shredded or made into a powder. Overall, it was observed that the ignition temperature was lower in fuels in their powder form than fuels in a shredded or natural form. Furthermore, the findings here align with prior works, indicating that the presence of chemical compounds such as lignin and proteins may hinder ignition. Additionally, to support the ignition behavior analysis, thermogravimetric (TG) testing has been added to the analysis.

4.1 Materials and methods

4.1.1 Experimental apparatus and procedure

The experiments were conducted in a bench-scale wind tunnel, with the setup shown in Figure 4.1. A wind speed of 1.6 m/s was used, identified as optimal for producing flaming ignitions across all fuel types. The wind temperature was maintained at 60.5 ± 10°C, using a controller connected to the wind tunnel's electric heater. The fan was positioned on the left side of the wind tunnel.

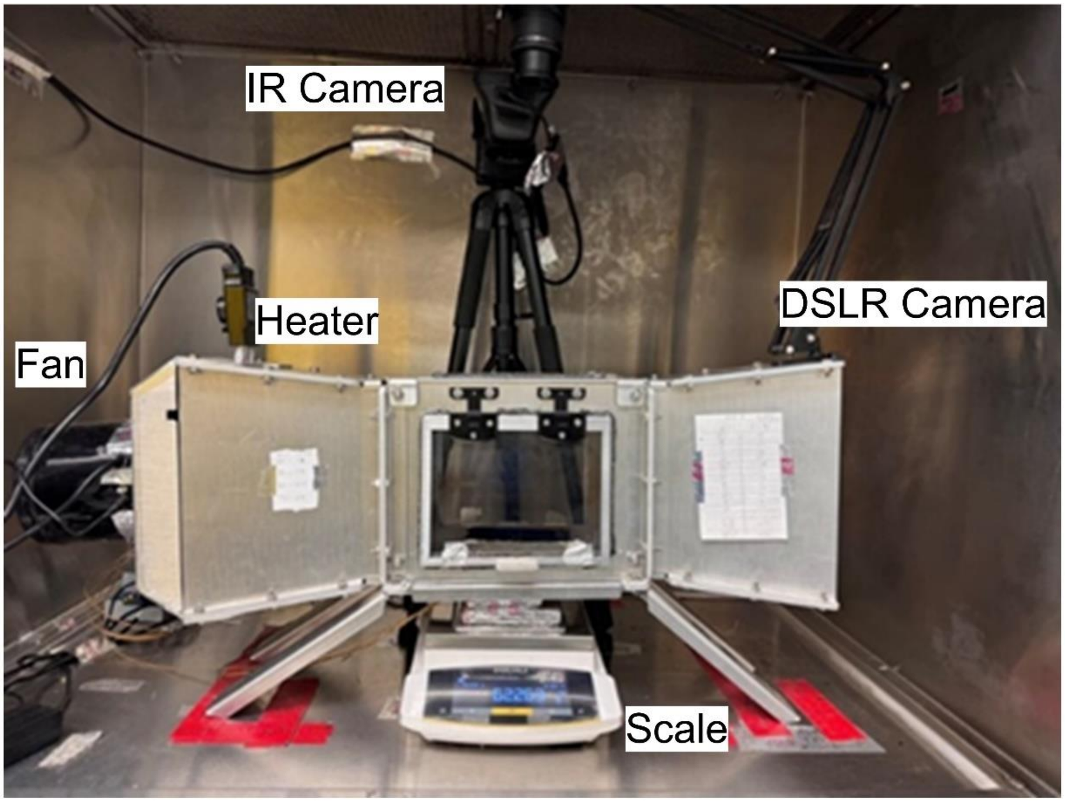

Figure. 4.1 Photograph of experimental apparatus and procedure

An aluminum tray, measuring 17.78 cm in length, 10.16 cm in width, and 7.62 cm in height, was used as the fuel bed, with a scale underneath to measure mass loss during the experiments. A DSLR and an infrared camera, on a nearby table, recorded the process. The tray, made in the lab from an aluminum sheet, had one side covered with a net to ensure proper airflow. Further details of the setup are shown in Figure 4.2.

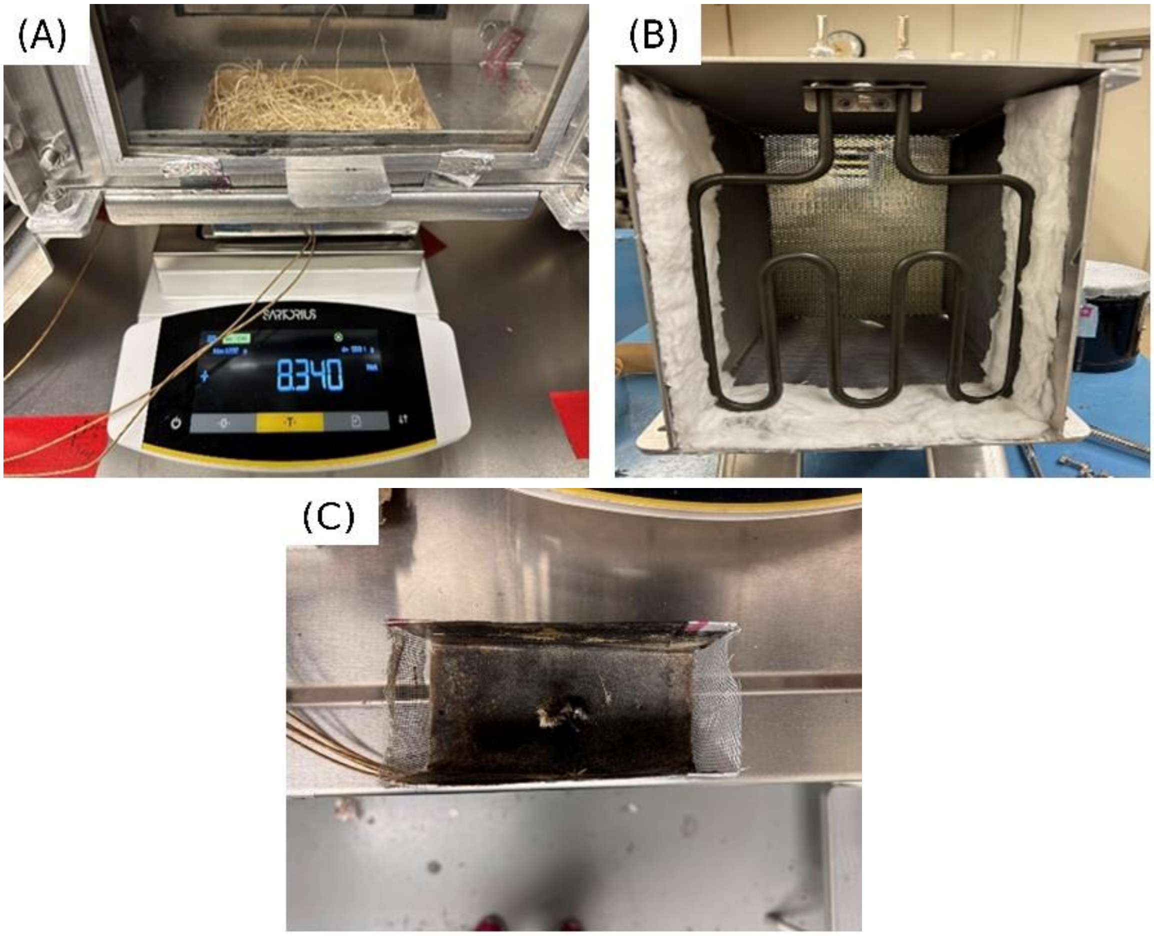

Figure. 4.2 Photographs of additional experimental apparatus from left (a) setup of fuel tray, (b) heated element placement inside the wind tunnel, (c) use of perforated mesh on the fuel tray.

For preparing the fuel beds, three Californian wildland fuel named bromus *(Bromus tectorum),* avena (*Avena fatua*), and wheatgrass (*Thinopyrum ponticum*) -and one prefabricated fuel, excelsior (Aspen wood), were used. All the fuels were prepared in three different structures in this study, as shown in Figure 4.3. The three different morphologies studied were: (a) powdered structure, (b) shredded structure, and (c) natural structure. The powdered structure was created by blending the natural fuels until they formed a fine powder. The shredded structure consisted of fuel cut into pieces measuring between 6 and 6.5 cm. The natural structure referred to uncut fuels, kept in large pieces and only trimmed as necessary to fit into the fuel bed tray.

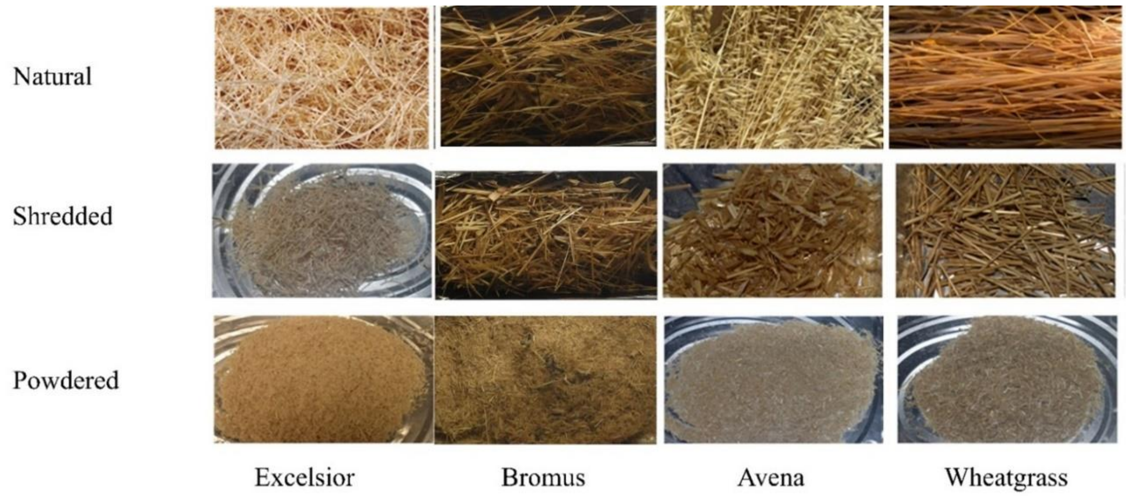

Figure. 4.3 Photographs of the fuels tested

The chemical compositions of the different fuels are shown in Table 3.1. The fuels were dried in an oven at 90 °C for 24 hours to control their moisture content. To ensure a lower moisture content, the dried fuels were tested using a moisture analyzer, to verify that the moisture content was below 3%. For each experiment, 10 grams of fuel were evenly distributed in the fuel bed steel tray. In this study, we focused on standardizing the mass of fuel, rather than the bulk density. This approach allows us to consistently control the amount of fuel used in each experiment.

After preparing the fuel bed, 304 C stainless steel spherical particles were heated with a propane torch for 90 seconds and dropped from a height of 5-10 cm to examine ignition behavior. The particles were held with a steel spoon, measuring 34 cm in length and 8.2 cm in bowl diameter. Heating time was carefully timed to prevent the particles from breaking or melting. A stopwatch and video recording were used to verify the heating and ignition times.

Four K-type thermocouples (18-gauge, 0.1 cm diameter) with fiberglass insulation were placed at the center of the fuel bed to measure initial particle and ignition temperatures. The photograph in Figure 4.4 (A) shows the thermocouple arrangement within the fuel bed. Thermocouple were placed in the middle of the tray since the heated particles were always dropped in the center of the steel tray. The thermocouples were positioned to directly contact the fuel bed where the heated particles were dropped, with the heads facing upwards to ensure accurate temperature readings (shown in Figure 4.4 (A) and (B)). Data from the thermocouples were collected using an NI-9425 DAQ system.

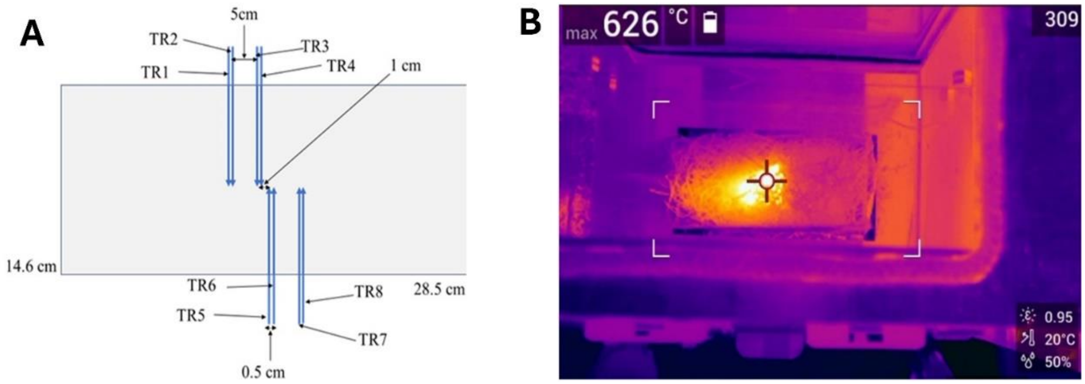

Figure. 4.4 (A) Thermocouple setup details inside the fuel bed, (B) IR Camera details on measuring the ignition temperatures.

An infrared (IR) camera (FLIR-E5-XT) was positioned above the fuel bed to measure temperatures at the center. Thermocouple readings were cross-referenced with IR temperature measurements. The IR camera settings were adjusted according to the camera manual and relevant studies, including a relative humidity of 50%, a distance of 1 meter, an ambient temperature of 20°C, and an emissivity reading of 0.95. The temperature range for the IR camera was set between 20°C and 660°C. Despite the varying emissivities of components in the fire environment, a constant emissivity was assumed for temperature calculations, as the IR camera tracks a specific isotherm, minimizing emissivity variation effects [130], [131]. The camera provided two types of temperature readings: a spatial reading of surface temperature and a point measurement. In this study, the point measurement focused on the center of the fuel bed where ignition occurred, approximating the ignition temperature and serving as a cross-reference for thermocouple-derived temperatures. Figure 4.4 shows a sample IR temperature reading, with the maximum surface temperature on the left and the point temperature on the upper right.

Initial particle temperatures, referred to as the "initial temperature" throughout this paper, were recorded just before the heated particles contacted the fuel beds, after 90 seconds of heating. Because all experiments used consistent heating duration and heat flux, particle temperatures were nearly uniform. These temperatures were measured using an infrared (IR) camera, capturing readings just before the particles were dropped into the fuel bed to avoid radiative cooling during transfer. The spoon holding the particles was also heated to prevent cooling from conduction and radiation. Average initial temperatures ranged between 620°C and 650°C, with a standard deviation of 15–35°C across particle sizes. Figure 4.5 presents an IR photograph with the temperature reading of the heated particles in the upper left corner, highlighting the maximum temperature observed. The ignition temperature was recorded during the transition from smoldering to flaming, and the ignition time was marked by this transition, which was measured using a stopwatch and verified with video recordings. A digital camera was used to document the experiments. In some experiments, significant particle scattering occurred due to human error during the drop, causing particles to land outside the fuel bed center, where temperature measurements were taken. Since thermocouples and the IR camera were centered on the fuel bed, data from these scattered drops were incomplete. As a result, experiments with particle scattering were considered outliers and excluded from the dataset.

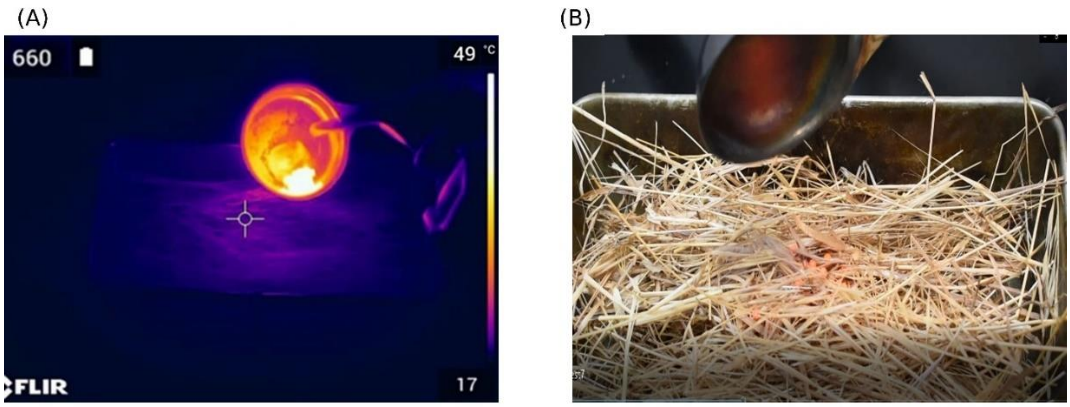

Figure. 4.5 Photograph of the experimental procedure, from left (A) showing particle heating with a propane torch - captured with an IR camera and (B) the moment of particle drops onto the fuel bed - captured with a DSLR camera.

4.1.2 Experimental Matrix

The parameters used in the study are presented in the experimental matrix below in Table 4.1. The sample size was kept at a minimum of 5 and at a maximum of 12 for each type of configuration. The metals used for the ignition particles were 304 C stainless steel, with 15 particles, each having a diameter of 4 mm. In selecting particle size for this study, our starting point was previous studies focusing on investigating the effects of heated particles effects on spot fire ignitions [22], [24], [47]. Therefore, using sizes within the range previously used, we chose 4 mm, which was helpful to replicate results from previous studies and represent real-world conditions of particle sizes produced during hot work. The relevant thermal and material properties are shown below in Table 3.3 (properties taken from matweb (https://www.matweb.com/index.aspx)).

Table 4.1. Experimental Matrix

Metal Particle	Fuel	Fuel Structure
304 C Stainless Steel, 4mm of 15 particles	Excelsior	Powdered, Shredded, Natural structure.
	Bromus	Powdered, Shredded, Natural structure.

	Avena Wild Oat	Powdered, Shredded, Natural structure.
	Wheatgrass Fuels	Powdered, Shredded, Natural structure.

4.1.3 Ignition behavior analysis protocol

The metrics of ignition behavior used in this study were the type of ignition (flaming, smoldering to flaming transition or smoldering), ignition temperature, and ignition time, total burn out time. The criteria for determining successful ignition were as follows: a flame ignition was considered successful if the flame remained active for at least 10 seconds, while smoldering ignition was defined as sustained smoldering for a minimum of 30 seconds. Flaming ignition occurs more quickly because it is highly visible and takes place at a higher temperature. In contrast, smoldering ignition required a longer observation period, typically 10–15 seconds for the formation of a char layer or glowing particles. Smoldering was confirmed when flameless fire spread was observed, with a visible char layer or glowing sustained for at least 30 seconds. The ignition determination approach was based on previous studies to ensure that smoldering was self-sustaining and propagating independently from its ignition source which was confirmed by visually observing the color transition of the fuel surface [22], [34] . This color change indicated the oxidation of the solid char in the fuels and served as a reliable marker for the ignition point at the same location where pyrolysis oxidation occurred (in situ oxidation), ultimately leading to smoldering ignition during the experiments [22], [34], [39], [132] . For instance, Snapshot in 4.6 (D) shows the smoldering regime of wheatgrass fuels in 30 seconds. Ignition time was measured by analyzing experiment videos, with the initial time set as the moment when the heated particles first contacted the fuel bed.

To ensure reliable results and minimize the effects of uncontrolled parameters on the experiments, at least five tests were conducted for each material at a specific morphology of the fuel bed.

4.1.4 Thermogravimetric Analysis

To gain deeper insights into species-specific ignition patterns, we analyzed thermogravimetric (TG) data for each fuel species in its natural structure. TG analysis has been widely used to obtain important ignition behavior indicators raging from ignition temperature to activation energy [133]–[137]. Samples of each wildland fuel were sent to a commercial vendor, INNOVATECH Laboratories, for analysis of weight loss thermograms. The instrument used for the analysis was a TA Instruments Q50 TGA. The test specimens were placed in a standard platinum pan and the experiment was conducted in a nitrogen atmosphere. The heating profile followed a standard ramp of 10˚C/min from 30˚C to 950˚C with a sample purge flow rate of 50.00 mL/min of pre-purified nitrogen and a balance purge flow rate of 40.00 mL/min of pre-purified nitrogen.

4.2 Results

In this study we conducted bench-scale experiments to examine the effect of fuel bed physical characteristics on ignition behavior and utilized thermogravimetric analysis data to understand the effect of fuel species on ignition behavior. The bench-scale experiments focused on investigating the role of fuel particle size on ignition behavior. Here ignition behavior was characterized through measuring ignition temperature, ignition time and burnout time. In addition to ignition behavior, we also quantified smoldering-to-flaming transition behavior in fuels where this phenomenon occurred. To maintain the ignition source conditions constant, all ignitions were initiated using 15 steel particles heated using the process described in the methods section; all experiments were conducted under the presence of a 1.6 m/s wind. Representative results and trends in ignition modes are presented in the next section. Afterward, detailed results and analysis are presented for the bench-scale experiments. The section is concluded with results from the thermogravimetric analysis.

4.2.1 Representative Results and Modes of Ignition

In this study, flaming and smoldering ignitions were observed as well as smoldering-to-flaming transitions. Photographs of representative experiments of flaming and smoldering ignitions as well as smoldering-to-flaming transitions are presented in Figure 4.6. Each series of snapshots shows the time evolution of the ignition process.

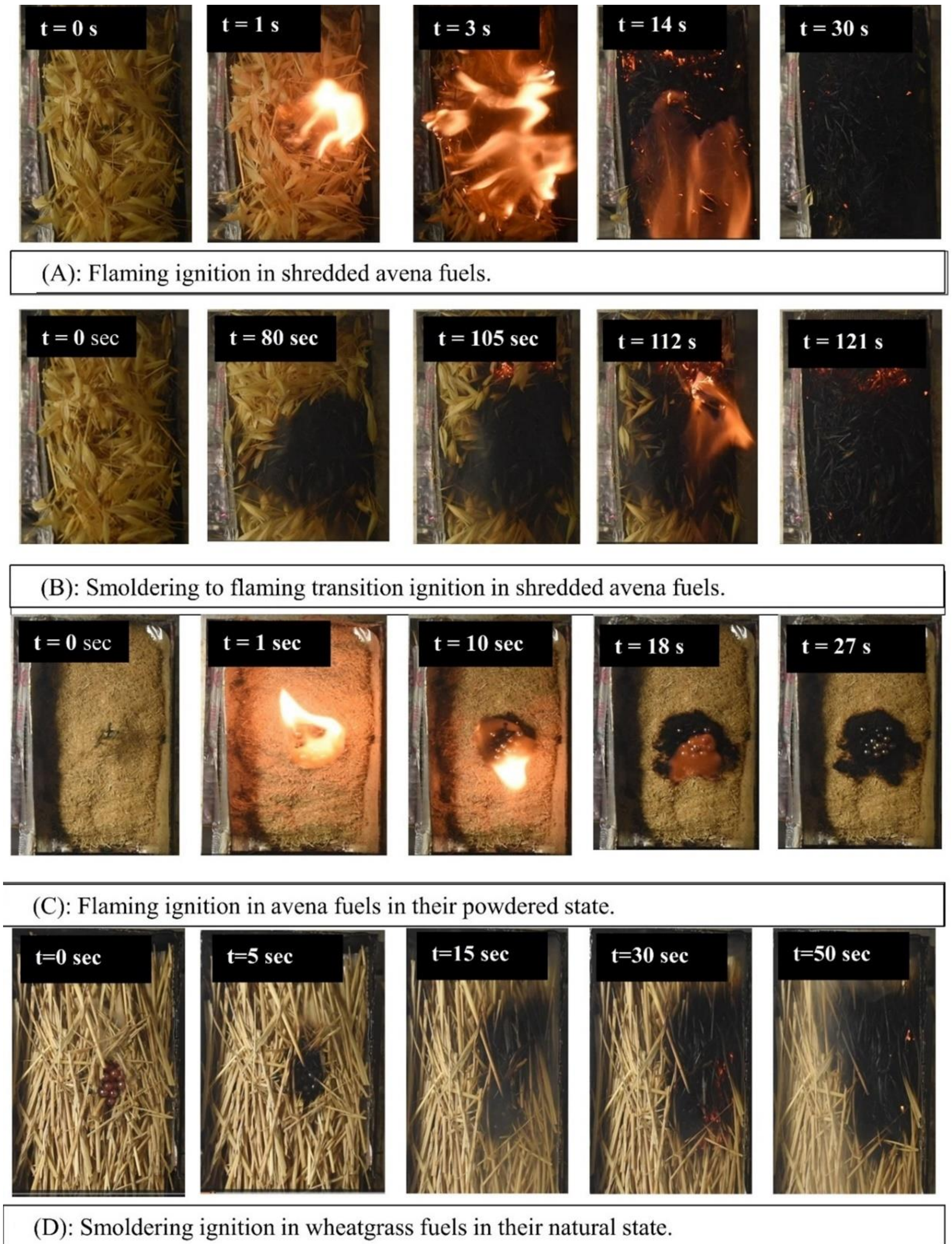

Figure. 4.6 Photograph of the experimental procedure, from left (A) showing particle heating with a propane torch - captured with an IR camera and (B) the moment of particle drops onto the fuel bed - captured with a DSLR camera.

Figure 4.6 (A) depicts a typical flaming ignition in shredded avena fuels. This ignition was characterized by a visible and sustained flame appearing immediately after the particle landed (t=0). The flame then quickly spread across the entire fuel bed within 20 seconds. Similar behavior was observed for all observed flaming ignitions.

Figure 4.6 (B) shows a group of snapshots for smoldering to flaming transition in shredded avena. Here we observed a smoldering ignition that spread for over one minute and eventually transitioned into a flame. The flame then quickly spread across the entire fuel bed within 20 seconds of the transition.

Figure 4.6 (C) shows a group of snapshots for smoldering to flaming transition in powdered avena fuels. The powdered fuels exhibit direct flaming ignition but could not spread across the entire fuel bed and stopped after 30 seconds from the ignition. In the last Figure in the series, smoldering ignition under natural conditions for wheatgrass fuels is illustrated.

Figure 4.6 (D) demonstrates that the smoldering ignition in wheatgrass fuels began to grow and stabilized within 30 seconds. Furthermore, the smoldering ignition was completed within 20 seconds after it started and, in a total of 50 seconds, finished the burning process. Note that in this work, the no ignition did not observe and investigated like some other previous studies [22], [39].

The distribution of modes of ignition among the various fuels and fuel particle sizes in this study are presented in Figure 4.7. There we observe that overall, all fuel species exhibited flaming ignitions across all fuel particle sizes examined (*i.e.* natural, shredded and powdered fuels). Moreover, wheatgrass exhibited smoldering ignition although as will be explained later, these were short lived. In addition, only two exceptional smoldering ignition results were found in Bromus fuels. StF transition was observed in all fuel species for solid and shredded fuels; powdered fuels did not exhibit transition behavior. Comparison between fuel species shows that bromus fuels were more likely to exhibit flaming ignition whereas avena fuels supported the greatest number of StF transitions. Wheatgrass was the only fuel to support smoldering ignitions that did not transition to flaming. Excelsior fuels, in the solid and shredded fuel particle configurations, were nearly equally likely to support flaming ignition as they were to support StF transition. Thus, our results indicate that the type of ignition might be correlated to fuel species.

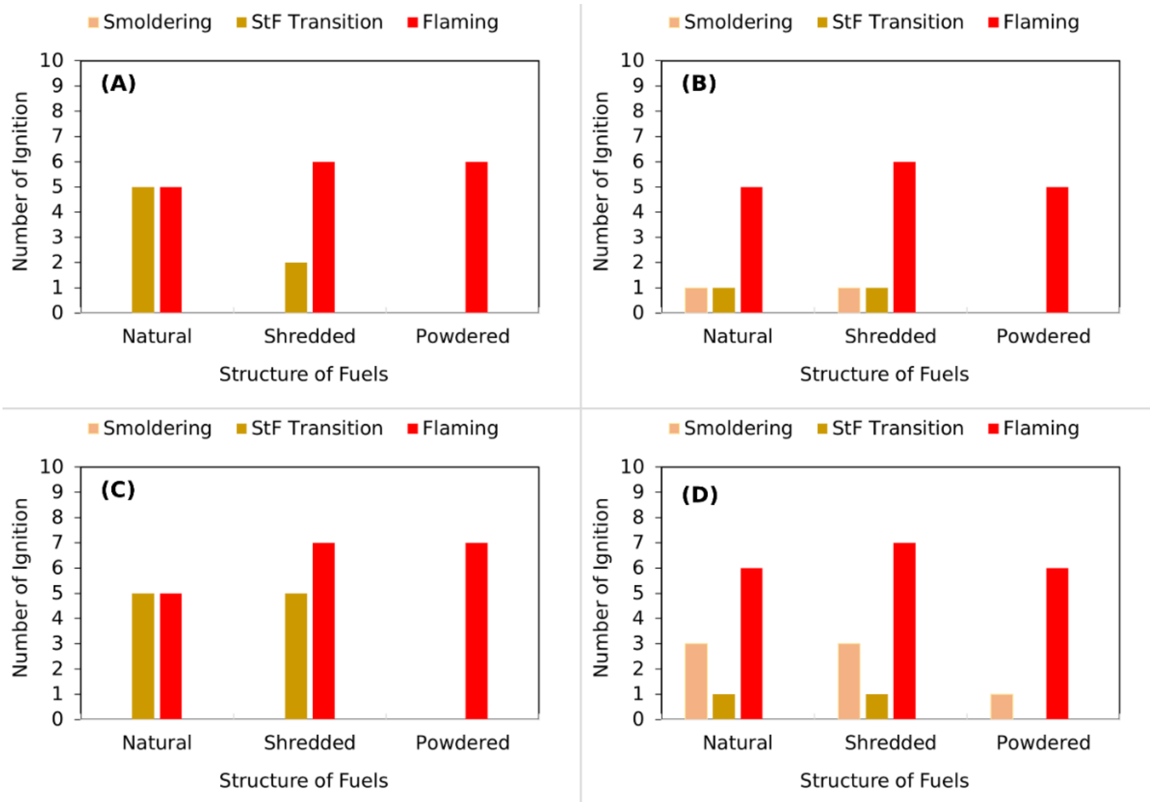

Figure. 4.7 type of ignitions of each kind of fuel in their different physical condition, from left (A) excelsior fuels (B) bromus (C) avena (D) wheatgrass.

There are two key factors influencing the ignition behavior of powdered fuel: a) the flaming ignition occurs at a much lower temperature for powdered fuels, which is easily provided by the heated particles, and b) the transition from smoldering to flaming is hindered by the lack of airflow within the fuel bed, due to the high bulk density of the densely packed powdered fuels.

In addition, the reconfiguration of the fuel particles for each fuel species allowed for an assessment of the role of fuel particle size on type of ignition supported. There the clearest trend is perhaps for powdered fuels in which flaming ignitions dominate across all fuels. Powdered or dusty fuels briefly exhibit smoldering ignition immediately after flaming ceases, this smoldering phase is often very short-lived. Several factors contribute to this behavior. First, the high surface area-to-volume ratio of fine particles facilitates rapid heat transfer and combustion, making them more prone to flaming rather than sustained smoldering. The quick ignition and high combustion efficiency result in minimal residual char, which is essential for sustaining smoldering combustion. Lastly, the airflow plays a critical role. The higher airflow 1.6 m/s in the wind tunnel setup, further accelerates flaming combustion and disrupts the thermal and oxygen gradients needed to sustain smoldering. This airflow can quickly extinguish the smoldering phase by cooling the residual particles and diluting the oxygen concentration around them. As a result, this brief smoldering phase was not emphasized in our analysis, as it had minimal impact on the overall combustion characteristics observed.

In fuel beds composed of shredded fuels, flaming ignitions significantly outnumbered smoldering ignitions in all fuels except excelsior. Fuels in their natural state exhibited perhaps the widest distribution of modes of ignition observed. For instance, in avena fuels, smoldering-to-flaming transitions outnumbered flaming ignitions whereas in bromus fuels, only one smoldering ignition was observed in contrast to five flaming ignitions. In excelsior fuels in their natural state, an equal number of flaming and smoldering-to-flaming transitions were observed. In wheatgrass fuels in their natural state, although flaming ignitions were the most numerous, a considerable number of smoldering ignitions were observed as well as one smoldering-to-flaming ignition.

4.2.2 Ignition Time and Burn out Time

Ignition time and smoldering-to-flaming transition trends for all fuels are shown in Figure 8. In general, the flaming ignition time did not vary significantly across the fuel particle sizes examined (see Figure 8(A)). For instance, in excelsior and wheatgrass fuels, the ignition time was the same across all fuel particle sizes. In bromus and avena fuels, the ignition time only differed for fuels in their natural state. Thus, for the conditions tested here, flaming ignition time did not show a notable variation with fuel particle size. In the case of variations between the various fuel species examined, however, very smaller and modest variations were observed. Bromus and wheatgrass on average ignited in 3 seconds whereas excelsior and avena on average ignited in two seconds.

When comparing the ignition during the smoldering-to-flaming transition, it was clearly observed that the transition time varied significantly and modestly across different fuel particle sizes and species (see Figure 8(B)). For example, for shredded excelsior, the smoldering-to-flaming transition time was observed to be 31 seconds, whereas it was 65 seconds for excelsior in its natural state. Similarly, for Bromus fuels, the transition time was 45 seconds for shredded fuels and 52 seconds for fuels in their natural state. Avena and wheatgrass fuels followed the same trend (see Figure 8(B)).

Consistent with previous studies on biomass fuels, this study highlights that fuel particle size plays a critical role in determining ignition behavior, particularly ignition time and temperature. Since the fuel particles size directly impacted the surface area of the fuels. The surface areas for fuels are described in table 4 in detail. In line with previous studies, this research also found that larger particles take longer to ignite and require higher temperatures to achieve ignition compared to smaller size particles because of lower surface area [109]–[111], [113], [117], [138]. For instance, Fernández-Añez et al. (2019) demonstrated that larger wood pellet fuels required more time and higher temperatures for ignition compared to their powdered form [109] . This is because finer particles have a larger surface area fully covering the heated metal surface, increasing the contact area and minimizing gaps between particles. This configuration of smaller fuel particle size has a higher surface to volume ratio enhances heat conduction within the fuel bed, reduces heat loss, and accelerates ignition.

As a result, smaller fuels, such as dusty or powdered fuels, ignite more quickly and at lower temperatures due to them because of their larger surface area with superior thermal connectivity. In contrast, larger particles act as thermal insulators, slowing heat penetration and delaying ignition. Although natural fuels with larger particles create larger gaps within the fuel bed, which can facilitate oxygen availability and support fire propagation, On the other hand, ignition is more difficult because the air is less conductive than the own substance. Also, these gaps reduce the contact area between the heated surface and fuel particles. This reduced contact hinders heat transfer, further slowing ignition. Consequently, larger fuels exhibit lower heat transfer efficiency, longer ignition times, and higher ignition temperatures [109]–[111], [113], [117], [138] .

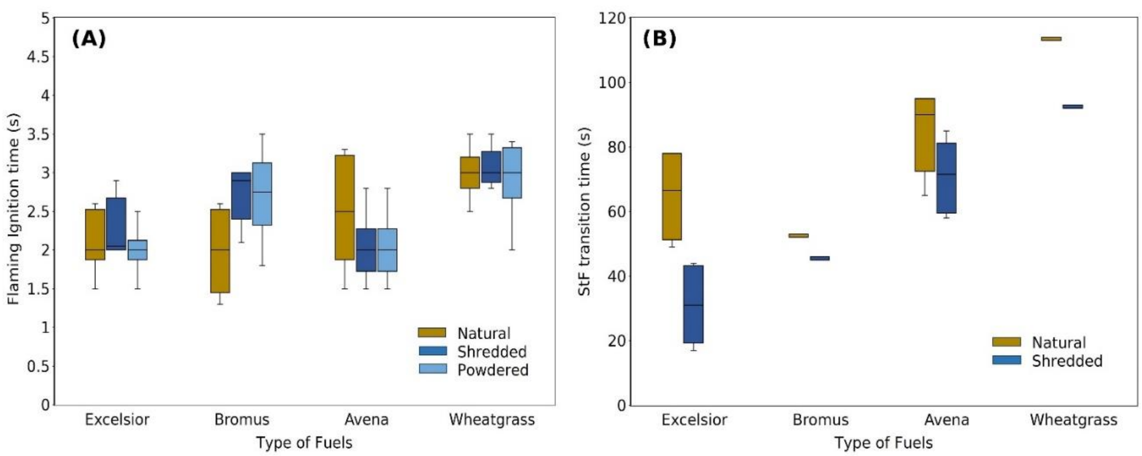

Figure. 4. 8 Ignition time analysis for all kinds of fuel structures (A) (left) flaming ignitions. (B) (right) smoldering-to-flaming (StF) transitions.

In addition to ignition time, a temporal parameter that provides important insight into the effect of fuel particle size on ignition behavior is burnout time. In this study, consistent with prior work, burnout time refers to the duration from the moment of ignition to the moment flaming ceases, regardless of whether all available fuel is fully consumed or not [101], [139], [140] . For instance, in natural structure fuels, flaming ignition ceases only after all the fuel is consumed, whereas in powdered fuels, flaming ignition may stop even before the entire fuel mass is burned. Examining burnout time is important for predicting fire behavior and duration, enabling better planning for fire suppression and risk assessment.

Overall, we observed that burnout time generally increased as fuel particle size increased. This is perhaps most apparent in flaming ignitions which support ignitions across all fuel particle sizes (*i.e.* powdered, shredded and natural fuels). There powdered fuels exhibited the lowest burnout times for all fuel species. Burnout time was higher for shredded fuels than powdered fuels and fuels in their natural state had the highest burnout time (see Figure 4.9). For example, in experiments with flaming ignitions, burnout time for powdered excelsior fuels was 59 seconds, compared to 71 seconds for shredded excelsior and 85 seconds for natural excelsior. Similarly, avena fuels burned out in 35 seconds for powdered, 65 seconds for shredded, and 80 seconds for natural states. Bromus and wheatgrass fuels followed the same trend (see Figure 4.9(A)), though the differences in burnout time for bromus fuels across all states were smaller compared to excelsior and avena fuels.

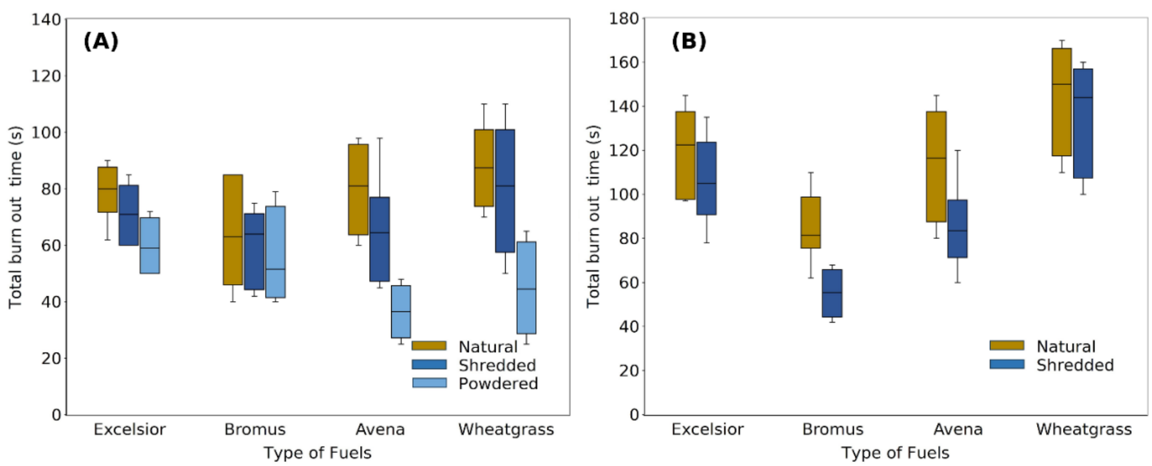

Figure. 4. 9 Burnout time (A) (left) flaming (B) (right) smoldering-to-flaming transition

A similar trend in the variation of burnout time with fuel particle size was also observed in the smoldering-to-flaming transition results. In the case of experiments in which smoldering-to-flaming transition occurred, burnout time was lower for shredded fuels than for fuels in their natural state, (see Figure 4.9 (B)). For instance, burnout time for shredded excelsior fuels was 106 seconds, compared to 120 seconds for natural excelsior. Similarly, avena fuels burned out in 85 seconds for shredded and 113 seconds for natural states. Bromus and wheatgrass fuels followed the same trend (see Figure 4.9 (A)).

Consistent with previous studies, it can be argued that ignition behavior, such as fuel burnout time, is directly impacted by fuel particle size in both flaming and smoldering-to-flaming transition ignitions [110], [111], [113], [141]. Fuels in their natural state have larger gaps within the fuel beds, promoting oxygen availability and abundant pyrolysis gas flow, which results in sustained burning. In contrast, the higher density of shredded fuels leads to much lower air flow and pyrolysis gas flow compared to natural fuels. As a result, ignition in shredded fuels extinguishes more quickly, leaving the fuel bed incompletely burned. Fuels in their powdered state have much smaller particle sizes and higher bulk density compared to shredded or natural fuels, significantly reducing total burnout time compared to the other two fuel conditions. However, it is noted that this trend was observed with only two particle sizes, natural and shredded. Future work could explore transition behavior across a broader range of particle sizes.

4.2.3 Ignition Temperature

As ignition time and burnout time have been discussed to characterize the ignition behaviors of the fuel bed species and particle sizes, it is important to note that ignition temperature is another key parameter analyzed in the experiments for flaming, smoldering, and StF transition behaviors. Each ignition phenomenon is discussed below.

Flaming

Figure 4.10 (A) shows the ignition temperature curve and Figure 4.10 (B) shows the ignition temperature trend for different fuel species and particle size. Flaming ignition temperatures were found to be significantly lower for certain fuels, such as excelsior, which aligns with temperatures reported in previous studies involving grassy fuel species [54], [142], [143] . This can primarily be attributed to their high surface-area-to-volume ratio, which facilitates faster heat absorption and promotes quicker ignition. The increased surface area allows for more efficient heat transfer, which in turn accelerates the ignition process at lower temperatures. Additionally, finer fuels, such as grasses and small particles, are more easily ignited due to their greater exposure to oxygen, further lowering their ignition threshold. For example, D Wragg et al. (2018) found that fire temperatures for various grasses and forbs ranged between 100-300°C, while Rallis et al. (2002) reported ignition temperatures for dry veld grass between 300-400°C, and W Cardoso et al. (2018) observed mean fire temperatures for dry savanna grasslands between 200-400°C [54], [142], [143].

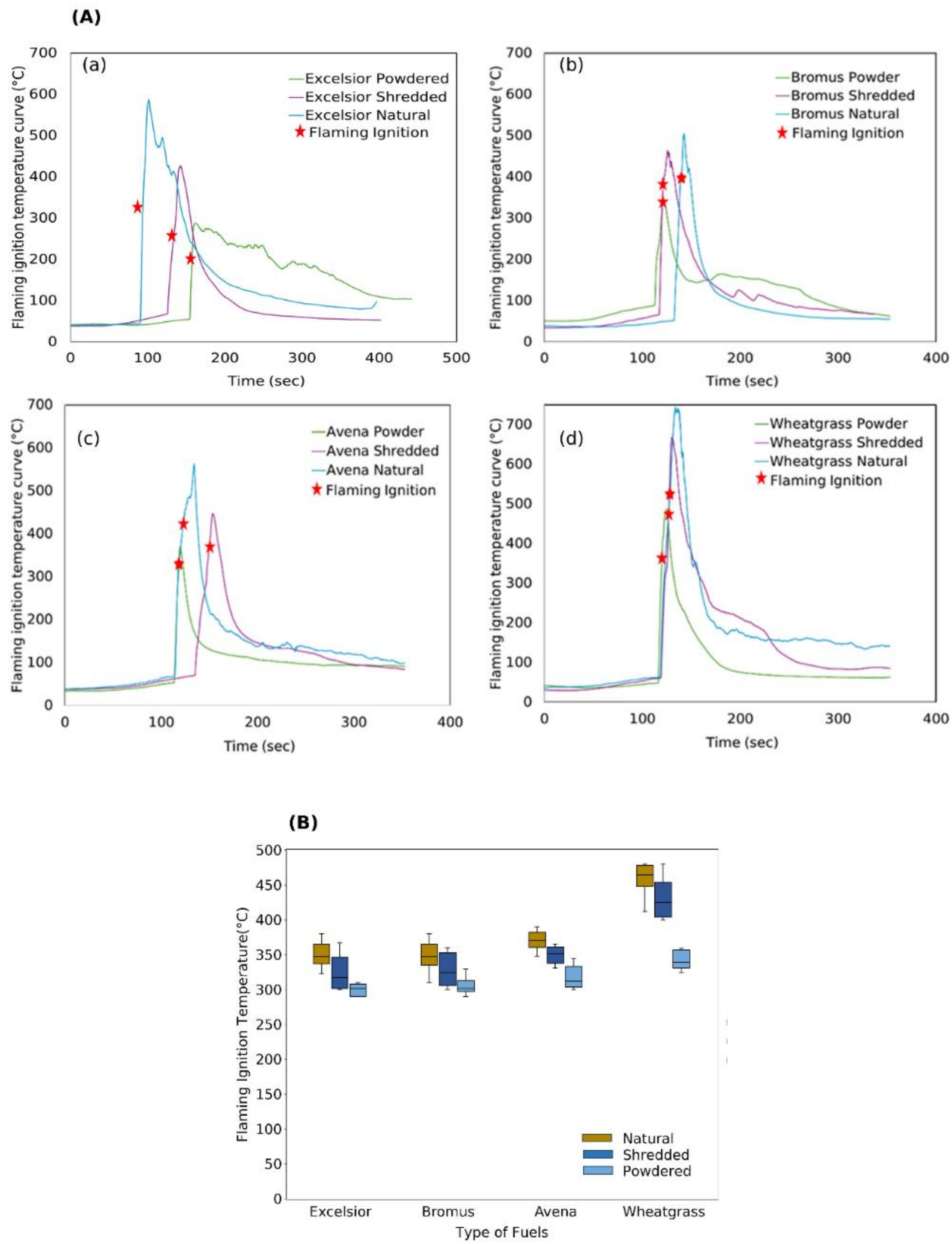

Figure. 4. 10 (A) Flaming ignition temperature curves; from left (a) excelsior (b) bromus (c) avena (d) wheatgrass. (B) Flaming ignition temperature analysis for all kinds of fuel structures.

Overall figure 4.10 clearly shows that the flaming ignition temperature for every fuel species is lowest in their powdered state and highest in their natural state, with shredded state falling in between. For example, in experiments with flaming ignitions, the ignition temperature for powdered excelsior fuels was 300 °C whereas it was 324°C for the shredded excelsior and 350°C for excelsior in its natural state. Similarly, for Bromus fuels, the flaming ignition temperature was 305°C for powdered fuels, 320°C for shredded fuels and 348°C for fuels in their natural state. Avena and wheatgrass fuels followed the same trend (see Figure 4.10 (a) and (b)).

Smoldering

Even though we aimed to analyze and quantify smoldering ignition alongside flaming ignitions throughout the experiments, very few instances of smoldering ignition remained as such. Most of the smoldering ignitions observed in the experiments transitioned into flaming ignition (see Figure 4.7). Simple smoldering ignitions were observed only in wheatgrass fuel species, particularly in their natural and shredded forms. Besides that, two exceptional smoldering ignition results were found in Bromus fuels where one in their natural form and one in their shredded form. The ignition temperature curves and trends for smoldering ignitions are illustrated in Figure 4.11.

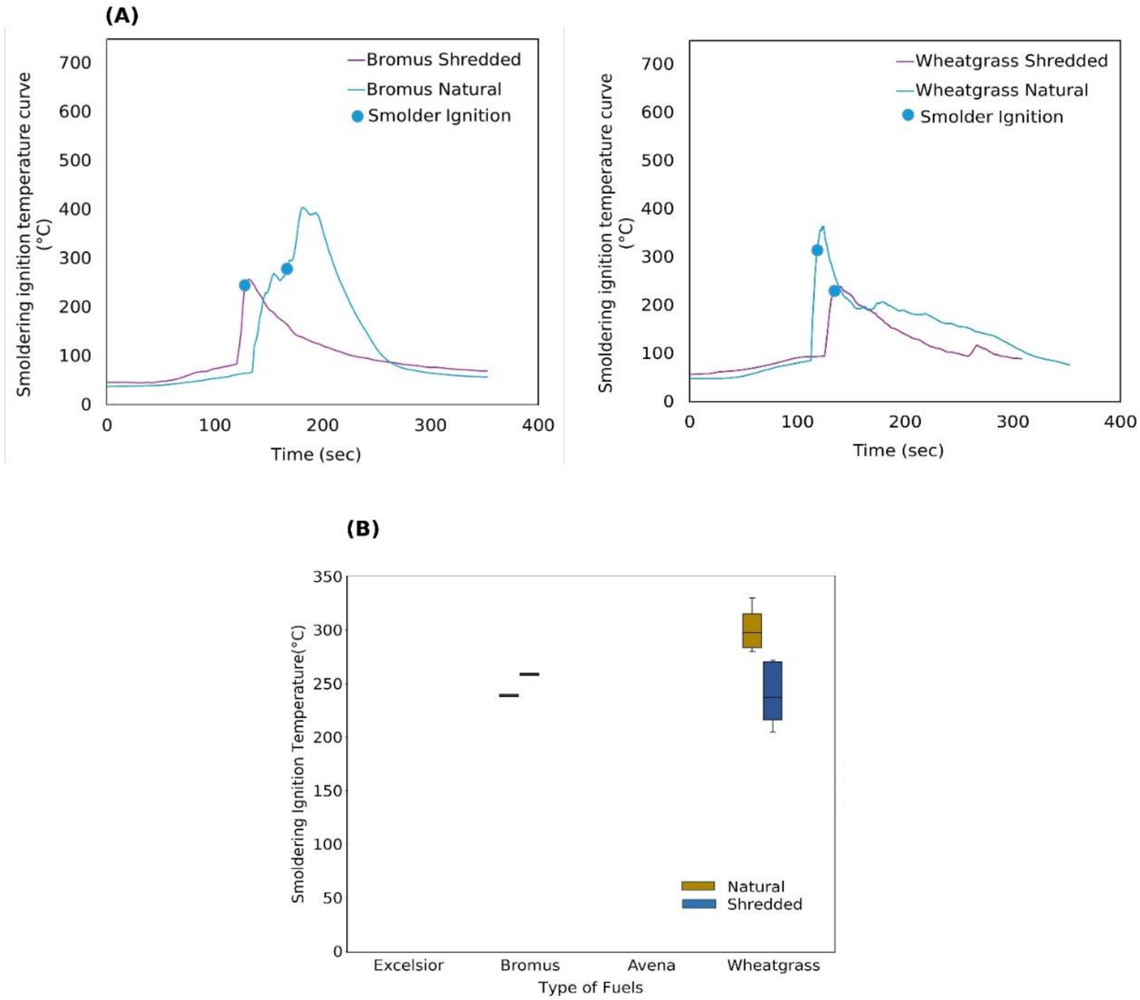

Figure. 4. 11 Smoldering ignition temperature curve (a) and trend (b) analysis for wheatgrass and bromus fuels (from left).

Figure 4.11 shows that smoldering ignition temperature also differs with fuel particle sizes in wheatgrass fuel species. For example, an average smoldering ignition occurred in wheatgrass fuels in 28 seconds at 240°C in their shredded form, whereas smoldering ignition was found in 15 seconds at 300°C in their natural form. It is also noteworthy that these five smoldering ignitions occurred at much lower temperatures in shredded wheatgrass fuel compared to the other five experiments in powdered wheatgrass fuels, preventing the transition to flaming despite the wind providing airflow to aid the transition. Furthermore, two exceptional smoldering ignitions were observed in Bromus fuels, in 19 seconds at 232°C in their shredded form, and in 42 seconds at 262°C in their natural form.

Smoldering to flaming transition

In this study, several experiments exhibited smoldering-to-flaming transition. It is worth noting that powdered excelsior fuels always ignited in flaming mode and therefore did not exhibit smoldering-to-flaming transition. This is why powdered excelsior trends are not included in Figure 4.12.

Figure 4.12 (A) shows the smoldering to flaming transition ignition temperature curve and Figure 4.12 (B) shows the ignition temperature trend for different fuel species in their different structures. Overall Figure 4.12 indicated that the StF transition into fuels with shredded structures compared to the fuels in natural structures. For instance, the smoldering to flaming transition ignition temperature for shredded excelsior fuels was 420 °C whereas it was 460°C for excelsior in its natural state. Similarly, for avena fuels, the flaming ignition temperature was 450°C for fuel in shredded structure whereas it was 500°C for fuels in their natural state. Besides the transition temperature, the temperature for first smolder also follows similar trends in ignition temperature. For instance, the first smolder occurred at 203°C for excelsior in shredded structure whereas it was at 245°C for excelsior in their natural structure. Similarly, for avena fuels, the first smolder temperature found at 234°C for fuel in shredded structure whereas it was 313°C for fuels in their natural state. Besides the transition temperature, the temperature for first smolder also follows similar trends in ignition temperature. Bromus and wheatgrass fuels followed the same trend (see Figure 4.12 (a) and (b)). Though it should be noted that bromus and wheatgrass fuels only show a single example of smoldering to flaming transition experiments. Overall, the trends observed in flaming ignitions across different fuel structures and species indicate that, as fuel particle sizes increase, the geometry becomes more complex, leading to varied ignition behaviors. As a result, the powder structure only exhibited flaming ignition, while the natural structure showed all three types of ignitions: smoldering, StF transition, and flaming.

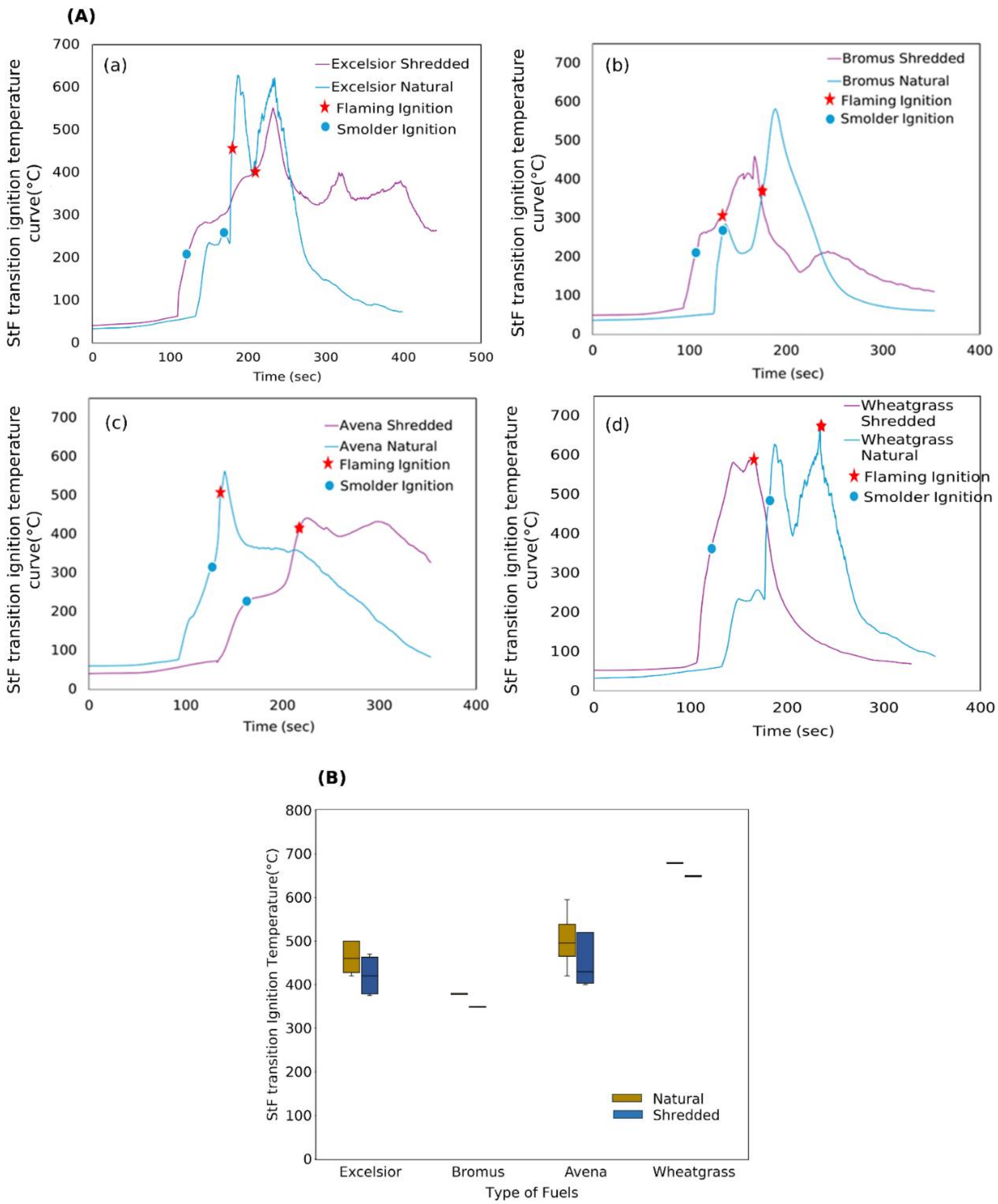

Figure. 4. 12 (A) Smoldering-to-flaming transition temperature curves. From Left (a) excelsior, (b) bromus, (c) avena, (d) wheatgrass, (B) Smoldering-to-flaming transition temperature trends

In line with previous studies on biomass fuels, this study emphasizes that fuel particle size significantly impacts the ignition behavior of fuels, as observed in wildland fuel structures [24], [109]–[111], [133], [144]. Previous studies have found that bulk materials generally require higher temperatures to ignite compared to their dust forms [109]–[112] . Our study also concludes that it has a similar effect on the ignition temperature in the various fuel structures. This study found that the ignition temperature for fuels in their natural structure is consistently higher than that for powdered fuels across all fuel species. Although fuels in their natural state have larger gaps within the fuel beds that promote oxygen availability, which could potentially ease ignition, these larger gaps also cause greater heat loss and reduce directly reduce the contact surface between the heated metal and fuel bed surfaces. In contrast, for powdered fuels, the finer particles fully cover the heated metal surface, resulting in a larger contact area, greater thermal conductivity between the fuels and heated surface. Besides that, the powdered configuration significantly reduces heat loss which also enhances ignition capability in powdered fuels.

4.2.4 Comparison of Powdered vs Natural Fuels

In addition to the particle size effects on ignition behavior mentioned above, interesting insight into the overall effect of fuel structure on ignition behavior can be obtained from comparing fuels in their natural state and fuels in the powdered state. Furthermore, analysis of ignition behavior in powdered fuels facilitates isolation of fuel species effects not related to fuel structure, namely, chemistry. Thus, in this section we provide a synopsis of major ignition behavior trends identified in powdered fuels and we briefly compare these to those occurring in natural fuels.

In the case of flaming experiments, we observed that fuel species affected ignition temperature across all fuel structures (i.e. natural, shredded and powdered fuels). However, powdered fuels exhibited the most modest variation in ignition temperature between fuel species. We therefore hypothesize that when evaluating fuel species' effects on ignition temperature, fuel structure may have a greater effect than chemical composition.

In terms of burnout time, fuel species sizes affected this parameter across all fuel particle sizes. The difference between fuel species was similar in natural and powdered fuels.

Similarly, in terms of ignition time, flaming ignition did not vary significantly across the fuel particle sizes examined. For instance, in excelsior and wheatgrass fuels, the ignition time was consistent across all their natural state and powdered state. In contrast, bromus and avena fuels, the ignition time only slightly differed for fuels in their natural state compared to the powdered state. We therefore hypothesize that when evaluating flaming ignitions and the effects of fuel species on ignition time, neither particle size nor chemical composition plays a significant role.

Additionally, in terms of mass loss analysis, the powdered structure of all types of fuels did not exhibit a significant change in mass from the initial state throughout the burnout time to the final mass, whereas other fuels, such as shredded and natural fuels, showed significant changes in mass loss during the burnout time. This is because powdered fuel ignites and extinguishes much faster than other fuel structures, such as shredded or natural forms, and does not burn long enough to significantly reduce the mass, resulting in minimal change to the total mass. To clarify the analysis, a comparison of mass loss during the burnout time is shown in Figure 4.13 below for excelsior, avena, and wheatgrass fuels.

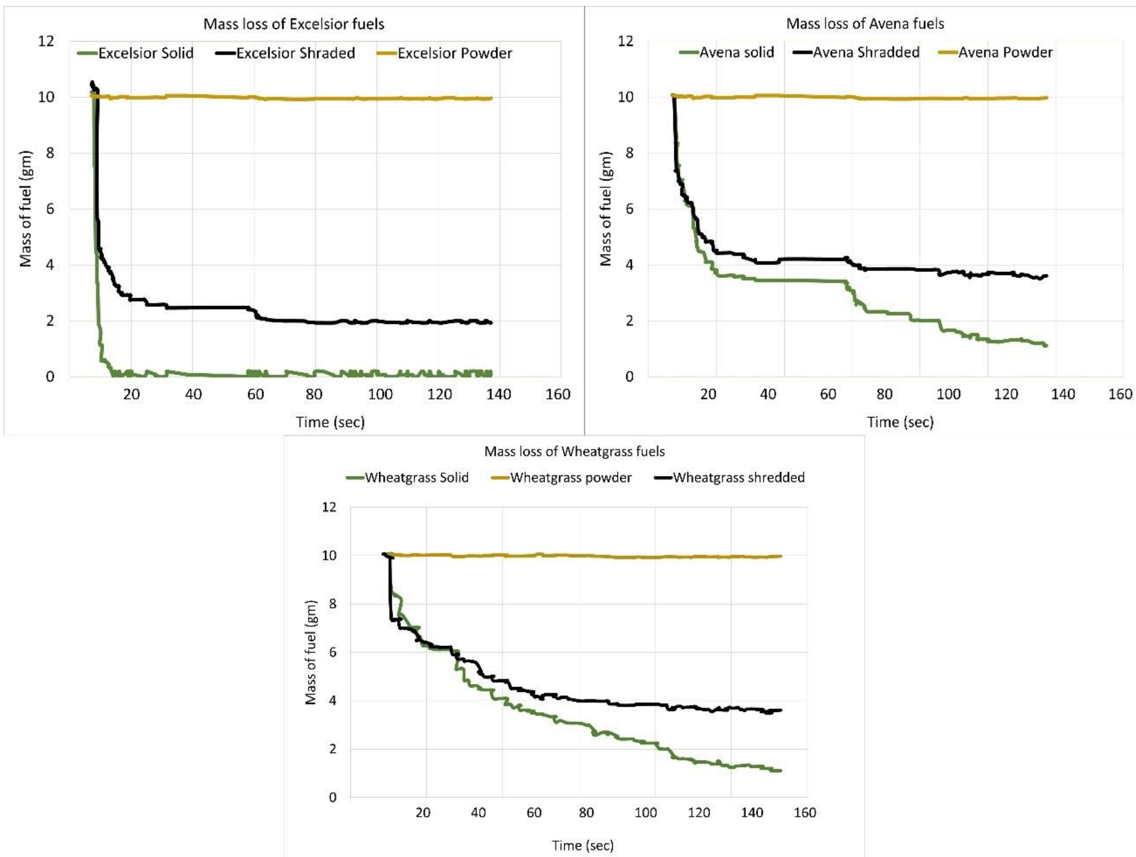

Figure 4.13: Mass loss vs burn-out time for excelsior, avena and wheatgrass fuels in all three structures.

4.2.5 Thermogravimetric Analysis

To better understand the fundamental thermal properties for each grass species, this study employs thermogravimetric (TGA) and differential thermogravimetric (DTG) analyses to assess their chemical degradation temperatures. TG analysis provides insight into the ignition characteristics by examining the kinetics of thermal degradation through the rate of weight loss under specific conditions. DTG analysis further refines this by pinpointing the specific temperatures at which the rate of weight loss is highest, identifying distinct degradation stages and thermal stability thresholds for each fuel type. These thermal degradation stages are critical for understanding the combustion behavior of wildland fuels, as the temperatures associated with maximum weight loss often correspond to the onset of key combustion phases, such as ignition. In this study, the DTG analysis results were used to correlate the thermal degradation patterns of Bromus, Avena, and Wheatgrass with their observed flaming and smoldering ignition temperatures and times. By identifying the temperature ranges at which each fuel undergoes its most significant decomposition, we can better understand the relationship between thermal stability and ignition behavior [134], [135], [141].

For instance, Bromus fuels with lower degradation temperatures demonstrated lower ignition temperatures as well as shorter flaming, smoldering, and transition ignition times, as well as lower ignition temperatures, compared to Wheatgrass fuels, which exhibited higher degradation temperatures as well as higher ignition temperature and longer ignition times. This correlation provides a mechanistic understanding of how thermal decomposition influences ignition dynamics, ultimately aiding in the prediction of wildfire ignition and propagation for different wildland grass species.

Followed by previous studies, this research aims to identify the specific temperature ranges associated with each stage of degradation [134], [135], [141]. Figure 4.14 presents the results of TG and DTG analysis for bromus, avena, and wheatgrass fuels together at a 10°C/min heating rate. Subsequently, the TG and DTG curves for each type of fuel are presented separately for further clarification.

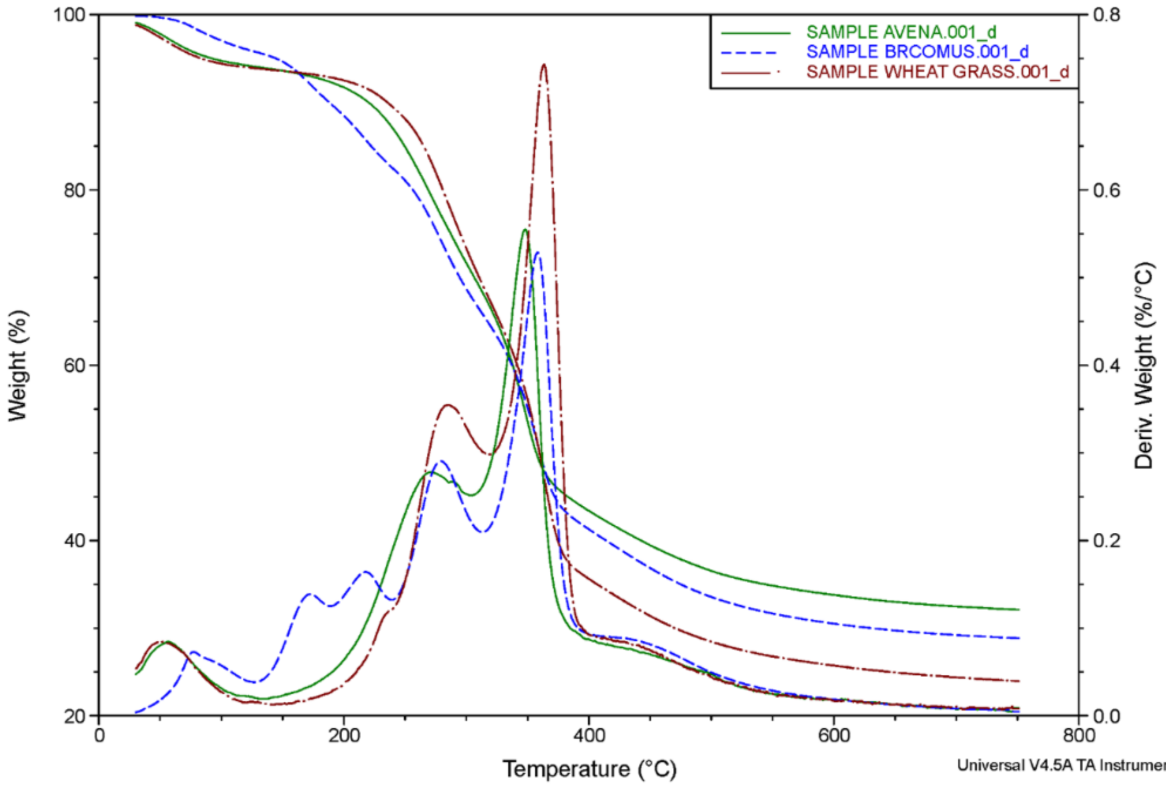

Figure 4.14 TG and DTG curves of wildland fuels combustion at 10 °C/min.

The DTG curves indicate a two-step process during biomass decomposition. In the first stage, volatiles are released and combusted, primarily involving the total thermal decomposition of hemicellulose and cellulose, along with partial lignin decomposition and the second stage involves char decomposition, which corresponds to the decomposition of the remaining lignin and the decomposition of the char residue[135], [136], [145]–[149]. To discuss the decomposition process in two stages, the TG and DTG curves for each fuel are presented separately below.

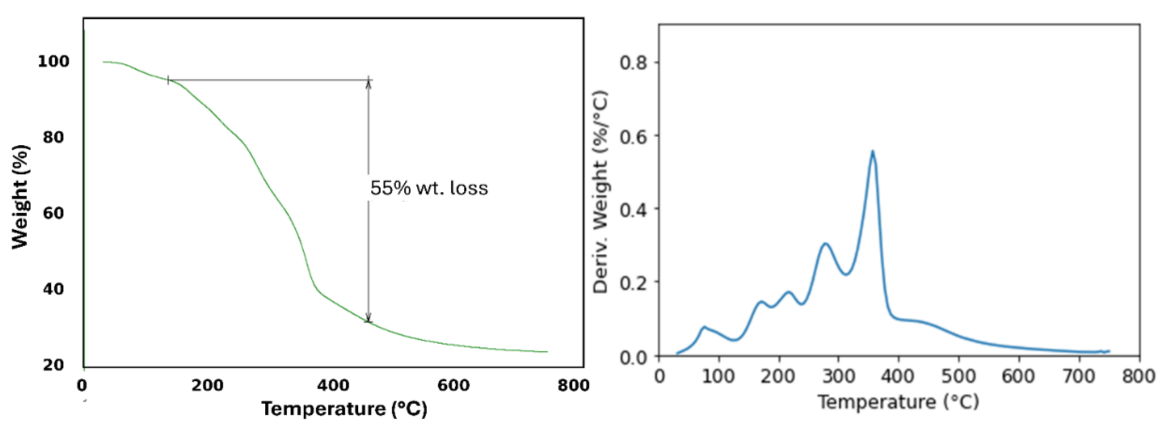

Figure 4.15 TG and DTG curves (from left) of bromus fuels combustion at 10 °C/min.

Figure 4.15 shows that the first peak of mass loss in bromus fuels occurred between 180-200°C, while the second peak appeared between 320-360°C during the TG decomposition process.

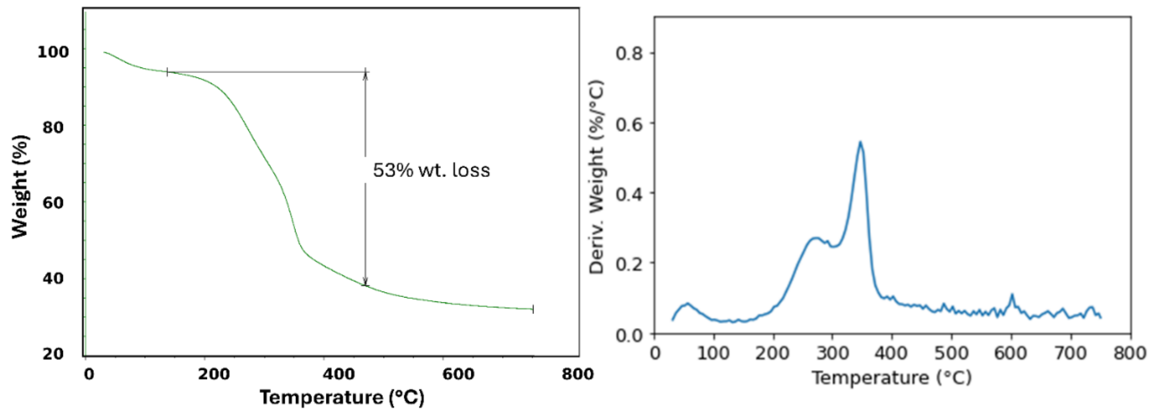

Figure 4.16 TG and DTG curves (from left) of avena fuels combustion at 10 °C/min.

Figure 4.16 shows that the first peak of mass loss started in avena fuels between 250-290°C, whereas the second peak occurred 330-360°C in this TG decomposition process.

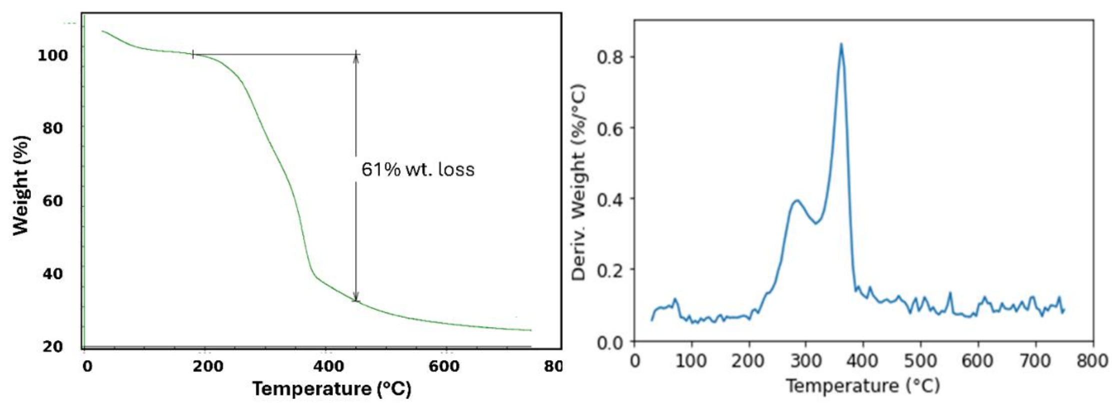

Figure 4.17 TG and DTG curves (from left) of wheatgrass fuels combustion at 10 °C/min.

Figure 4.17 shows that the first peak of mass loss started in wheatgrass fuels between 270-300°C, whereas the second peak occurred 380-390°C in this TG combustion process.

As observed in our experimental study analysis, wheatgrass fuels consistently ignite at higher temperatures compared to excelsior, avena and bromus fuels. The DTG curves indicate that the temperatures for both the first and second peaks are consistently higher for wheatgrass fuels followed by the bromus and avena fuels. This trend is also reflected in the decomposition temperature peaks observed in the TG analysis. According to the TG and DTG curves, maximum mass loss begins later in wheatgrass fuels compared to bromus and avena fuels. And it is worth noticing that DTG curve shows a peak at approximately 0.8%/°C for wheatgrass fuels which is much higher than that for bromus (0.57%/°C) and avena (0.59%/°C) fuels. Also, it is worth noting that the wheatgrass degradation is maximum in the second stage of decomposition which occurs due to high amount of lignin content as well as higher amount char decomposition.

Previous studies have shown that the chemical decomposition of fuel species has significant effects on ignition behavior, such as ignition temperature, ignition time [105], [136]. Though previous studies also show through the TG analysis that the fuel particle size also has an effect on the ignition temperature [133], [150]. Therefore, we hypothesized that, in our case study, fuel particle size would have an equally important effect on ignition behavior alongside chemical composition.

4.3 Summary

This study successfully elucidated the critical role that fuel structure and species play in spot the ignition behavior of wildland fuels. Through a series of bench-scale experiments, it was demonstrated that fuel beds with varied particle configurations, such as powdered, shredded, and natural states, exhibit distinct ignition patterns. The findings highlight that those powdered fuels, with their smaller particle size and cohesive structure, tend to ignite at lower temperatures, indicating a heightened susceptibility to ignition compared to shredded or natural fuels. The fact that without any big differences of volatile materials, the powder fuels were capable of ignition at lower temperatures indicates that some combination of smaller fuel particulate sizes and higher densities make ignition possible at lower temperatures [109], [111], [112], [133], [151]. The smaller particle size and higher bulk density of powdered fuels made ignition easier, consistently resulting in shorter ignition times compared to fuels in other states [110], [111], [141]. The effects of fuel particle size and bulk density were evident in the total burn-out time observed in this study. While ignition occurred more quickly and at lower temperatures in the high-density powdered fuels, the smaller gaps within the fuel bed led to faster extinguishment due to limited oxygen and restricted pyrolysis gas flow. In summary, this study finds that fuels in their powdered state consistently exhibit a much shorter total burn-out time compared to those in their shredded or natural states, a finding that aligns with previous studies [110], [111], [113].

Moreover, the thermogravimetric analysis provided valuable insights into the ignition parameters, revealing how besides their physical characteristics such as geometry and bulk density, their chemical composition such as lignin also affects ignition temperature, delay time, burning rate, and total burnout time. The DTG curves always show the peaks in higher temperatures for the wheatgrass fuels because of high amount of lignin content as well as higher amount char decomposition compared to the bromus and avena fuels.

In conclusion, this study contributes to this understanding by highlighting how ignition thresholds and heat transfer characteristics differ across fuel structures, particularly the differences between powdered and natural grasses, which can help inform the design of preventive measures. Regarding your question on whether to use an average or worst-case scenario for designing protective measures, we suggest considering the worst-case scenario for safety design, particularly in areas where wildfires are a concern. Our findings indicate that powdered grasses require lower ignition temperatures and shorter ignition times compared to natural grasses, making them more susceptible to ignition under certain conditions. Therefore, the worst-case scenario, which would involve the most easily ignitable fuels (such as powdered fuels), should be used to determine the temperature thresholds and required time to ensure comprehensive safety measures. Designing based on this scenario ensures that protective and preventive measures are effective even in the most challenging conditions.

In terms of recommendations, it would be prudent to focus on mitigation strategies that take into account the specific ignition characteristics of different wildland fuels. For example, the application of firebreaks, fuel treatment strategies (e.g., reducing the amount of fine, easily ignitable fuels like powdered grasses), and the establishment of defensible zones around properties could significantly reduce the risk of ignition. Additionally, the findings can help guide the development of fire-resistant materials and structures for buildings in the WUI, as well as inform firefighting tactics by identifying the most vulnerable fuel types.

Additionally, community-level fuel management strategies should be prioritized. These strategies include creating buffer zones, managing grasses, and controlling fine fuel distribution within neighborhoods. The 2003 Cedar Fire in San Diego, where unregulated vegetation accelerated fire spread into urban areas, underscores the need for strategic fuel management in WUI zones. Communities can enhance fire prevention by maintaining open spaces and regulating vegetation density, with a particular focus on reducing fine fuels near structures.

This approach, grounded in our study's findings and informed by past wildfire incidents, supports more resilient and fire-adaptive communities in WUI areas.

For future research, we recommend integrating our experimental findings into numerical modeling simulations using the Fire Dynamics

Simulator (FDS). This approach will allow us to simulate various scenarios and conditions, offering deeper insights into the ignition process and uncovering complex interactions that may not be fully captured through experiments alone.

Acknowledgement

I thank Cobian-Iñiguez Fire Lab for their support in the research work. My special thanks go to the undergraduate students – Juan Hernandez, Jason Estevez, and Gen Duenas for their invaluable assistance and contribution in conducting experiments. This research is supported through startup funding from the University of California, Merced, School of Engineering.

Chapter 5

Wind-Driven Ignition Behavior of Wildland Fuels: Experimental Insights Under Controlled Conditions

Wildfires are driven by complex interactions between fuels, ignition sources, and environmental conditions among which wind plays a critical role. This study investigates the influence of wind speed on the ignition behavior of wildland fuels using a controlled wind tunnel setup. Four fuel types (excelsior, bromus, avena, and wheatgrass) were exposed to stainless steel spheres as heated ignition sources under four wind conditions (0.5, 1.0, 1.5, and 2.0 m/s). The analysis focuses on key combustion parameters including ignition temperature, ignition delay, StF transition, burnout time, rate of spread (ROS), and heat release rate (HRR). Results show that higher wind speeds significantly increased ignition and peak temperatures while reducing ignition delay and transition times, likely due to increased oxygen supply and enhanced heat transfer. This effect might be explained by the fact that higher wind speeds increased convective heat transfer to the fuel surface, raising its temperature more rapidly and leading to quicker ignition. When comparing all fuels, bromus and excelsior consistently ignited more quickly than avena and wheatgrass, suggesting that these fuels had higher flammability potential and required less time to transition into flaming combustion likely due to their fine structure and greater oxygen accessibility. Similarly, HRR values rose with wind, indicating more intense combustion. The study highlights how wind-enhanced convective heat transfer and oxygen availability accelerate combustion dynamics and fire spread. Which indicates that higher wind speeds increase local flame fuel contact frequency and enhance intermittent convective heating of the fuel bed surface. These insights improve our understanding of wind-driven fire behavior and provide valuable input for predictive fire modeling, risk assessment, and wildfire mitigation strategies.

5.1 Materials and methods

5.1.1 Experimental apparatus and procedure

The experiments were conducted in a bench-scale subsonic wind tunnel measuring 82.3 cm in length, 15.6 cm in width, and 42.5 cm in height. The tunnel was constructed from 4 mm thick aluminum sheets, as shown in Figure 5.1. A 6-inch inline axial fan was positioned on the left side of the wind tunnel and controlled by a Raspberry Pi module. Downstream of the fan, the system includes a diffuser, honeycomb, mesh screens, an electric heater, and the test section. In addition, a DSLR camera, an infrared camera, and thermocouples are used to assist with the methodology.

The test section measures 15.6 cm in width and 28 cm in height, with a length of 30 cm. It is enclosed with heat-resistant ceramic glass on both sides and has an open top. Inside the test section, a custom aluminum tray was used as the primary fuel bed, which measures 20 × 9.8 × 7.62 cm (length × width × height). To ensure airflow consistency, we used a standardized aluminum tray with a perforated mesh on the wind-facing side to reduce obstruction. Air velocity was also calibrated using an anemometer within the fuel bed. The fuel bed was always placed on top of a measuring scale to monitor mass loss throughout the experiments. A thermostat is connected to the electric heater to control the airflow at 30.5 ± 1.3 °C inside the wind tunnel. A steel spoon measuring 34 cm in length and 8.2 cm in bowl diameter is also used to hold the metal particles, which are heated with a propane torch to initiate the ignition source in the fuel bed. The wind tunnel is enclosed in a fireproof fume hood, and the full setup is depicted in Figure 5.1. A moisture analyzer MX-50 used in this study to ensure the moisture content in the fuels.

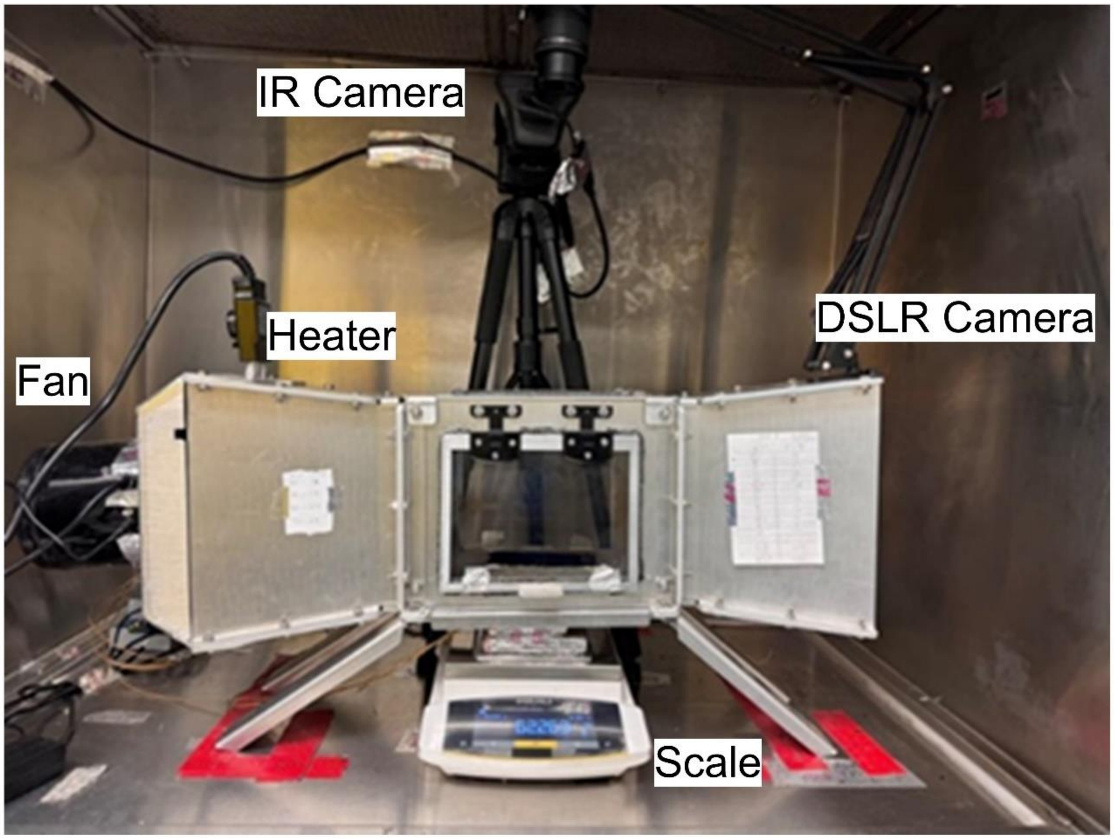
IR Camera
Heater
Fan
DSLR Camera
Scale

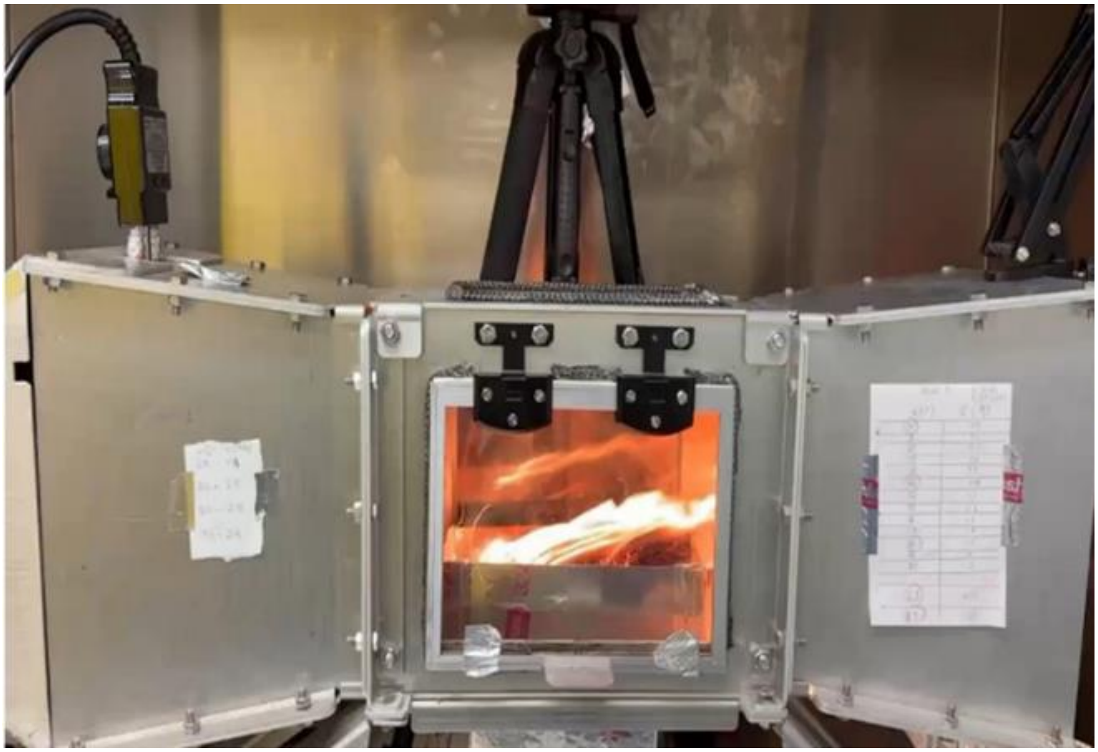

Figure 5.1 Photograph of experimental apparatus and procedure.

Fuel bed preparation

Four types of fuels were examined to investigate ignition behavior in this study. The details of the fuel properties are shown in Table 5.1. One prefabricated fuel (excelsior) was considered the standard fuel, while the other three fuels were classified as wildland fuels, as they were collected from the field (as shown in Figure 5.2).

Table 5.1. Fuel bed properties

Grass Fuel Species	**Chemical Composition**	**Heat of combustion for flaming ignition (MJ/kg)**
Excelsior (Aspen Wood Fiber)	Cellulose (48%), Lignin (18%), Hemicellulose (20%), Extractives (11.5%), and Minerals (Ash, 3%) [152]	32.37 [122], [152]
Bromus	Protein (8%), Fat (1.5) %, Fiber (31.3%), Lignin (8.4%), Ash (8.1%) [153]	18.707 [153]
Wild Oats	Protein (15.4%), Fat (6.4%), Fiber (15%), Starch (35.9 %), Ash (3.8%), lignin (13%) [154]	18.07 [154]

Wheatgrass Fuels	Protein (25.4%), Starch (51.6%), Fiber (9.5%), Ash (5.2%), Fat (1.7%), and Lignin (20-22%) [155]	16.94 [155]

All fuels were oven-dried at 90 °C for 24 hours to reduce moisture content and confirm that it was below 3%. Moisture content was then tested with a moisture analyzer with a measurement accuracy ±0.10%. For each experiment, 15 grams of fuel were evenly distributed in the steel tray, focusing on standardizing fuel mass rather than bulk density to ensure consistent fuel quantity across experiments.

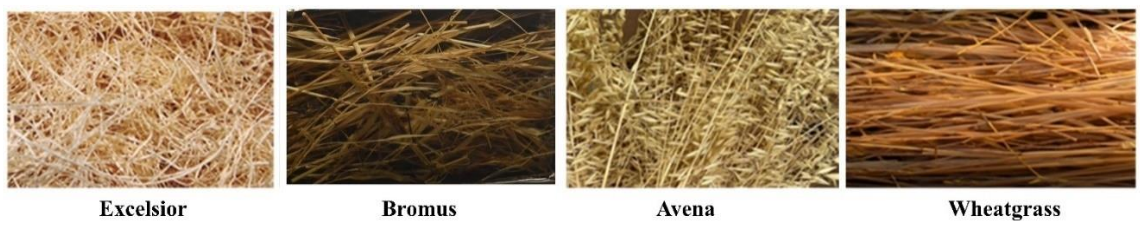

Figure 5.2 Photograph of fuels

Ignition source

15 spherical particles of 304C stainless steel, each 4 mm in diameter, were heated with a propane torch for 90 seconds and were dropped simultaneously from a height of 8-10 cm to assess ignition behavior. The heating time was carefully controlled to avoid breaking or melting the particles, with a stopwatch and video recording used to verify both heating and ignition times. In choosing the particle size for this study, we based our selection on previous research examining the impact of heated particles on spot fire ignitions [24], [26], [47]. To align with the sizes used in these studies, we selected 4 mm particles, which not only allowed us to replicate previous findings but also to simulate real-world particle sizes generated during hot work. The thermal and material properties are provided in Table 3.3.

Thermocouple setup

Four K-type thermocouples (18-Gauge, 0.04" diameter) with fiberglass insulation and jackets were positioned at the center of the fuel bed to measure the initial particle and ignition temperatures. The thermocouples were placed in the middle of the tray, where the heated particles were consistently dropped, ensuring direct contact with the fuel bed for precise temperature readings. Data from the thermocouples were recorded using an NI-9425 DAQ system. A schematic representation of the thermocouple setup is shown in Figure 5.3 for clarity.

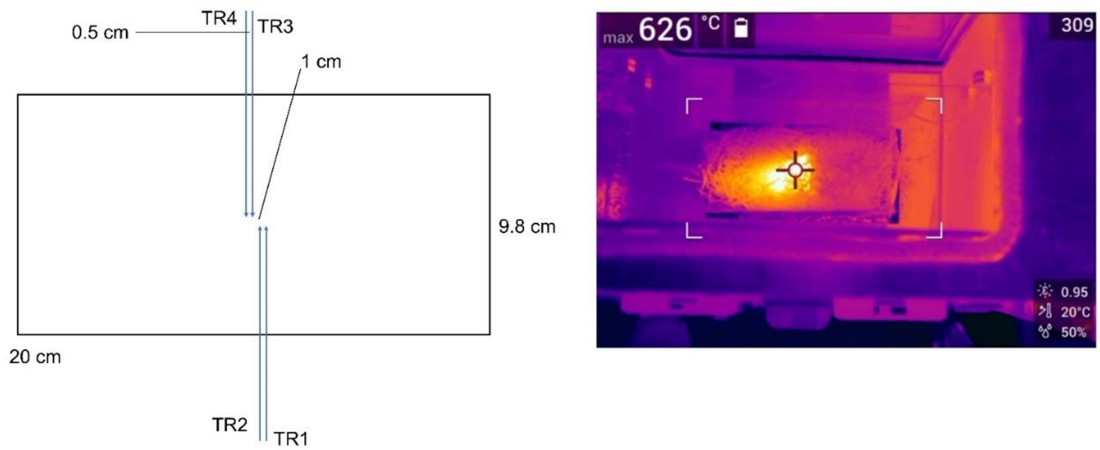

Figure 5.3 A schematic visual representation of the thermocouple setup (left) & IR camera details (right).

Infrared (IR) camera setup

An infrared (IR) camera (FLIR-E5-XT) was positioned above the fuel bed to monitor temperatures at the center. The spectral range of the infrared camera is 7.5 to 13 micrometers (µm). There was no window or barrier between the camera and the sample during the experiments, ensuring that the thermal readings were not affected by any intermediate surface. Thermocouple readings were compared with the IR temperature measurements for validation. The IR camera settings were configured according to the manual and guidelines from relevant studies, including a relative humidity of 50%, a distance of 1 meter, an ambient temperature of 20°C, and an emissivity value of 0.95. The temperature range for the IR camera was set between 20 °C and 660°C. Although the emissivity of different components in the fire environment may vary, a constant emissivity was used for temperature calculations, as the IR camera tracks a specific isotherm, reducing the effects of emissivity variation [130], [131]. The camera provided two types of temperature readings: a spatial surface temperature and a point measurement. In this study, the point measurement focused on the center of the fuel bed where ignition occurred, helping to approximate the ignition temperature and serving as a cross-check with thermocouple data. Figure 5. 3 displays an example of the IR temperature readings, showing the maximum surface temperature on the left and the point temperature on the upper right.

5.1.2 Experimental Matrix

The parameters used in this study are presented in the experimental matrix below in Table 5.2. Four different airflow speeds were selected for achieving all three types of ignitions, smoldering, smoldering-to-flaming transition, and flaming ignition across all fuel samples. The selected wind speeds (0.5, 1.0, 1.5, and 2.0 m/s) were chosen to represent a realistic range of low-to-moderate ambient wind conditions frequently observed during the early stages of wildland fires and in WUI zones. This range allows for systematic investigation of how incremental increases in airflow affect ignition characteristics and flame behavior, without introducing excessive turbulence or flame detachment that occurs at higher velocities. Furthermore, these controlled wind speeds are consistent with previous laboratory studies on fire spread and ignition dynamics [67], [156]. Which enables meaningful comparison and validation of the observed trends in ignition delay, heat transfer, and flame development. The 0.5 m/s condition serves as a near-ambient baseline, while 2.0 m/s represents an upper bound for steady wind in many experimental fire environments.

Table 5.2. Experimental matrix

Metal Particle	**Wind Velocity (m/s)**	**Fuel**
304C Stainless Steel, 4mm of 15 particles	0.5 1 1.5 2	Excelsior (Aspen Wood Fiber)
		Bromus (*Bromus tectorum and Bromus diandrus*)
		Avena Wild Oat (*Avena fatua*)
		Wheatgrass Fuels *(Thinopyrum ponticum)*

5.1.3 Ignition behavior analysis protocol

This study assessed several ignition behavior metrics, including the ignition type (flaming, smoldering-to-flaming transition, or smoldering), ignition temperature, ignition time, and total burnout time. Additionally, the fire spread rate and heat release rate were also measured to provide a comprehensive understanding of the fire spread dynamics.

The criteria for defining successful ignition were as follows: a flame ignition was deemed successful if the flame persisted for a minimum of 10 seconds, while smoldering ignition was considered successful if it lasted for at least 15 seconds. Figure 5.4, provided below, aids in understanding the ignition regime through visual observation. Flaming ignition occurs rapidly, as it is highly visible and takes place at a higher temperature. On the other hand, smoldering ignition requires a longer observation time, typically 10~15 seconds, to allow the formation of a char layer or glowing particles. Smoldering was confirmed when flameless fire spread was observed, accompanied by a visible char layer or sustained glowing for at least 15 seconds. The method for determining ignition was based on previous studies to ensure that smoldering was self-sustaining and propagating independently of the ignition source, which was confirmed by visually observing the color change of the fuel surface [22], [34]. This color transition signified the oxidation of solid char in the fuel and served as a reliable indicator of the ignition point, coinciding with the location where pyrolysis oxidation occurred, ultimately leading to smoldering ignition in the experiments [22], [34], [39], [45].

Figure 5.4 A visual representation of the different ignition process.

Ignition time refers to the moment when ignition becomes visible during the experiments. It was recorded using a stopwatch and verified by analyzing the DSLR video recordings, with the start time marked when the heated particles made contact with the fuel bed. For smoldering-to-flaming transition experiments, the transition time was defined as the moment when visible signs of flaming combustion first appeared following a period of smoldering on the fuel surface.

Ignition temperature was recorded using the thermocouples and verified by analyzing the IR camera data. Initial particle temperatures were primarily recorded with the IR camera which just before the heated particles touched the fuel beds. The spoon was already heated along with metal particles which prevented direct radiative and conductive cooling of the particles by the spoon. On average, the initial particle temperatures were found to be between 620 °C and 650 °C, with a standard deviation ranging from 15 °C to 35 °C across all particle sizes.

To improve reliability and minimize the influence of uncontrolled factors, each fuel material was tested at least five times.

5.2 Results

This section summarizes the ignition behavior of wildland fuels by analyzing critical ignition parameters, including ignition temperature, ignition time, and different ignition modes under various wind conditions. To ensure the robustness of our findings, we repeated the experiments with three different types of wildland fuels and excelsior, allowing for a comparative analysis of their ignition responses. Additionally, we incorporated a spread behavior analysis, which includes the total burnout time, rate of spread, and heat release trends during combustion under varying wind conditions. By integrating these results, we identified significant patterns in ignition behavior and combustion efficiency across different fuel types. The following subsections provide a detailed analysis of the experimental findings and dataset.

5.2.1 Modes of Ignitions on varying wind speeds

Figure 5.5 shows the significant impact of wind speed on ignition behavior across different fuel types. The results indicate that all fuel types exhibit sensitivity to wind variations, leading to diverse ignition outcomes, including flaming, smoldering, and transition ignitions across all wind speeds. In many cases, higher wind speeds promote flaming ignition and StF transitions, suggesting that increased airflow enhances oxygen availability and accelerates combustion. In contrast, lower wind speeds tend to result in more pure smoldering ignitions with no transition, likely due to reduced convective heat transfer and slower oxidation rates. Comparing ignition transitions among the fuels, bromus exhibits a stronger tendency for flaming transitions as wind speed increases, more so than avena and wheatgrass. Although avena and wheatgrass follow a similar trend – where higher wind speeds increase transition ignitions - the number of transitions is lower compared to bromus. This suggests that bromus is highly flammable and ignites readily in windy conditions, likely due to its fuel structure, which facilitates oxygen flow and accelerates combustion. In contrast, avena and wheatgrass tend to extinguish smoldering combustion more quickly rather than sustaining smoldering or transitioning between combustion modes. A striking difference emerges when comparing these wildland fuels to excelsior, which displays a high variation in ignition types across different wind speeds. Excelsior supports multiple ignition pathways, demonstrating high susceptibility to environmental changes.

Overall, Figure 5.5 highlights a key trend: increasing wind speed generally shifts ignition behavior toward flaming combustion, reinforcing the role of oxygen supply in sustaining flames. However, in some cases, wind-induced convective cooling may counteract this effect, leading to more varied ignition outcomes. These findings align with previous studies suggesting that greater oxygen availability enhances the oxidizer concentration in the combustion zone, promoting flames and increasing overall ignitability [97], [157], [158]. Though sometimes wind significantly increases convective heat losses and induced a cooling effect from the smoldering surfaces, which in turn may offset the increase in smoldering intensity related to the higher oxygen flux at higher wind speeds [37], [159].

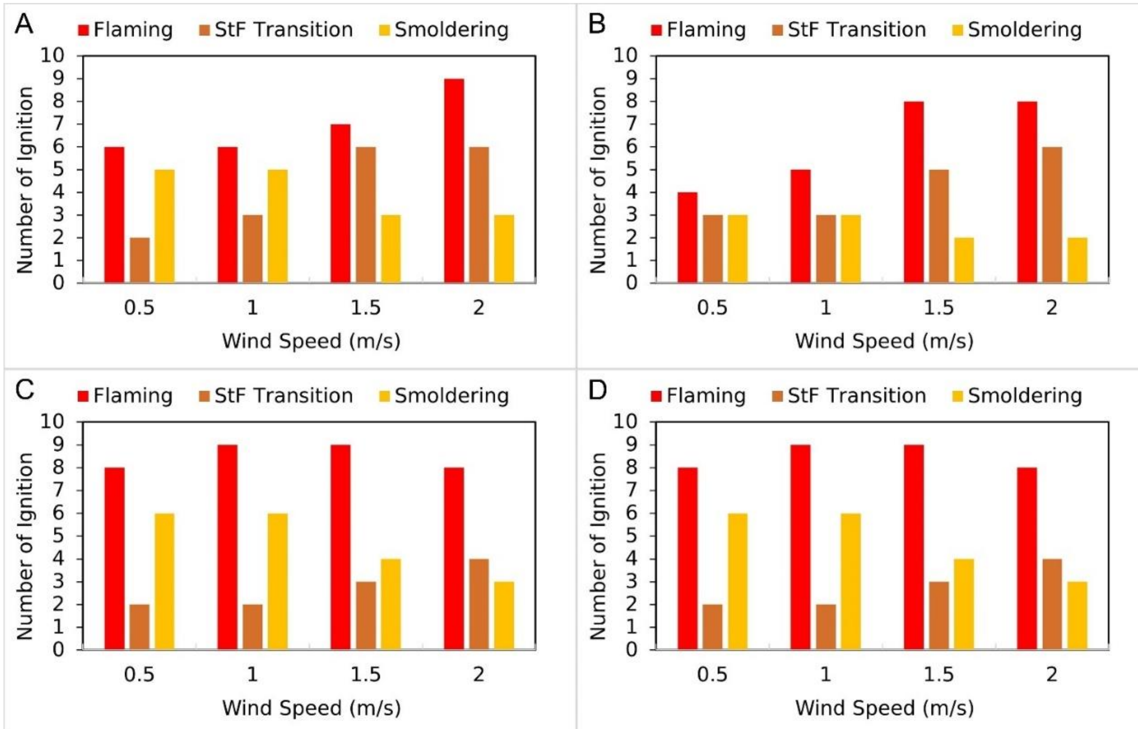

Figure 5.5 Type of ignitions of each kind of fuel in their different wind velocity condition, from left (A) excelsior fuels (B) bromus (C) avena (D) wheatgrass.

5.2.2 Ignition Time

Ignition times were measured for each ignition experiment, as ignition time provides crucial insights into the fuel's flammability and ignition delay under varying conditions, helping to predict fire behavior more accurately. While the majority of experiments exhibited direct flaming ignition characterized by the immediate appearance of flames upon the impact of heated metal particles on the fuel bed, some initially underwent sustained smoldering before gradually transitioning to flaming.

Therefore, when comparing ignition times across experiments, three ignition times were taken into account: smoldering time, StF transition time, and flaming ignition time.

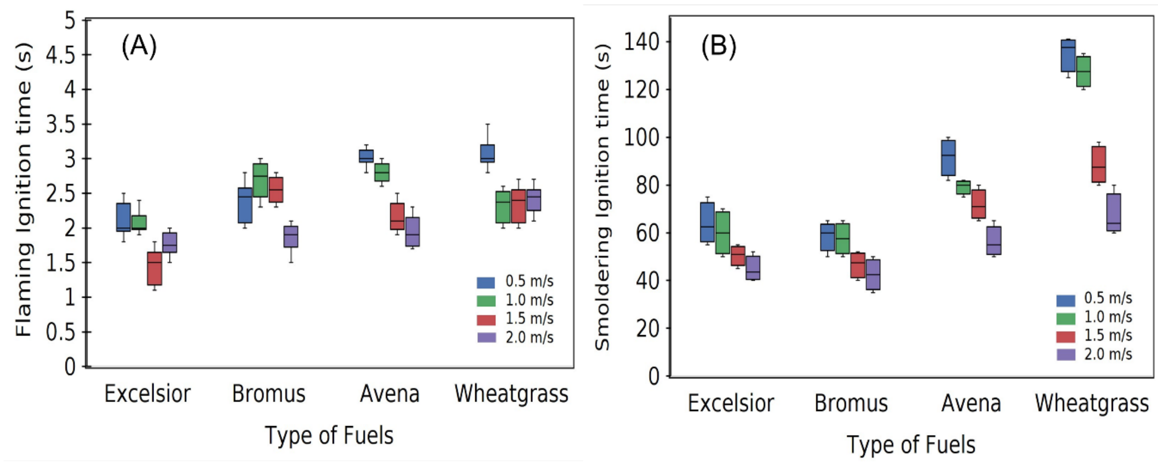

Figure 5. 6 Ignition time for each fuel species from left (A) for Flaming ignition, (B) smoldering ignition with varying wind conditions.

Figure 5.6 illustrated the impact of wind speed on flaming and smoldering ignition times across different fuel types. Flaming ignition time tended to decrease with increasing wind speed, indicating enhanced oxygen availability accelerated combustion initiation. Excelsior and bromus exhibited the shortest flaming ignition times, suggesting that these fuels were more easily ignitable under all wind conditions. In contrast, wheatgrass consistently took longer to ignite in flaming mode, implying a higher resistance to rapid combustion.

For smoldering ignition time, the trend was more variable. While excelsior and bromus ignited relatively quickly in smoldering mode, avena and wheatgrass showed prolonged smoldering ignition times, particularly at lower wind speeds. Wheatgrass stood out with the longest smoldering ignition times, especially at 0.50 and 1.0 m/s, which may have indicated lower thermal conductivity or a more compact fuel structure. The general trend suggested that higher wind speeds reduced smoldering ignition time by enhancing convective heat transfer.

When comparing the ignition times for smoldering ignitions that transitioned to flaming, we observed a similar trend. Figure 5.7 presented only transition experiments, showing the influence of wind speed on smoldering ignition time (A) and smoldering-to-flaming (StF) transition time (B) across different fuel types. The transition times shown in Figure 5.7(B) refer to the time elapsed from the moment the hot particles were dropped onto the fuel bed until the onset of flaming combustion. For instance, in excelsior fuels, at wind speeds of 0.50 and 1.0 m/s, the StF transition occurred within 40–58 seconds. As wind speed increased to 1.5 and 2.0 m/s, the transition time dropped to an average of 32 and 21 seconds, respectively.

A similar decreasing trend in StF transition time was evident for avena fuels, though the absolute values were higher than those for excelsior. At 0.5 m/s, the transition time for avena ranged from 82 to 101 seconds, whereas at 1.0 m/s, it reduced to 78 seconds. As wind speed increased, the transition time further dropped to 52 seconds at 1.5 m/s and 40 seconds at 2.0 m/s, indicating that wind played a crucial role in accelerating the combustion process.

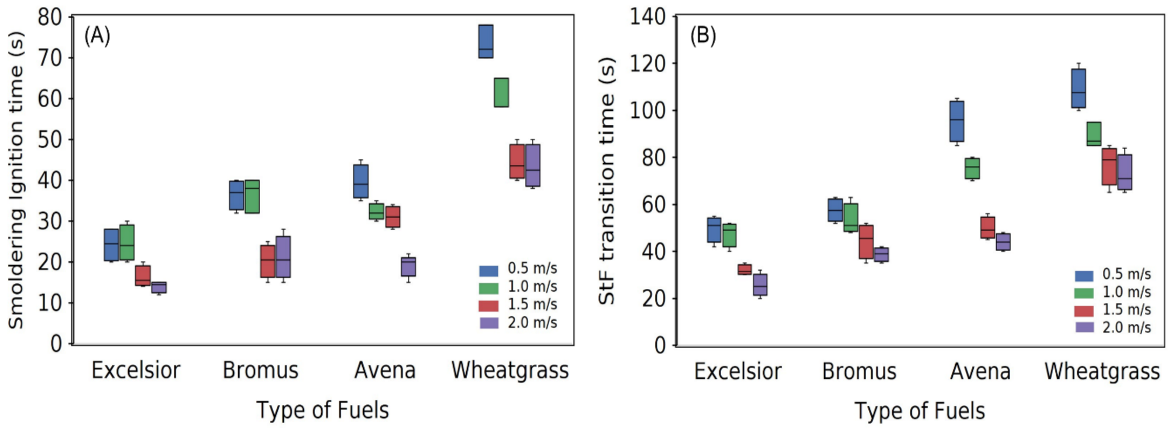

Figure 5.7 Ignition time for each fuel species from left (A) for smoldering ignition, (B) for StF transition ignition with varying wind conditions.

Overall, the trends showed that higher wind speeds reduced all types of ignition times, including transition times across most fuels, likely due to increased oxygen supply and enhanced heat transfer. This effect might be explained by the fact that higher wind speeds increased convective heat transfer to the fuel surface, raising its temperature more rapidly and leading to quicker ignition. This closely aligns with previous works such as those by Wang et al. which showed that as the wind speed increases, the flaming delay time decreases, regardless of whether it is direct flaming or a transition from smoldering [22]. Their analysis leveraged a theoretical framework that considered the inherent complexity of the fuel bed structure and the dynamic nature of particle deposition. In applying such model they noted that in cases of rapid direct flaming ignition, the hot particle serves as both the heating and pilot source [100]. As a result, the classical pilot ignition theory for thermally thin fuels, as described by Quintiere et al, was employed to estimate the ignition delay time [160]. This approach was similarly used by Wang et al. to perform heat transfer analysis [22]. As described by Quintiere (2006), the ignition time,

$$t_f = \frac{\rho_f \delta_f [c_f(T_{ig} - T_a) + FMC\Delta H_{ev}]}{\dot{q}_p''} = \frac{\rho_f \delta_f [c_f(T_{ig} - T_a) + FMC\Delta H_{ev}]}{h_p[\overline{T_p} - \overline{T_f}]} \quad (1)$$

Where t_f is time to ignition, ρ_f fuel density (kg/m³), δ_f is the characteristic length of fuel for the current discrete and porous fuel bed, $\dot{q}_p''$ is the heat flux from particle to fuel, c_f specific heat capacity of the fuel (J/kg·K), T_{ig} ignition temperature, T_a ambient temperature, FMC fuel moisture content, ΔH_{ev} is the heat of water evaporation = 2.26 MJ/kg, h_p convective heat transfer coefficient, $\overline{T_p}$ average initial particle temperature, $\overline{T}_f$ fuel surface temperature to the ignition zone. Given that the heat transfer coefficient is directly affected by the wind flow, equation (1) clearly points to a decrease in ignition delay time due to enhancements to the heat transfer coefficients occurring as a result of increasing wind speeds.

When comparing all fuels, bromus and excelsior consistently ignited more quickly than avena and wheatgrass, suggesting that these fuels had higher flammability potential and required less time to transition into flaming combustion likely due to their fine structure and greater oxygen accessibility [20], [40].

Overall comparing Figures 5.6 and 5.7, two key observations should be noted: (1) variation in ignition time across different wind speeds and fuel types was significantly lower in flaming ignition compared to smoldering ignition, (2) faster smoldering promoted a successful transition to flaming ignition, whereas slower smoldering often led to extinction before transitioning.

5.2.3 Burnout Time

In addition to ignition time, another temporal parameter that provided important insight into the effect of wind on ignition behavior was burnout time. In this study, consistent with prior work, burnout time referred to the duration from the moment of ignition to the moment flaming ceased, regardless of whether all available fuel was fully consumed or not [101], [139], [140]. Examining burnout time was important for predicting fire behavior and duration, enabling better planning for fire suppression and risk assessment.

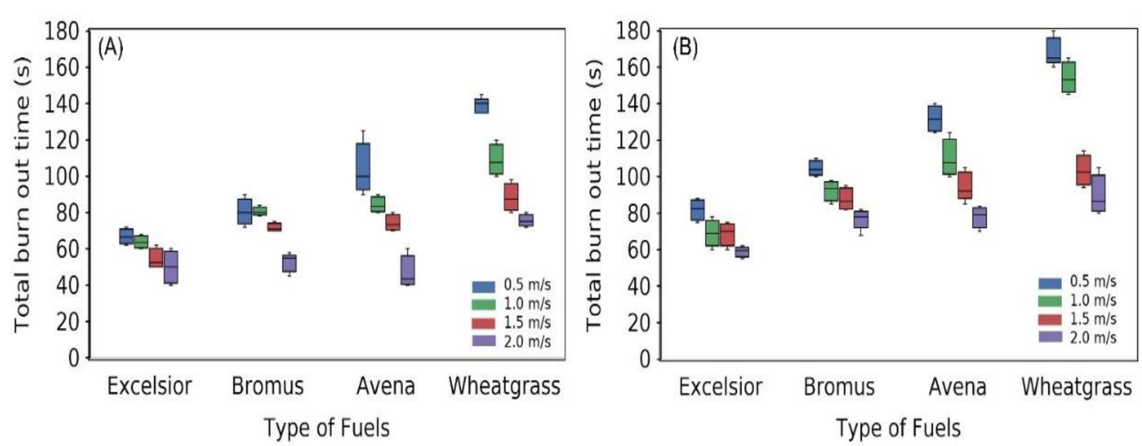

Figure 5. 8 Total burnout time for each fuel species from left from left (A) for Flaming ignition, (B) for StF transition ignition with varying wind conditions.

Figure 5.8 illustrated a clear trend in which higher wind speeds led to shorter burnout times across all fuel types. For instance, in the flaming ignition cases shown in Figure 5.8 (A), the total burnout time for excelsior fuels decreased from approximately 60–70 seconds at 0.50 m/s to around 40–50 seconds at 2.0 m/s. Avena and bromus also exhibited similar reductions in burnout time with increasing wind speed, indicating that higher wind speeds promoted faster combustion completion. Interestingly, wheatgrass showed the longest burnout duration at low wind speeds, exceeding 140 seconds at 0.50 m/s, but dropped significantly under higher wind conditions, reaching 60-70 seconds at 2.0 m/s.

The observed decrease in total burnout time with increasing wind speed can be attributed to the combined effects of enhanced oxygen supply and convective heat transfer. Increasing the wind speeds helps two ways to make the total burn efficiently which makes the total burn out time shorter. The two ways are:

1. Increased Oxygen Supply → Faster Reaction Rate and
2. Enhanced Convective Heat Transfer → Rapid Flame Propagation.

As explained by the general convective heat transfer coefficient equation and supported by previous studies, the convective heat transfer coefficient increases with wind speed [67], [161], [162]. This increase in the heat transfer coefficient leads to greater convective heat transfer to adjacent unburned fuel, which promotes faster ignition across the fuel bed. As a result, the time required for complete combustion is reduced, whether the ignition is smoldering, or direct flaming or a transition from smoldering [38], [67], [69], [163]. Another study by Andrews et al. explained that higher wind speeds allow the fire to spread more rapidly while consuming less fuel per unit area before advancing, thereby reducing fire residence time through intensified convective heat transfer [66].

Another observation from this study was that total burnout times for StF transitions were generally longer and exhibited more variability than those for flaming ignitions. This suggested that the smoldering phase prolonged the combustion duration before transitioning to complete burning. While the wind effect was still noticeable, the differences in burnout time between wind conditions appeared less pronounced in bromus and wheatgrass, suggesting that some fuels might not experience the same oxygen-driven acceleration in combustion.

5.2.4 Ignition temperature

Figure 5.9 presents the flaming ignition temperature curves for different fuel types (excelsior, bromus, avena, and wheatgrass) under varying wind conditions (0.50 m/s, 1.0 m/s, 1.5 m/s, and 2.0 m/s). Figure 5.9 consists of four subplots (A–D), showing the temperature evolution over time for each fuel type. Each plot in Figure 5.9 displays a sharp rise in temperature, reaching a peak before declining, representing the ignition and combustion phases. The heated particles drop point is shown with the dotted line with its individual color for the wind speed and the red stars indicate the exact moment of flaming ignition. To improve the visibility of each temperature curve and avoid overlapping, the x-axis values were intentionally offset. This adjustment was made to ensure that the individual ignition trends could be distinguished more clearly, as flaming ignition occurs within a very short timeframe after the heated particles are dropped onto the fuel bed. Without this offset, the curves would largely overlap due to their close ignition timings. It is important to note, however, that all experiments were conducted following the same procedure, and the x-axis shifts are solely for visual clarity.

In Figure 5.9, the ignition time is recorded around 9–12 seconds after the drop of the heated particles, whereas in Figure 5.6, ignition times are observed between 1–3 seconds for all flaming ignition cases. This discrepancy is due to a time lag in the thermocouple data. Upon examining the thermocouple readings, it was found that ignition appeared to lag by approximately 10 seconds compared to the timing captured in the video and IR images. This delay reflects the preheat response time of the thermocouples. The 10-second lag observed in the thermocouple data indicates the time it takes for the thermocouples to reach steady-state conditions after the heated particles drop onto the fuel bed. When the particles initially make contact, the thermocouples, which are at atmospheric temperature, require this time to accurately measure the rise in temperature due to the ignition. This delay is through calibration and assessment. It does not necessarily indicate that the thermocouples are too large or improperly placed but rather reflects the expected due to the thermocouples' response time, which determined inherent response time of the sensors to stabilize at the new temperature conditions.

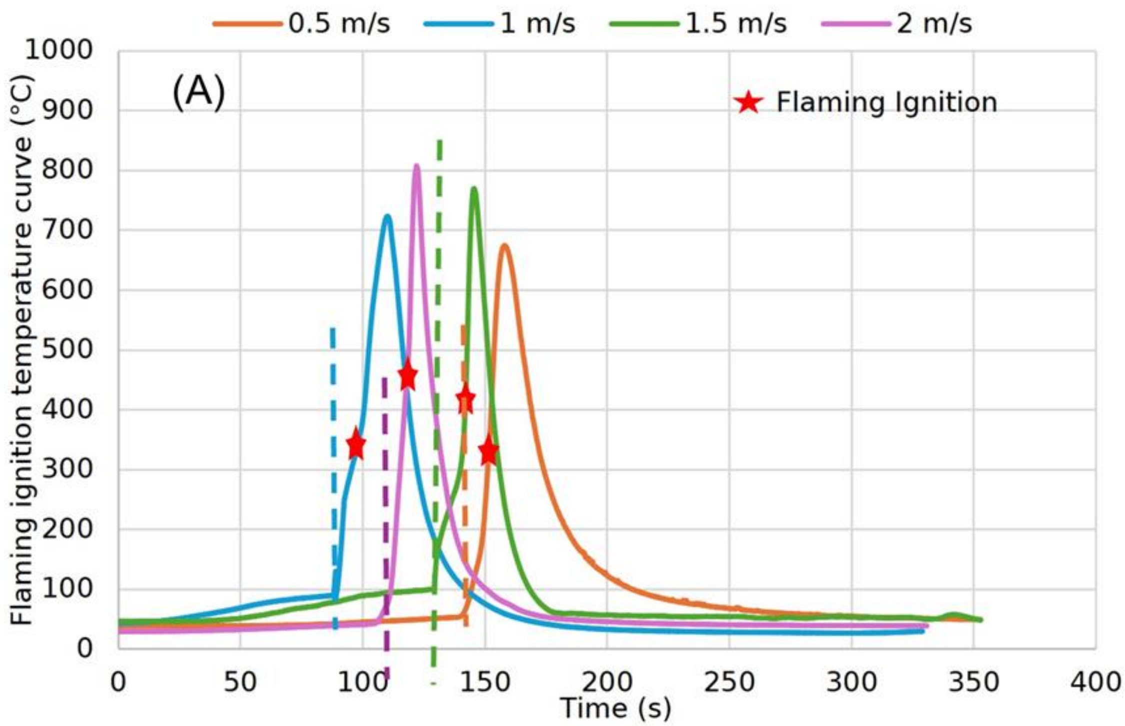
0.5 m/s
1 m/s
1.5 m/s
2 m/s
(A)
Flaming Ignition
Flaming ignition temperature curve (°C)
Time (s)

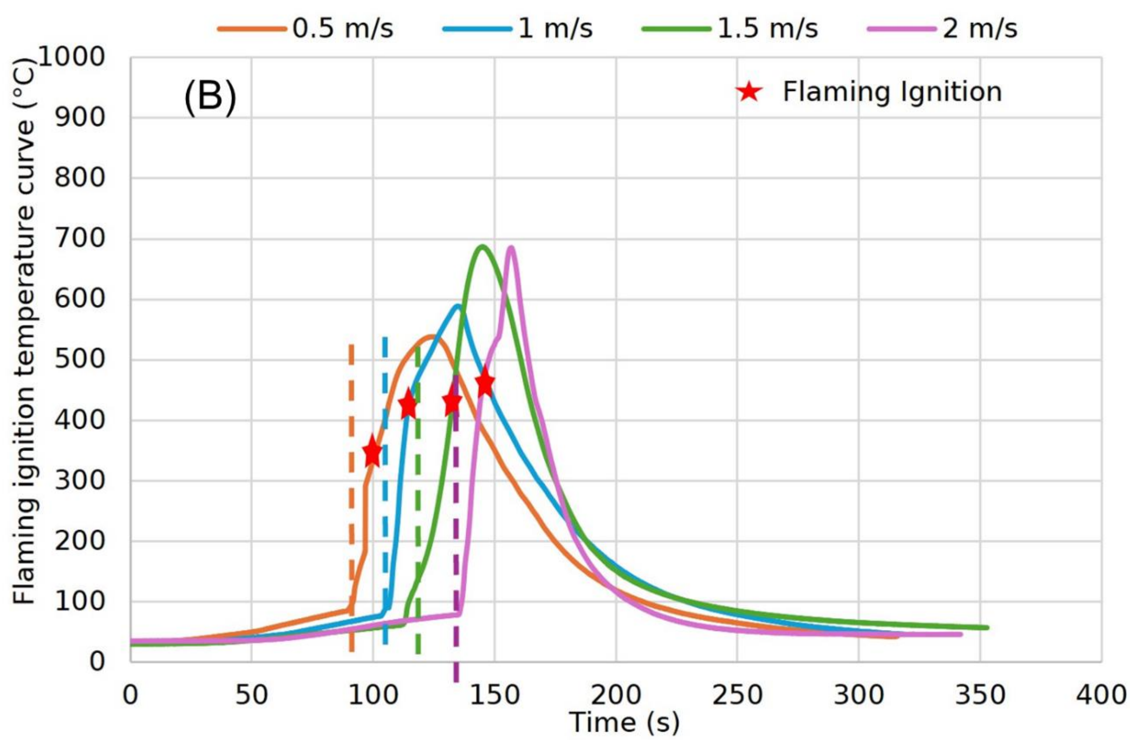
0.5 m/s
1 m/s
1.5 m/s
2 m/s
(B)
Flaming Ignition
Flaming ignition temperature curve (°C)
Time (s)

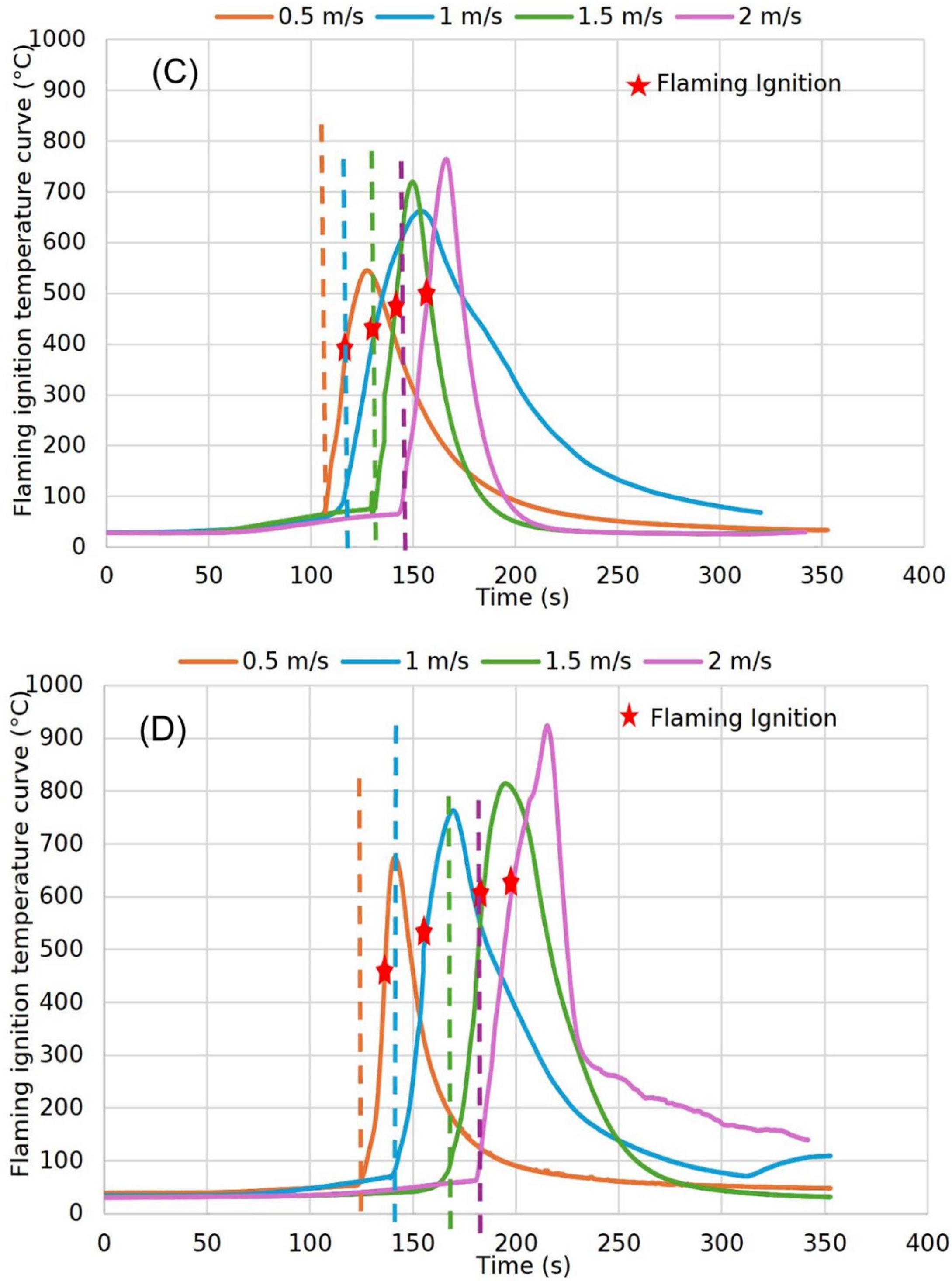

Figure 5. 9 Flaming ignition temperature curves for various fuel in different wind speeds, from left (A) excelsior fuels (B) bromus (C) avena (D) wheatgrass.

Figure 5.9 reveals a clear trend in which higher wind speeds generally result in elevated ignition and peak temperatures. To gain a clearer insight into the effects of wind speed on ignition temperature, Figure 5.10 presents the ignition temperatures for both flaming and smoldering ignitions. The figure highlights three key observations: (1) Flaming ignition temperatures were significantly higher than smoldering ignition temperatures for all fuel types; (2) Wind speed had a considerable impact on ignition temperature in both ignition modes; and (3) Wheatgrass consistently exhibited higher ignition temperatures compared to the other fuels.

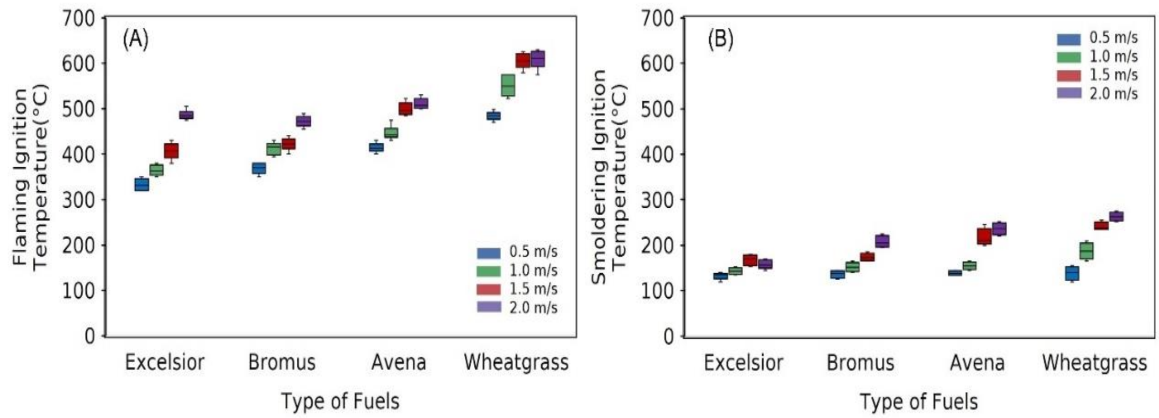

Figure 5. 10 Comparison of flaming (A) and smoldering (B) ignition and temperature for various fuels in different wind speeds.

For instance, in flaming ignition cases, the ignition temperature for excelsior increased with wind speed, reaching nearly 500 °C at 2.0 m/s, compared to around 330 °C at 0.50 m/s. A similar trend was observed in wheatgrass, where ignition temperatures rose from approximately 450 °C at 0.50 m/s to around 620 °C at 2.0 m/s. Likewise, bromus and avena and wheatgrass followed this pattern, with higher wind speeds leading to faster ignition (Figure 5.6) and elevated peak temperatures (Figure 5.10). Similar trends have been followed in smoldering ignition cases as well. The smoldering ignition temperature for excelsior reached nearly 180 °C at 2.0 m/s, compared to around 130 °C at 0.50 m/s. This trend suggested that increased wind speeds enhanced convective heat transfer, leading to higher ignition temperatures. The rise in temperature at the point of ignition could be attributed to the greater availability of oxygen and the increased transfer of heat to the fuel surface, which together accelerated combustion. Consequently, stronger winds could create a more intense ignition environment, characterized by elevated hot gas temperatures and a shift in the ignition regime toward higher temperature thresholds [159]. Further supporting this relationship, studies by Chen et al. and Xie et al. demonstrated that increased airflow enhances combustion behavior [36], [38] . Chen et al. found that higher oxygen flow rates (4–24 m/s) resulted in higher peak temperatures during both flaming and smoldering ignition, primarily due to intensified char oxidation under stronger airflow [38] . Similarly, Xie et al. observed a near-linear increase in both the smoldering spread rate and peak temperature with rising wind velocity, highlighting the critical role of oxygen availability in promoting combustion efficiency [36] . Together, these findings reinforce the conclusion that wind not only supplies oxygen but also enhances convective heat transfer, thereby contributing to higher ignition temperatures.

While comparing the ignition temperature only for smoldering ignitions that transitioned to flaming (Figure 5.11), we observed a similar trend. In addition to smoldering ignition temperatures, the smoldering-to-flaming (StF) transition temperatures were also examined and are presented Figure 5.11.

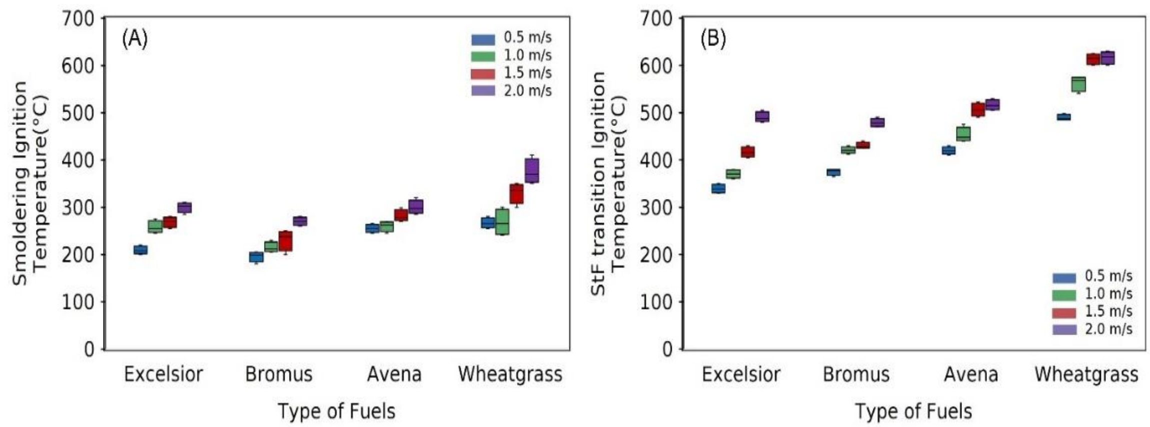

Figure 5. 11 Comparison of smoldering ignition and StF transition ignition temperature for various fuel in different wind speeds.

The data indicated a clear trend in which higher wind speeds resulted in elevated ignition temperatures across all tested fuels, similar to the trend observed for flaming ignition temperatures. This increase in ignition temperature with wind speed was likely due to enhanced convective heat transfer and higher oxygen availability, which accelerated heat release and flame propagation.

Additionally, when comparing Figures 5.10 and 5.11, it was evident that smoldering ignition temperatures were higher in cases where a transition to flaming occurred, whereas smoldering with lower ignition temperatures tended to extinguish rather than transition to a flaming state. This highlights the point that smoldering ignition temperature establishes a threshold beyond which a proper transition to flaming ignition becomes unlikely, leading instead to extinction. If the temperature does not surpass this critical level, sustained combustion may not occur, reinforcing the importance of ignition temperature as a key factor in fire spread dynamics.

5.2.5 Rate of spread analysis

This study also examined the rate of spread (ROS), which helps analyze ignition behavior by indicating how quickly fire propagates after ignition - reflecting energy release and combustion dynamics. A common method was used to determine the fire spread rate in this study: the cumulative spread rate, calculated as the total distance traveled by the fire divided by the total time of travel [158] .

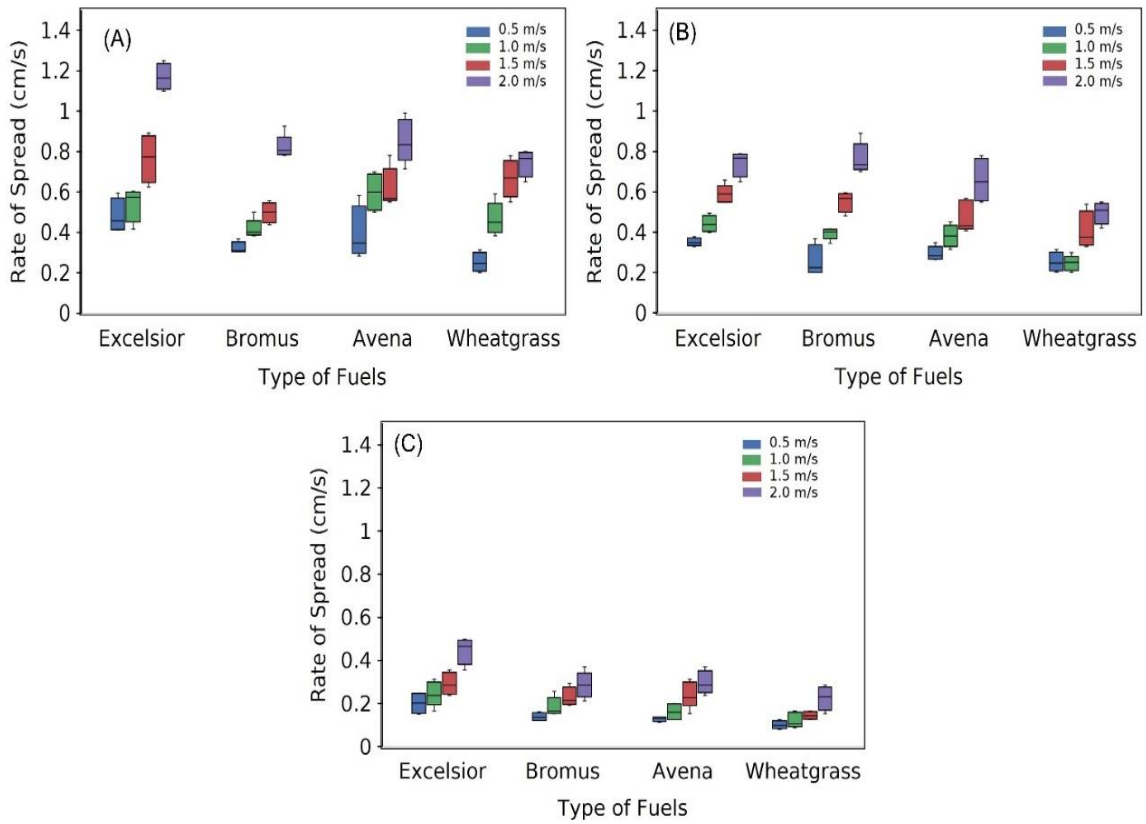

Figure 5. 12 Average calculated Rate of spread for various fuels in different wind speeds, both for flaming (A), StF transition (B) and smoldering (C) ignitions.

Figure 5.12 presents a comparative analysis of the Rate of Spread (ROS) across different fuel types under varying wind conditions. The comparisons highlight the significant influence of wind speed on ROS across all fuel types and ignition types, including flaming, smoldering, and StF transitions. For instance, in Excelsior fuels, the ROS during flaming ignition peaked at approximately 1.2 cm/s at a wind speed of 2.0 m/s, and dropped to 0.42 cm/s when the wind speed was reduced to 0.5 m/s. Similarly, in Wheatgrass fuels, the ROS for flaming ignition peaked at 0.79 cm/s at 2.0 m/s and decreased to 0.22 cm/s at 0.5 m/s. A similar trend where increasing wind speed resulted in higher ROS was also observed for the other two fuels, Bromus and Avena. The results further indicate that ROS values are significantly lower during smoldering ignition compared to StF transition and flaming ignition. For example, in Avena fuels, the ROS was 0.31 cm/s during smoldering ignition, whereas it increased substantially to 0.79 cm/s and 0.62 cm/s during flaming and StF transition ignition, respectively, at the same wind speed of 2.0 m/s.

The relationship between wind speed and ROS has been consistently observed in both experimental and modeling studies [67], [70], [122], [158], [164]. A study by Butler et al higher wind speeds enhance convective heat transfer, resulting in faster preheating and ignition [67]. Under wind speeds below 10 m/s, ROS increased linearly by about 3% per unit wind speed, aligning with models, which aligned with other laboratory-based models and found the similar trend [68], [165], [166].

Wind effects were also evident in smoldering and smoldering-to-flaming transitions [36], [38] . A study by Chen et al. showed that durations for all combustion (smoldering and flaming) processes decrease, as the airflow velocity increases due to rising oxygen supply and oxidation rate increase the smoldering or flaming ignition temperature, thus, accelerating both the heat-transfer and burning processes, results decrease the rate of spread [38]. Particularly for smoldering ignition cases, a study by Xie et al. observed that the smoldering spread rate increases with increasing airflow, as it resembles a burning or fuel-regression process, similar to candle combustion or a premixed flame, where the smoldering mass burning flux rises with greater air mass flux supply within the fuel bed [36]. Although the maximum wind speed in our study was limited to 2 m/s, a sharper rise in ROS might have been observed if wind velocities above 2.5 m/s had been tested, as demonstrated by previous experimental and theoretical studies [162], [165]–[168].

In addition, some studies suggest that fire spread in windy conditions is governed by buoyancy and inertia, resulting in two distinct fire types: plume-dominated fires and wind-driven fires. Plume-dominated fires are primarily influenced by radiation, where the upward movement of hot gases (due to buoyancy) drives fire spread. In contrast, wind-driven fires are mainly controlled by convection, where wind pushes the flames forward, facilitating spread. In some cases, both radiation and convection contribute to fire propagation [68], [78], [169].

5.2.6 Heat release rate analysis

This study also examined the heat release rate (HRR) at different wind speeds to determine whether higher airflow significantly affected sustained ignition behavior. The heat release analysis further explored whether wind speed influenced ignition behavior favorably or unfavorably meaning that higher winds could either enhance oxygen availability, promote ignition, or increase heat loss, thereby extinguishing the ignition process. Studying HRR is important because it plays a crucial role in understanding the combustion process, fire behavior, and fire propagation rates. It is also one of the most significant predictors of fire hazard [170]–[172].

The heat release rate was calculated using the mass loss rate, by multiplying the heat of combustion [122].

$$HRR = MLR * Heat\ of\ Combustion$$

Where HRR is heat release rate and MLR is the mass loss rate, and the heat of combustion is given in MJ/kg for each fuel. The following heating values were used for flaming ignition in the calculations: 32.37 MJ/kg for excelsior, 18.707 MJ/kg for bromus, 18.07 MJ/kg for avena, and 16.94 MJ/kg for wheatgrass [122], [159], [173]–[176]. Since specific data on the heat of combustion during smoldering combustion for the selected fuels are not readily available from existing literature, previous studies suggest using an effective heat of combustion in the range of 6–12 MJ/kg for smoldering ignition, compared to typical values of 16–30 MJ/kg for flaming combustion [45], [177]. As the previous study suggests the following heating values were used for smoldering ignition in calculations: 14.6 MJ/kg for excelsior, 8.42 MJ/kg for bromus, 8.13 MJ/kg for avena, and 7.62 MJ/kg for wheatgrass.

Figure 5.13 presents a comparative analysis of heat release rate (HRR) across different fuel types under varying wind conditions. The results indicate that HRR is surely affected by wind speed for all fuel types and ignition conditions including flaming, smoldering or StF transition ignitions.

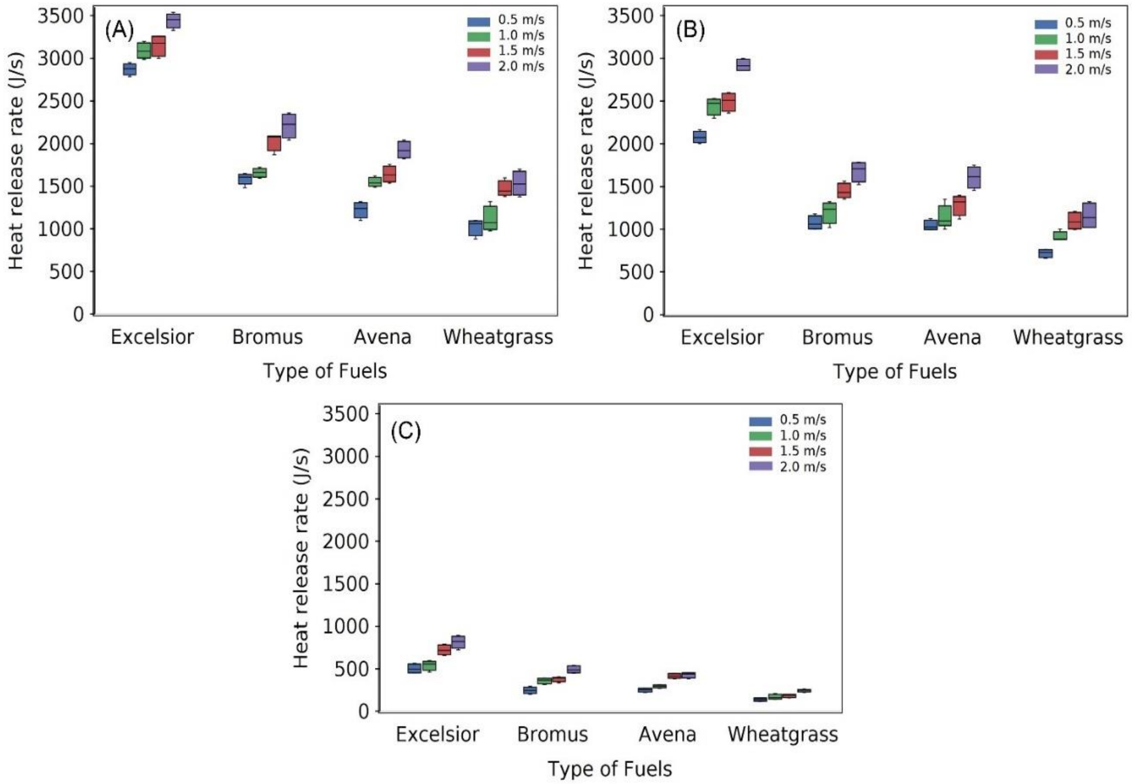

Figure 5. 13 Average calculated Heat release rate for various fuels at different wind speeds, from left (A) for flaming ignition, (B) for StF transition, (C) for Smoldering Ignition.

For instance, in Excelsior fuels, the HRR during flaming ignition peaked at approximately 3498 J/s at a wind speed of 2.0 m/s, and dropped to 2985 J/s when the wind speed was reduced to 0.5 m/s. Similarly, in Wheatgrass fuels, the ROS for flaming ignition peaked at 1621 J/s at 2.0 m/s and decreased to 1013 J/s at 0.5 m/s. A similar trend where increasing wind speed resulted in higher HRR was also observed for the other two fuels, Bromus and Avena. The results further indicate that HRR values are significantly lower during smoldering ignition compared to StF transition and flaming ignition. For example, in Avena fuels, the HRR was 485 J/s during smoldering ignition, whereas it increased substantially to 1825 J/s and 1551 J/s during flaming and StF transition ignition, respectively, at the same wind speed of 2.0 m/s. These lower HRR values from smoldering ignition indicate that when the HRR remains too low, the heat output is insufficient to sustain the transition from smoldering, leading to extinction rather than flame propagation. This analysis aligned with previous studies which found that increasing the flow increases the total mass flux is much higher in case of smoldering to flaming transition compared to simple smoldering experiments [36], [38]. In parallel, wind speed appears to play a dual role while it enhances oxygen supply and convective heating, it may also disrupt heat retention within the smoldering zone, thereby suppressing the transition and promoting extinction.

This HRR trend with wind speed aligns with previous studies, which indicate that higher wind speeds increase local flame - fuel contact frequency and enhance intermittent convective heating of the fuel bed surface. [158], [164]. Previous studies have shown that total heat flux, whether radiative or convective - increases with rising wind velocity [73], [161], [162]. To further explain this increase, these same researchers have emphasized the role of flame angles. As wind velocity increases, the flame angle decreases, causing the flame to tilt closer to the fuel surface. This alignment enhances convective heat transfer between the flame and the unburnt fuel, thereby increasing the overall heat flux delivered to the fuel bed. It can summarize that stronger winds push flames forward, increasing the rate of heat transfer to unburned fuel, which accelerates ignition and promotes faster fuel consumption. Consequently, this leads to higher HRR values, as the effects of more rapid ignition also enhance mass loss [70], [71], [164].

5.3 Summery

This study provided a comprehensive investigation into the ignition behavior and StF transition of various fuels (excelsior, bromus, avena, and wheatgrass) under controlled wind tunnel conditions. Key combustion parameters, including ignition temperature, ignition time, total burnout time, rate of spread (ROS), and heat release rate (HRR) were analyzed across a range of wind speeds (0.5–2.0 m/s), revealing how airflow dynamics and fuel properties interact to influence fire development.

Ignition behavior showed consistent trends across all fuel types with varying wind speeds. As wind speed increased, ignition temperatures rose while ignition times decreased, reflecting enhanced convective heat transfer and oxygen availability. This indicated a strong correlation between wind-enhanced convective heat transfer and the elevated fuel temperatures leading to ignition. Similarly, ignition time was found to be related to ignition temperature, with higher ignition temperatures resulting in faster ignition. Fuels with more open structures (e.g., excelsior and bromus) demonstrated quicker ignitions, while denser fuels like wheatgrass exhibited delayed response due to restricted airflow. In continuation, burnout time exhibited contrasting behavior depending on wind conditions as well as the combustion mode. Flaming ignitions tended to burn out faster under higher winds due to rapid combustion, while smoldering-to-flaming transitions showed longer and more variable durations, influenced by the fuel's structural properties and the energy required for sustained transition. Wheatgrass showed the longest burnout duration at low wind speeds but experienced significant reduction under high wind, suggesting wind-driven oxygen enhancement overcame its structural resistance. Further, both the rate of spread (ROS) and heat release rate (HRR) increased with wind speed across all ignition modes. These trends highlight the role of wind in promoting flame-fuel interaction and intensifying combustion. The study identified a higher HRR required for smoldering fires to transition into sustained flaming combustion, reinforcing the importance of energy output in fire dynamics.

Finally, the study also focuses on fuel properties to highlight the physical and chemical influences of different fuels on ignition behavior, even under varying wind conditions. The results demonstrate that fuel structure and composition significantly affect how a material responds to heating and airflow. Excelsior and bromus, with their fibrous, low-density structures and moderate lignin content and higher cellulose content, facilitated quicker ignition and higher combustion intensity. In contrast, avena and wheatgrass, which possess denser matrices and higher lignin and protein content, exhibited delayed ignition, lower HRR, and longer burnout times. These properties are associated with restricted oxygen diffusion, and slower char oxidation. The higher activation energy required for lignin decomposition further contributes to their resistance to ignition. These observations underscore the importance of considering intrinsic fuel characteristics when assessing ignition potential and fire dynamics, particularly in wind-driven wildfire scenarios.

These findings underscored the vital role of wind in accelerating ignition, intensifying fire energy output, and enhancing sustained ignitions, while also highlighting that fuel properties critically influence ignition thresholds, combustion behavior, and fire spread potential. Together, these insights support improved fire modeling, risk assessment, and the development of targeted wildfire mitigation strategies. Such insights are crucial for wildfire management, especially in Wildland–Urban Interface (WUI) areas, where fire behavior is highly dynamic. Incorporating wind effects into predictive fire models can improve fire prevention strategies, enhance safety protocols, and support more effective firefighting approaches. Future research should consider additional factors, such as fuel moisture content and localized temperature variations, to further refine fire behavior predictions, enhance fire modeling accuracy, and strengthen risk mitigation efforts.

Acknowledgement

I thank Cobian-Iñiguez Fire Lab for their support in the research work. My special thanks go to the undergraduate students – Juan Hernandez, Jason Estevez, and Gen Duenas for their invaluable assistance and contribution in conducting experiments. This research is supported through startup funding from the University of California, Merced, School of Engineering.

Chapter 6

Influence of Wind Gusts on Ignition Dynamics and Heat Release in Wildland Fuels.

Wind gusts are known to significantly influence wildfire behavior, yet their direct role in ignition dynamics remains underexplored in laboratory settings. This study investigates how controlled wind gusts affect ignition behavior, combustion transitions, and heat release characteristics of wildland fuels using a bench-scale wind tunnel. Three fuel types, excelsior, wild oat (avena), and wheatgrass were exposed to heated stainless-steel particles under varying wind speeds (1.0 and 2.0 m/s) and gust frequencies (0.03, 0.05, and 0.07 Hz). Key ignition parameters, including ignition temperature, ignition delay, StF transition, burnout time, and heat release rate (HRR), were measured and analyzed. Results show that increasing gust frequency consistently reduces ignition and transition times across all fuels while raising ignition temperatures and HRR. HRR also increased notably, rose in excelsior during flaming ignition at high gust frequencies. These findings indicate that gusty winds enhance convective heat transfer and oxygen availability, accelerating fire initiation and intensifying combustion. The results offer valuable insights for improving predictive fire spread models, ignition risk assessments, and wildfire mitigation strategies under transient wind conditions.

6.1 Materials and methods

6.1.1 Experimental apparatus and procedure

The experiments were conducted in a bench-scale subsonic wind tunnel measuring 82.3 cm in length, 15.6 cm in width, and 42.5 cm in height. The tunnel was constructed from 4 mm thick aluminum sheets, as shown in Figure 6.1. A 6-inch inline axial fan was positioned on the left side of the wind tunnel and controlled by a Raspberry Pi module. Downstream of the fan, the system includes a diffuser, honeycomb, mesh screens, an electric heater, and the test section. In addition, a DSLR camera, an infrared camera, and thermocouples are used to assist with the methodology.

The test section measures 15.6 cm in width and 28 cm in height, with a length of 30 cm. It is enclosed with heat-resistant ceramic glass on both sides and has an open top. Inside the test section, a custom aluminum tray was used as the primary fuel bed, which measures 20 × 9.8 × 7.62 cm (length × width × height). The fuel bed was always placed on top of a measuring scale to monitor mass loss throughout the experiments. A thermostat is connected to the electric heater to control the airflow at 30.5 ± 1.3 °C inside the wind tunnel. A steel spoon measuring 34 cm in length and 8.2 cm in bowl diameter is also used to hold the metal particles, which are heated with a propane torch to initiate the ignition source in the fuel bed. The wind tunnel is enclosed in a fireproof fume hood, and the full setup is depicted in Figure 6.1. A moisture analyzer MX-50 used in this study to ensure the moisture content in the fuels.

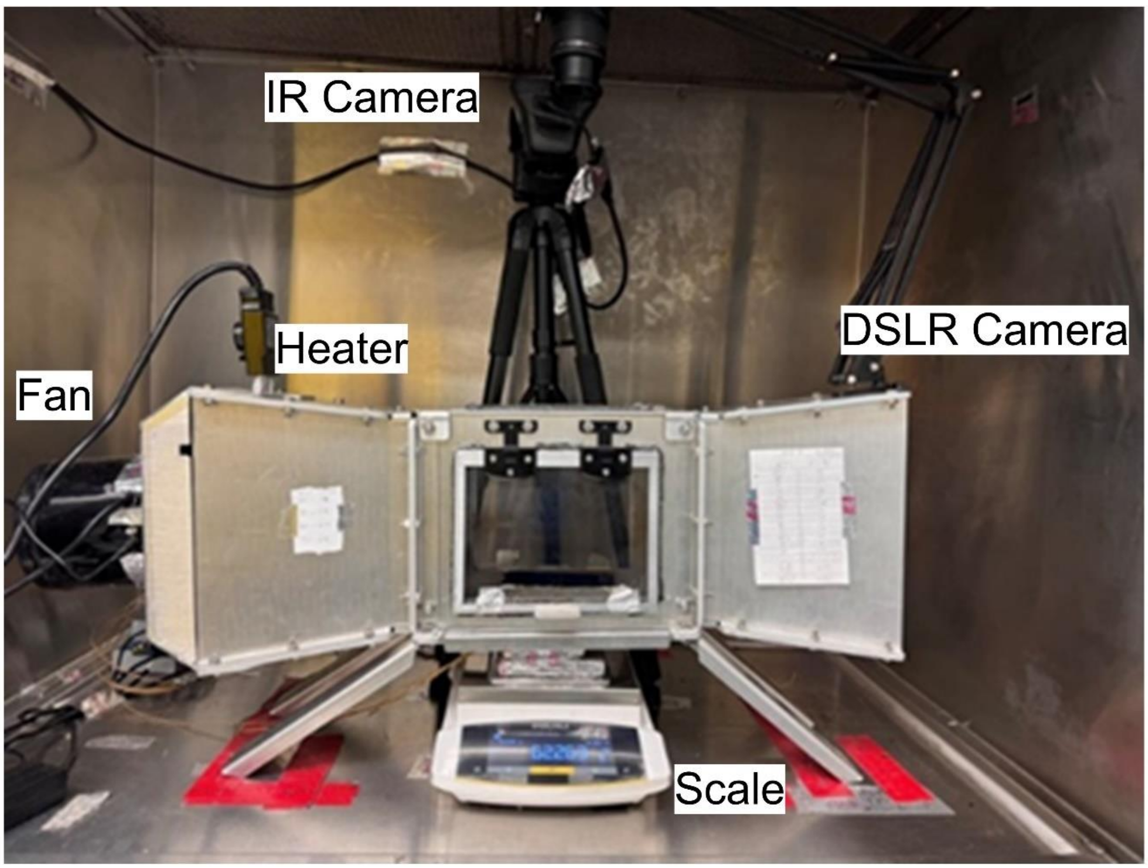

Figure 6.1 Photograph of experimental apparatus and procedure.

Fuel bed preparation

Four types of fuels were examined to investigate ignition behavior in this study. The details of the fuel properties are shown in Table 5.1. One prefabricated fuel (excelsior) was considered the standard fuel, while the other three fuels were classified as wildland fuels, as they were collected from the field (as shown in Figure 6. 2).

All fuels were oven-dried at 90 °C for 24 hours to reduce moisture content and confirm that it was below 3%. Moisture content was then tested with a moisture analyzer with a measurement accuracy ±0.10%. For each experiment, 15 grams of fuel were evenly distributed in the steel tray, focusing on standardizing fuel mass rather than bulk density to ensure consistent fuel quantity across experiments.

Figure 6. 2 Photograph of fuels.

Ignition source

15 spherical particles of 304C stainless steel, each 4 mm in diameter, were heated with a propane torch for 90 seconds and were dropped simultaneously from a height of 8-10 cm to assess ignition behavior. The heating time was carefully controlled to avoid breaking or melting the particles, with a stopwatch and video recording used to verify both heating and ignition times. In choosing the particle size for this study, we based our selection on previous research examining the impact of heated particles on spot fire ignitions [24], [26], [47]. To align with the sizes used in these studies, we selected 4 mm particles, which not only allowed us to replicate previous findings but also to simulate real-world particle sizes generated during hot work. The thermal and material properties are provided in Table 3.3.

Thermocouple setup

Four K-type thermocouples (18-Gauge, 0.04" diameter) with fiberglass insulation and jackets were positioned at the center of the fuel bed to measure the initial particle and ignition temperatures. The thermocouples were placed in the middle of the tray, where the heated particles were consistently dropped, ensuring direct contact with the fuel bed for precise temperature readings. Data from the thermocouples were recorded using an NI-9425 DAQ system. A schematic representation of the thermocouple setup is shown in Figure 6.3 for clarity.

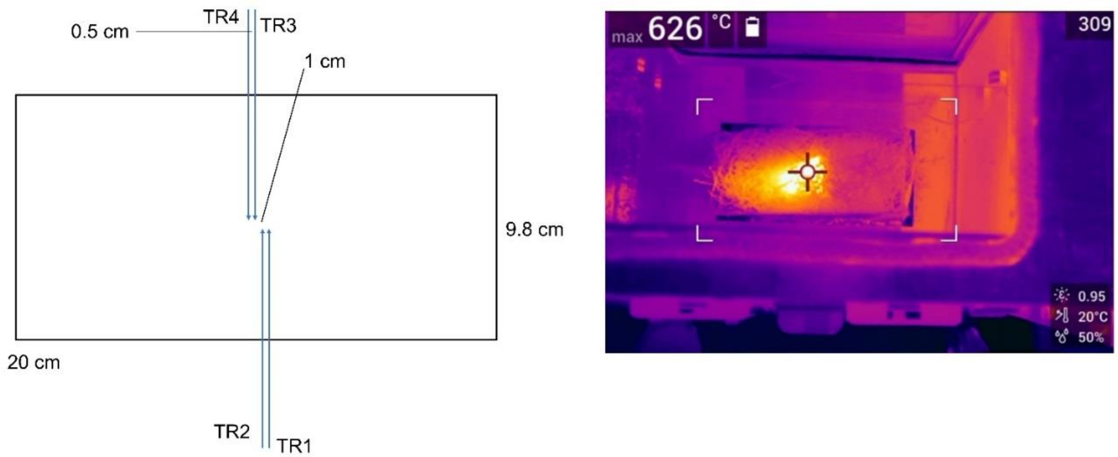

Figure 6.3 A schematic visual representation of the thermocouple setup (left) & IR camera details (right).

Infrared (IR) camera setup

An infrared (IR) camera (FLIR-E5-XT) was positioned above the fuel bed to monitor temperatures at the center. Thermocouple readings were compared with the IR temperature measurements for validation. The IR camera settings were configured according to the manual and guidelines from relevant studies, including a relative humidity of 50%, a distance of 1 meter, an ambient temperature of 20°C, and an emissivity value of 0.95. The temperature range for the IR camera was set between 20 °C and 660°C. Although the emissivity of different components in the fire environment may vary, a constant emissivity was used for temperature calculations, as the IR camera tracks a specific isotherm, reducing the effects of emissivity variation [130], [131]. The camera provided two types of temperature readings: a spatial surface temperature and a point measurement. In this study, the point measurement focused on the center of the fuel bed where ignition occurred, helping to approximate the ignition temperature and serving as a cross-check with thermocouple data. Figure 6.3 displays an example of the IR temperature readings, showing the maximum surface temperature on the left and the point temperature on the upper right.

6.1.2 Experimental Matrix

The parameters used in this study are presented in the experimental matrix below in Table 6.1. Four different airflow speeds were selected for achieving all three types of ignitions, smoldering, smoldering-to-flaming transition, and flaming ignition across all fuel samples. The selected wind speeds (0.5, 1.0, 1.5, and 2.0 m/s) were chosen to represent a realistic range of low-to-moderate ambient wind conditions frequently observed during the early stages of wildland fires and in Wildland–Urban Interface (WUI) zones. This range allows for systematic investigation of how incremental increases in airflow affect ignition characteristics and flame behavior, without introducing excessive turbulence or flame detachment that occurs at higher velocities. Furthermore, these controlled wind speeds are consistent with previous laboratory studies on fire spread and ignition dynamics [67], [156]. Which enables meaningful comparison and validation of the observed trends in ignition delay, heat transfer, and flame development [67], [162]. The 0.5 m/s condition serves as a near-ambient baseline, while 2.0 m/s represents an upper bound for steady wind in many experimental fire environments [178], [179]. To capture the unsteady nature of real wildfire conditions, controlled gust frequencies (0.03, 0.05, and 0.07 Hz) were also introduced. These frequencies simulate intermittent bursts of wind observed in the field and allow for a systematic investigation of how dynamic airflow affects ignition behavior and combustion transitions [156], [180]. Also, these are the maximum gust levels (0.03, 0.05, and 0.07) that our wind tunnel could generate. The system was limited in its ability to produce stronger gusts. Therefore, our experiments were conducted using these three intensities. Higher gust values were beyond the tunnel's operational capability.

Table 6.1 Experimental matrix

Metal Particle	**Wind Velocity (m/s)**	**Wind Gust Frequency (Hz)**	**Fuel**
304C Stainless Steel, 4mm of 15 particles	1 2	0.03 0.05 0.07	Excelsior (Aspen Wood Fiber)
			Bromus (*Bromus tectorum and Bromus diandrus*)
			Avena Wild Oat (*Avena fatua*)
			Wheatgrass Fuels *(Thinopyrum ponticum)*

6.1.3 Ignition behavior analysis protocol

This study assessed several ignition behavior metrics, including the ignition type (flaming, StF transition, or smoldering), ignition temperature, ignition time, and total burnout time. Additionally, the fire spread rate and heat release rate were also measured to provide a comprehensive understanding of the fire spread dynamics.

The criteria for defining successful ignition were as follows: a flame ignition was deemed successful if the flame persisted for a minimum of 10 seconds, while smoldering ignition was considered successful if it lasted for at least 15 seconds. Figure 6.4, provided below, aids in understanding the ignition regime through visual observation. Flaming ignition occurs rapidly, as it is highly visible and takes place at a higher temperature. On the other hand, smoldering ignition requires a longer observation time, typically 10~15 seconds, to allow the formation of a char layer or glowing particles. Smoldering was confirmed when flameless fire spread was observed, accompanied by a visible char layer or sustained glowing for at least 15 seconds. The method for determining ignition was based on previous studies to ensure that smoldering was self-sustaining and propagating independently of the ignition source, which was confirmed by visually observing the color change of the fuel surface [22], [34]. This color transition signified the oxidation of solid char in the fuel and served as a reliable indicator of the ignition point, coinciding with the location where pyrolysis oxidation occurred, ultimately leading to smoldering ignition in the experiments [22], [34], [39], [45].

Figure 6.4 A visual representation of the different ignition process.

Ignition time refers to the moment when ignition becomes visible during the experiments. It was recorded using a stopwatch and verified by analyzing the DSLR video recordings, with the start time marked when the heated particles made contact with the fuel bed. For smoldering-to-flaming transition experiments, the transition time was defined as the moment when visible signs of flaming combustion first appeared following a period of smoldering on the fuel surface.

Ignition temperature was recorded using the thermocouples and verified by analyzing the IR camera data. Initial particle temperatures were primarily recorded with the IR camera which just before the heated particles touched the fuel beds. The spoon was already heated along with metal particles which prevented direct radiative and conductive cooling of the particles by the spoon. On average, the initial particle temperatures were found to be between 620 °C and 650 °C, with a standard deviation ranging from 15 °C to 35 °C across all particle sizes.

To improve reliability and minimize the influence of uncontrolled factors, each fuel material was multiple times.

6.2 Results

This section summarizes the ignition behavior of wildland fuels by analyzing ignition parameters, including ignition temperature, ignition time, and different ignition modes under various gusty wind conditions. To ensure the robustness of our findings, we repeated the experiments with different types of wildland fuels and excelsior, allowing for a comparative analysis of their ignition responses. Additionally, we incorporated a spread behavior analysis, which includes the total burn out time, rate of spread, and heat release trends during combustion under varying wind gust conditions. By integrating these results, we identified significant patterns in ignition and spread behavior across different fuel types. The following subsections provide a detailed analysis of the experimental findings and dataset.

6.2.1 Modes of Ignition

The distribution of ignition modes - flaming, smoldering to flaming (StF) transitions, and smoldering, across wind gust frequencies for three fuel types (Excelsior, Avena, and Wheatgrass) at two wind speeds (1 m/s and 2 m/s) is presented in Figure 6.5. Both wind speeds were tested across the same gust frequencies (0.03, 0.05, and 0.07 Hz) to ensure consistency and strengthen the reliability of the observed trends. Using two wind conditions allows for a more robust understanding of how wind gusts influence ignition behavior, rather than relying on a single-speed comparison.

At both wind speeds, Excelsior fuels exhibited a clear increase in flaming ignitions with increasing gust frequency, alongside a notable rise in StF transitions. Smoldering ignitions were present but declined as gust frequency increased, indicating that higher frequency gusts promote the transition from smoldering to flaming. Avena fuels followed a similar pattern, with flaming ignitions increasing and smoldering decreasing as gust frequency rose. StF transitions were consistently present across all gust conditions but were most prominent at 0.05 and 0.07 Hz and less frequent at 0.03 Hz for both wind speeds.

In contrast, Wheatgrass fuels were predominantly characterized by smoldering ignitions, particularly at 0.03 and 0.05 Hz across both wind speeds, with only a few instances of smoldering to flaming (StF) transitions. At 1 m/s, flaming ignitions were observed only in limited numbers, even at the highest gust frequency (0.07 Hz), suggesting that the airflow at this speed was insufficient to consistently trigger flaming combustion in denser fuels like wheatgrass. However, at 2 m/s, flaming ignitions increased noticeably, with the highest number occurring at 0.07 Hz. Despite this rise, StF transitions remained minimal, indicating that flaming ignition was more likely to occur directly rather than through a transitional smoldering phase.

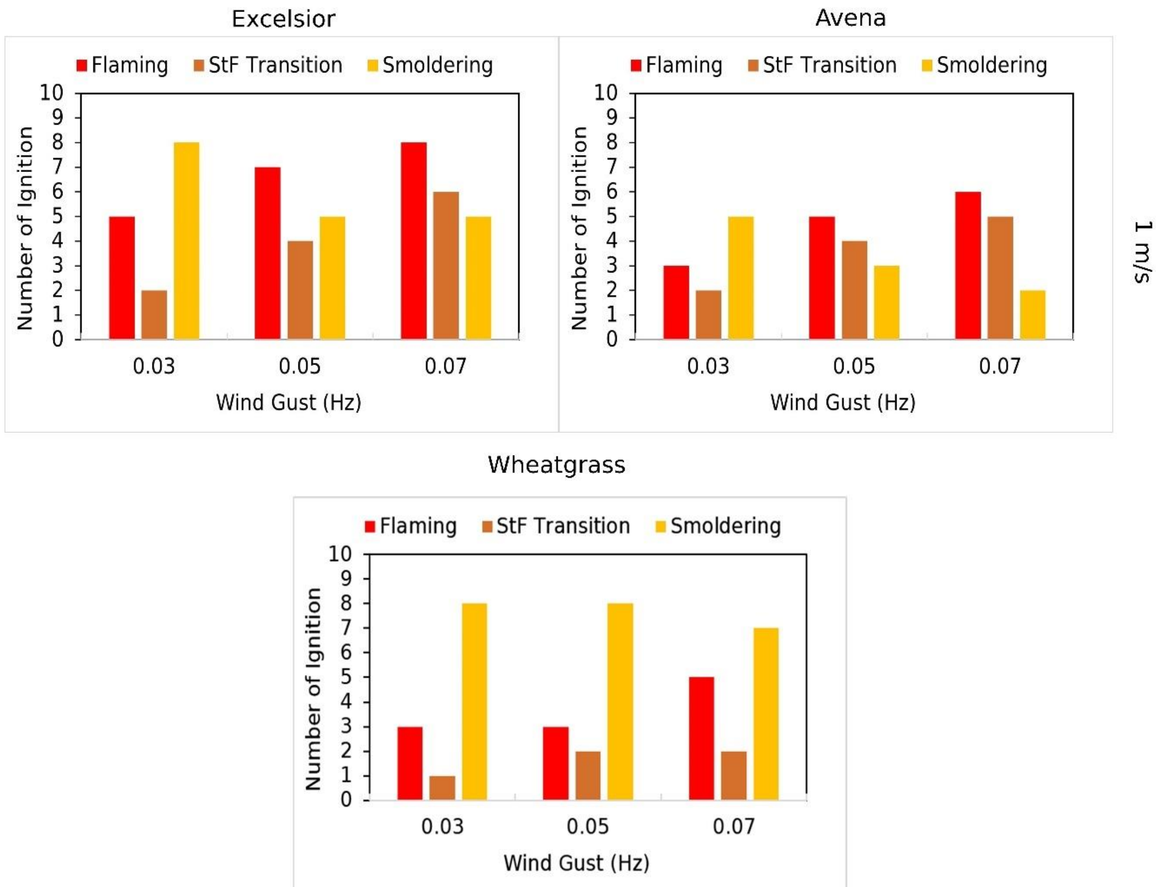
Excelsior
Avena
Wheatgrass
Flaming
StF Transition
Smoldering
Number of Ignition
Wind Gust (Hz)
0.03
0.05
0.07
1 m/s

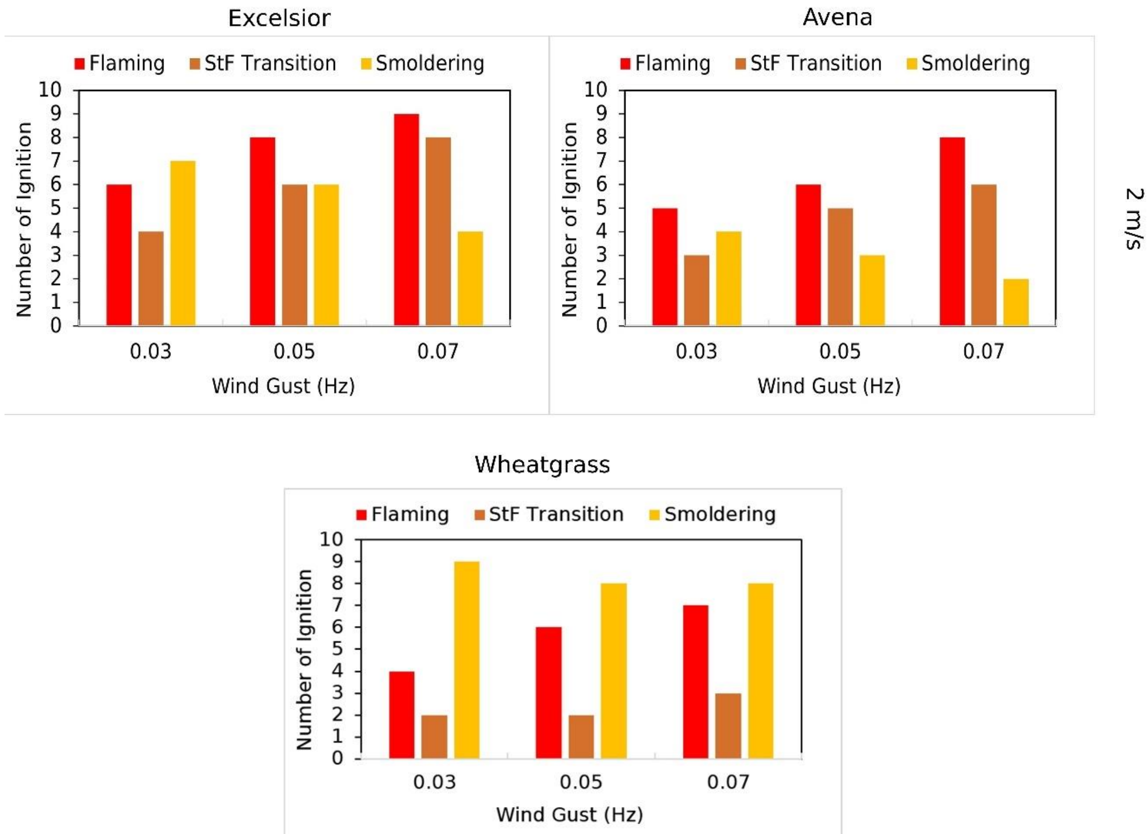

Figure 6.5 Type of ignitions of each kind of fuel in different wind gust conditions, from left (A) excelsior fuels (B) bromus (C) avena (D) wheatgrass.

6.2.2 Ignition Time

Ignition times are measured for each ignition experiment since ignition time provides crucial insights into the fuel's flammability and ignition delay under varying wind gust frequency conditions, helping to predict fire behavior more accurately. While the majority of experiments exhibited direct flaming ignition characterized by the immediate appearance of flames upon the impact of heated metal particles on the fuel bed some initially underwent sustained smoldering before gradually transitioning to flaming. Therefore, when comparing ignition times across experiments three ignition times including smoldering time, StF transition time and flaming ignition time were taken into account. To understand the impact of gust wind frequency, two wind conditions were tested across fuel types and frequency conditions.

Fig. 6 presents the effects of gust wind frequency (0.03 Hz, 0.05 Hz, and 0.07 Hz) on flaming, smoldering, and StF transition times for three fuel types: excelsior, avena, and wheatgrass, under two wind speeds (1 m/s and 2 m/s). The transition times shown in Figure 6.6 refer to the time elapsed from the moment the hot particles were dropped onto the fuel bed until the onset of flaming combustion. The StF transition for excelsior, at 1 m/s, increasing gust frequency from 0.03 to 0.07 Hz results in a decrease in StF transition time from approximately 82 to 63 seconds. A similar reduction is observed at 2 m/s, where transition times drop from 58 to 34 seconds as gust frequency increases. In Avena fuels, the effect of gust frequency is also evident; at 1 m/s, StF transition times decrease from around 72 to 50 seconds, while at 2 m/s, they fall from 59 to 42 seconds. Wheatgrass shows the most pronounced sensitivity to gust frequency, with transition times decreasing from 135 to 98 seconds at 1 m/s and from 110 to 70 seconds at 2 m/s. These trends indicate that higher gust wind frequencies significantly enhance the transition from smoldering to flaming, likely due to more dynamic airflow increasing oxygen supply and localized heating, thereby promoting quicker combustion transitions.

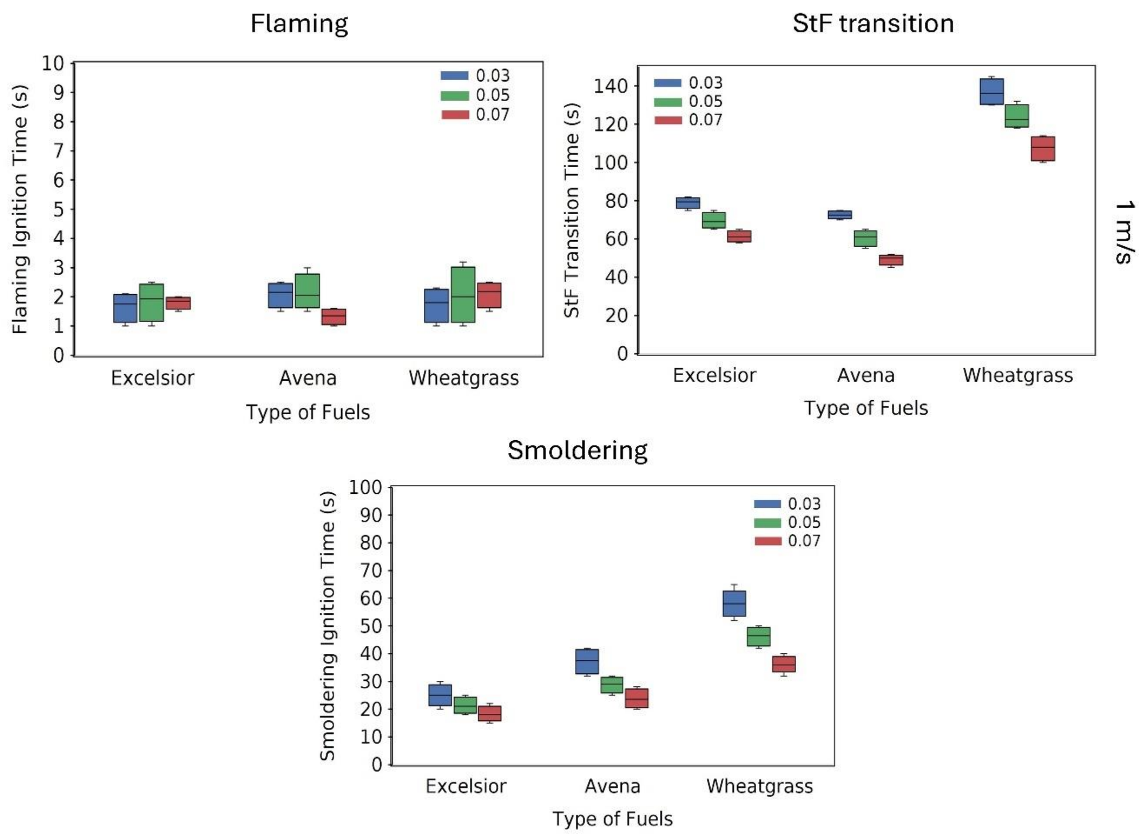

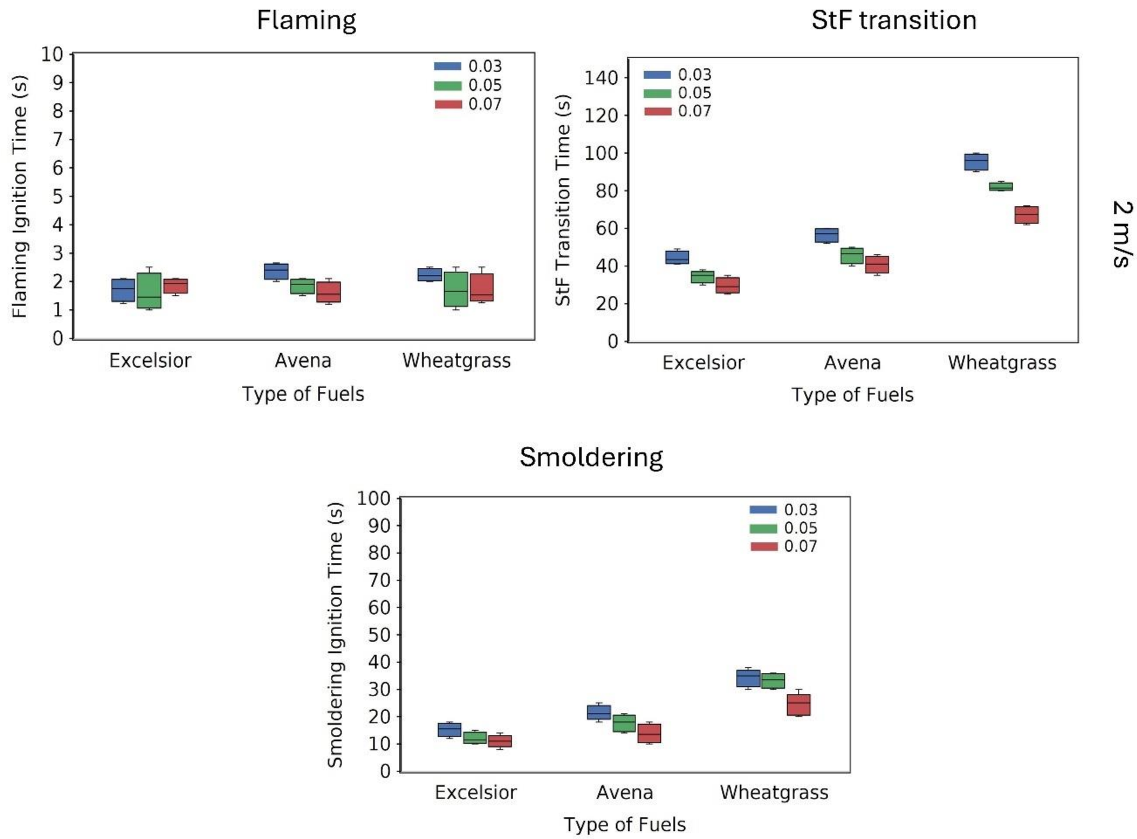

Figure 6.6 Ignition time for each fuel species in different wind gust frequency (0.03 Hz, 0.05 Hz, and 0.07 Hz)

In general, increasing gust frequency tends to reduce ignition and transition times across all fuel types and ignition modes. This trend is particularly evident for StF transition and smoldering ignition, where higher gust frequencies (0.07 Hz) result in significantly faster transitions, likely due to more frequent bursts of convective heating enhancing oxygen transport and heat penetration into the fuel bed. Wheatgrass consistently shows longer ignition and transition times across all gust frequencies, suggesting a more resistant structure or lower thermal responsiveness. The results collectively suggest that higher gust frequencies facilitate earlier ignition and faster transition to flaming, particularly in fuel types with denser or less aerated structures.

It might be because of more wind gusts supply more oxygen which helps to increase the convective heat transfer to the fuel surface, raising its temperature more rapidly and leading to quicker ignition. Also, wind delivers more oxygen to the combustion zone, supporting faster chemical reactions and reducing ignition time. Besides comparing all fuels, wheatgrass always needs longer time to ignition compared to excelsior and avena which suggests that these fuels have a lower flammability potential and require longer time to transition into flaming combustion, likely due to their resistant structure.

Overall, comparing the results across gust wind frequencies, two key observations have been found: (1) The variation in ignition and transition times across different gust frequencies is more prominent in smoldering ignition and StF transition than in flaming ignition, suggesting that smoldering phases are more sensitive to airflow fluctuations. (2) Higher gust frequencies consistently promote faster smoldering and more rapid transitions to flaming ignition, whereas lower frequencies often result in prolonged smoldering durations or failed transitions. This indicates that increasing wind frequencies increases heat transfer and oxygen delivery, which provokes sustaining smoldering and ensuring successful progression to flaming combustion.

6.2.3 Burnout Time

In addition to ignition time, a temporal parameter that provides important insight into the effect of fuel particle size on ignition behavior is burnout time. In this study, consistent with prior work, burnout time refers to the duration from the moment of ignition to the moment flaming ceases, regardless of whether all available fuel is fully consumed or not [101], [139], [140]. Examining burnout time is important for predicting fire behavior and duration, enabling better planning for fire suppression and risk assessment.

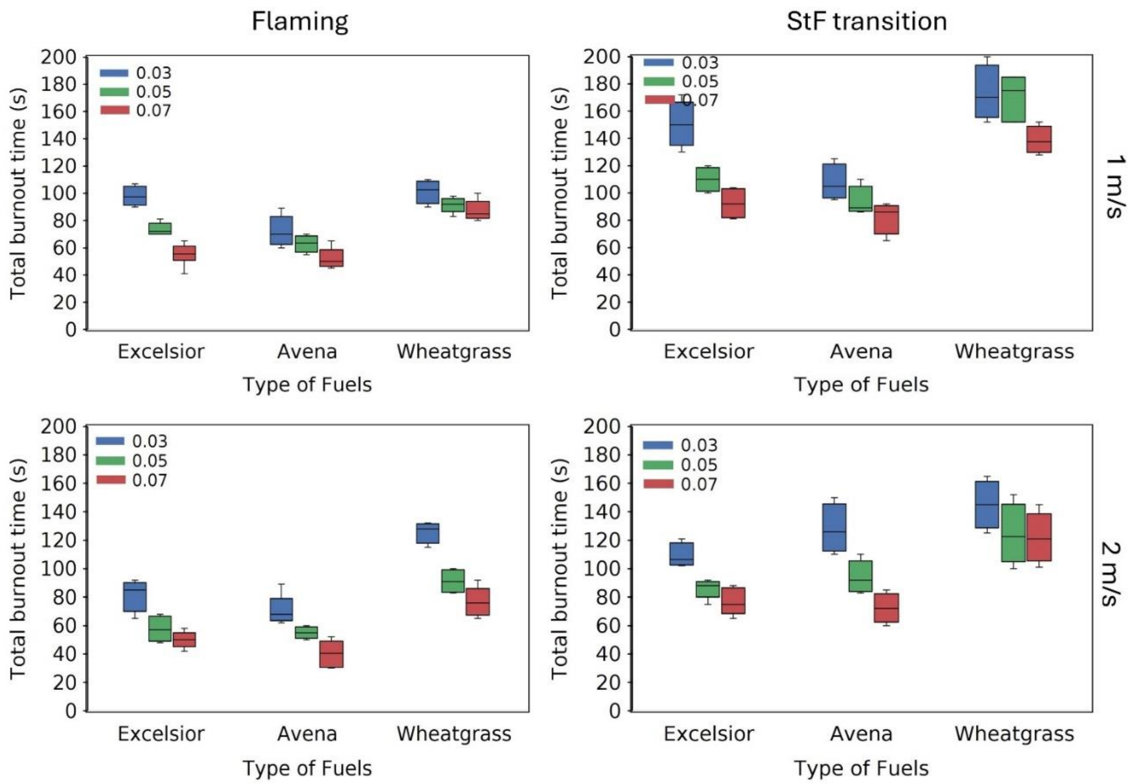

Figure 6.7 Ignition time for each fuel species in different wind gust frequency (0.03 Hz, 0.05 Hz, and 0.07 Hz)

Figure 6.7 demonstrates the influence of gust wind frequency (0.03, 0.05, and 0.07 Hz) on the total burnout time for flaming and smoldering-to-flaming (StF) transitions across three fuel types: excelsior, avena, and wheatgrass-under two wind speeds (1 m/s and 2 m/s). A consistent pattern is observed in both ignition modes: increasing gust frequency tends to reduce total burnout time, indicating a more in-tense and efficient combustion process. For flaming ignition (left panels), Excelsior shows a clear reduction in burnout time from ~100 s at 0.03 Hz to ~56 s at 0.07 Hz under 1 m/s, and from ~80 s to ~40 s under 2 m/s. Avena and wheatgrass follow a similar trend, with wheatgrass initially exhibiting the longest burnout time (~130 s at 0.03 Hz) but dropping to ~65 s at 0.07 Hz. This suggests that higher frequency gusts increase flame propagation efficiency by improving oxygen availability and enhancing convective heat transfer within the fuel bed.

In the case of StF transitions (right panels), the effect of gust frequency is even more pronounced, with both Excelsior and Avena showing reductions in burnout time as gust frequency increases. For example, excelsior's total burnout time at 1 m/s decreases from ~145 s at 0.03 Hz to ~100 s at 0.07 Hz. Similarly, Avena shows a reduction from ~130 s to ~85 s. At 2 m/s, the trend persists, although with increased variability, especially in avena and wheatgrass, where higher gust frequencies result in broader data spread, indicating fluctuating combustion stability under more turbulent airflow conditions. Wheatgrass, which typically sustains longer burnout times, also shows notable reductions with gust frequency increases, particularly under 2 m/s where total burnout drops from ~180 s to ~120 s.

These observations suggest that higher gust frequencies accelerate combustion processes. It might be because of higher gusts providing more winds which help to introduce more air to the fuel bed and helps the combustion process. As described by Nelson (2002) and Butler et al. (2019), wind introduces more oxygen into the combustion zone, leading to a more intense but shorter duration burn as fuel is consumed more rapidly [67], [69]. Andrews et al. (2013) explained how higher wind speeds reduce the fire residence time by intensifying convective heat loss, allowing fire to move quickly while consuming less fuel per unit area before advancing [66]. Besides that, frequent gusts intermittently disrupt boundary layers, facilitating oxygen penetration, and intensifying heat feedback to unburnt fuel.

However, this trend shows a different behavior under higher gust frequencies combined with higher wind speeds. At 2 m/s, gust frequencies, particularly at 0.07 Hz, lead to increased variability in total burnout time, most notably in StF transitions. The experiments explained that the higher deviation in total burnout time happens since in burnout duration since the brief flameouts were followed by gust-driven reignition, delaying final burnout and amplifying result variability. For excelsior, while the average burnout time remains low (~90 seconds), several trials show extended durations up to ~130 seconds. Avena also shows a similar spread, with burnout times ranging from ~75 to ~120 seconds. Lastly, wheatgrass displays the widest range, with burnout times varying from ~100 to ~160 seconds under the same conditions. This greater deviation is likely attributed to intermittent reignition events caused by strong gusts, which can reignite fuels that are nearly extinguished, thereby prolonging combustion and contributing to the spread in burnout times. These results collectively suggest that at higher wind speeds, strong and frequent gusts can introduce turbulence that disrupts steady burning, leading to intermittent combustion and greater spread in total burnout durations.

6.2.4 Ignition Temperature

Figures 6.8 and 6.9 investigate the impact of gust wind frequencies (0.03, 0.05, and 0.07 Hz) on flaming ignition, smoldering ignition, and smoldering-to-flaming (StF) transition temperatures across different fuel types (Excelsior, Avena, and Wheatgrass) at two wind speeds (1 m/s and 2 m/s).

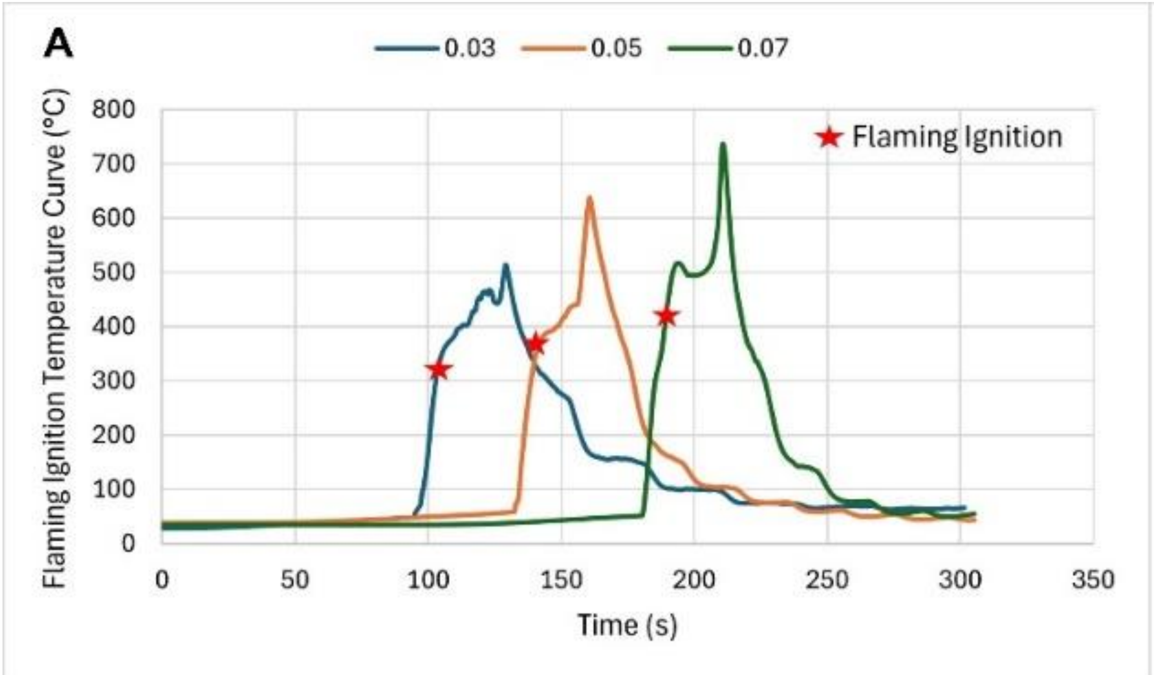
A
0.03
0.05
0.07
Flaming Ignition
Flaming Ignition Temperature Curve (°C)
Time (s)

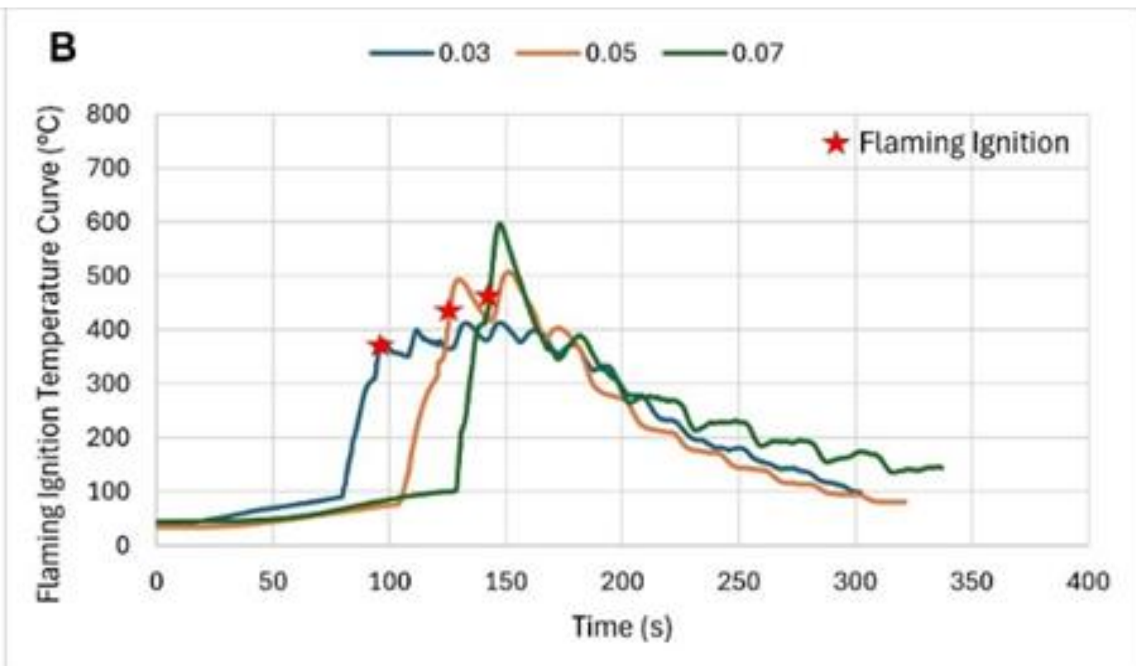
B
0.03
0.05
0.07
Flaming Ignition
Flaming Ignition Temperature Curve (°C)
Time (s)

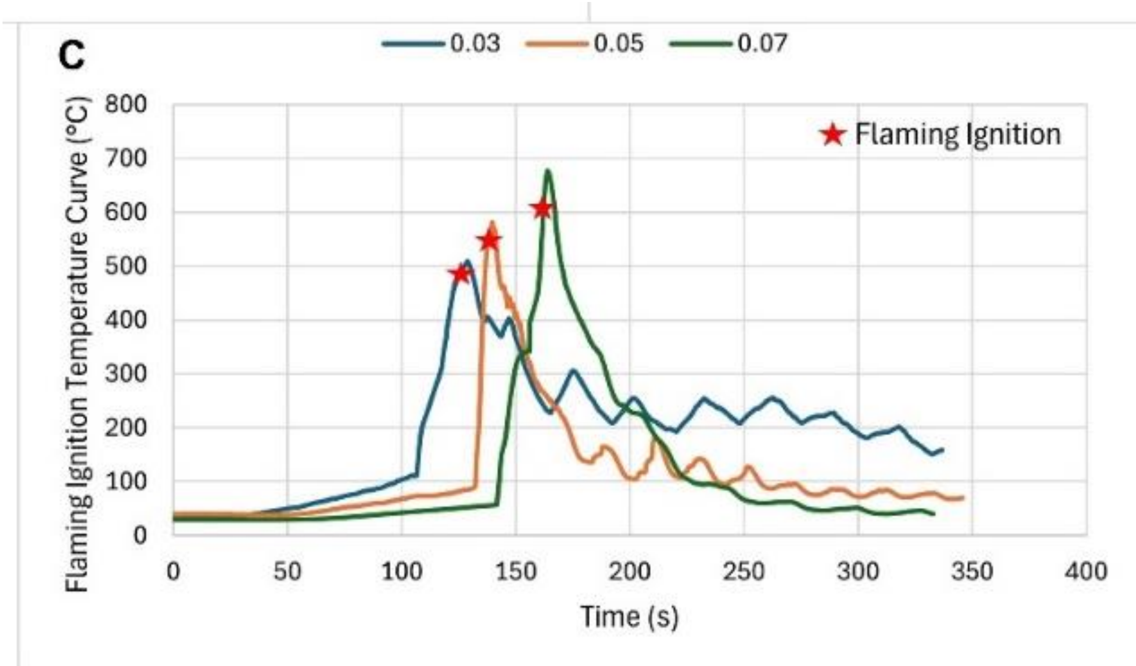

Figure 6.8 Flaming ignition temperature curves for various fuel in wind gusts at 1m/s wind condition.

Figure 6.8 provides ignition temperature curves for different fuels under varying wind gust frequencies. The temperature curves show the flaming ignition temperature at the moment of flaming ignition with red star in the flaming ignition curve. These results clearly demonstrate that increasing gust wind frequency leads to higher flaming ignition temperatures across all fuels. For instance, in excelsior, the flaming ignition temperature increases from approximately 320°C at 0.03 Hz to around 400°C at 0.07 Hz, indicating a notable rise with higher gust frequency. Avena exhibits a similar trend, with ignition temperatures rising from about 390°C to 480°C across the same frequency range. In the case of wheatgrass, which has a denser structure and thus a higher ignition threshold, the increase is even more pronounced rising from approximately 500°C at 0.03 Hz to nearly 620°C at 0.07 Hz.

To gain a clearer insight into the effects of wind gusts on ignition temperature, figure 6.9 presents the box plots with ignition temperatures for both flaming smoldering and StF transition ignitions.

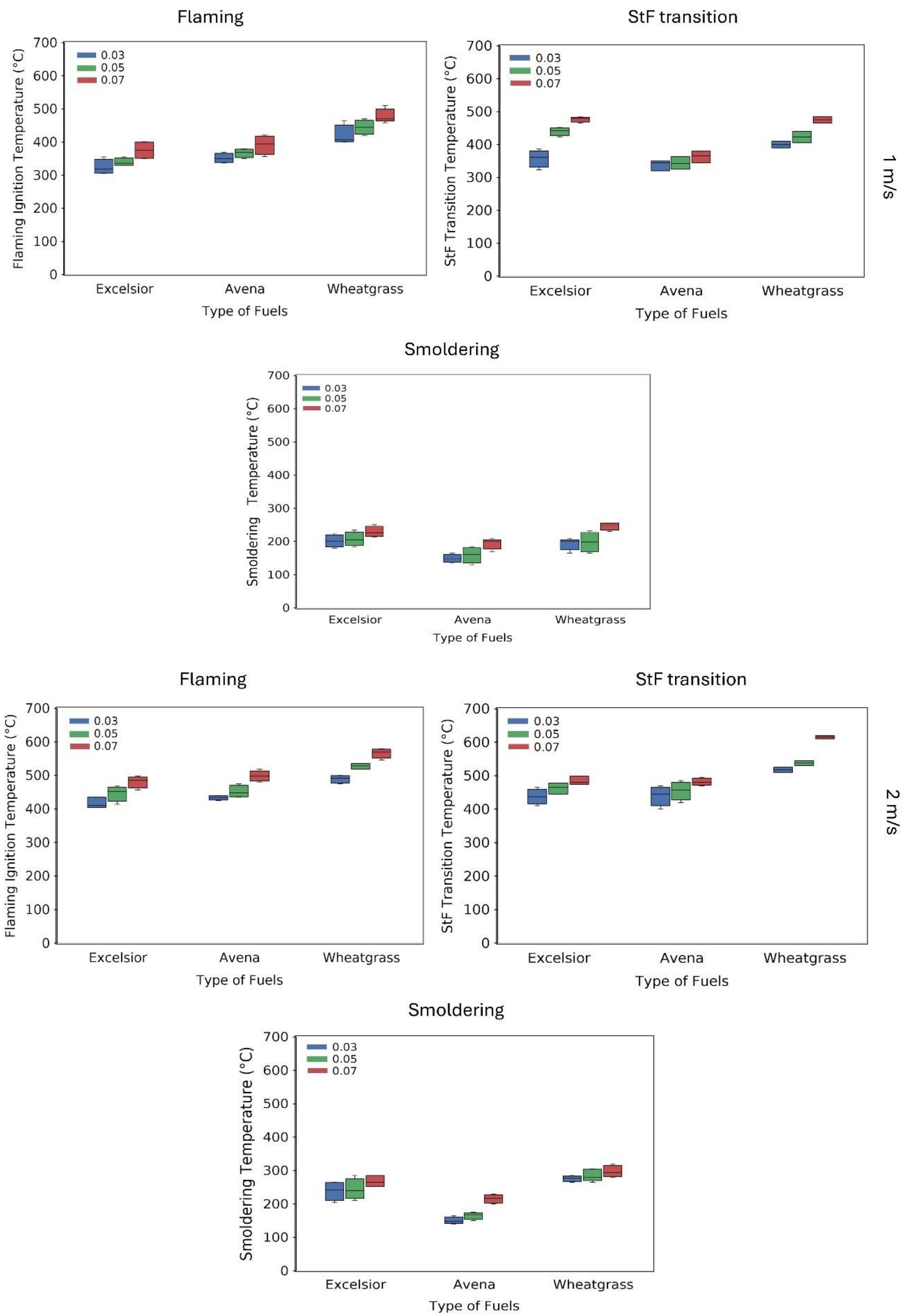
Flaming
Flaming Ignition Temperature (°C)
0.03
0.05
0.07
Excelsior
Avena
Wheatgrass
Type of Fuels
StF transition
StF Transition Temperature (°C)
1 m/s
Smoldering
Smoldering Temperature (°C)
2 m/s

Figure 6.9 Ignition temperature for each fuel species in different wind gust frequency (0.03 Hz, 0.05 Hz, and 0.07 Hz)

In Figure 6.9, the box plots show that flaming ignition temperatures consistently increase with rising gust frequency, across all fuel types and both wind speeds. For example, in Excelsior, flaming ignition temperature rises from ~405°C at 0.03 Hz to ~489°C at 0.07 Hz and 2m/s wind condition. A similar upward trend is evident in Avena and Wheatgrass. In avena fuels, flaming ignition temperature rises from ~415°C at 0.03 Hz to ~495°C at 0.07 Hz and 2m/s wind condition. Similarly, in wheatgrass, flaming ignition temperature rises from ~475°C at 0.03 Hz to ~530°C at 0.07 Hz and 2m/s wind condition. This suggests that higher gust frequencies intensify the ignition environment by intermittently enhancing oxygen supply and convective heat, pushing the ignition threshold to higher temperatures. A similar trend is observed for StF transition temperatures, where higher gust frequencies again correlate with increased transition temperatures, particularly in denser fuels like Wheatgrass. Smoldering ignition temperatures show a subtler, but still notable, increase with gust frequency. For instance, Wheatgrass ignition temperature rises from ~270°C at 0.03 Hz to ~320°C at 0.07 Hz and 1m/s wind condition. This indicates that, while the smoldering process is slower and less flame-dependent, the influence of dynamic airflow still enhances heat retention and oxygen access, raising the ignition point.

This trend suggests that increased wind gust frequencies add more air and enhance convective heat transfer, resulting in higher ignition temperatures. The rise in temperature at the point of ignition may be attributed to the greater availability of oxygen and the increased transfer of heat to the fuel surface, which accelerates combustion. Consequently, stronger winds can create a more intense ignition environment with hot gas temperature and shifting the ignition regime to higher temperature thresholds [159]. A study by Lai et al. (2022,) shows that the ignition temperature increase under low wind speed, the reason for the phenomenon is attributed to the increased oxygen supply [181]. This suggests that wind enhances convective heat transfer, leading to higher temperatures during ignition. Additional evidence supporting this relationship comes from the work of Chen et al. (2023) and Xie et al. (2020), who explored the influence of airflow on combustion dynamics [36], [38]. They summarized that increasing oxygen flow velocities from 4 to 24 m/s led to elevated peak temperatures during both smoldering and flaming ignition phases, attributing this to enhanced char oxidation under stronger airflow. In a related study, Xie et al. found that both the smoldering spread rate and peak temperature rose almost linearly with increasing wind speed, emphasizing the importance of oxygen supply in driving combustion performance [36]. Collectively, these studies indicate that wind not only enriches oxygen availability but also boosts convective heat transfer, ultimately leading to higher ignition temperatures and more efficient combustion.

6.2.5 Heat release rate analysis

This study also examined the heat release rate at different wind speeds to determine whether higher airflow significantly affects sustained ignition behavior. The heat release analysis also examines whether wind speed influences ignition behavior favorably or unfavorably, meaning higher winds may either enhance oxygen availability, promoting ignition, or increase heat loss, extinguishing the ignition process. Studying HRR is important as it plays a crucial role in understanding the combustion process, fire behavior, and fire propagation rates and it is one of the most significant predictor of fire hazard [170]–[172].

The heat release rate is calculated using the mass loss rate by multiplying the heat of combustion [122].

$$HRR = MLR * Heat\ of\ Combustion$$

Where HRR is heat release rate in (KJ/gr) and MLR is the mass loss rate in (gr/s) and heating value or heat of combustion value for each fuel in (MJ/kg). For calculating experiments, the heating value for excelsior is used 32.37 MJ/kg, for avena is 18.07 MJ/kg and for wheatgrass is 16.94 MJ/kg [122], [159], [173]–[176]. Since specific data on the heat of combustion during smoldering combustion for the selected fuels are not readily available from existing literature, previous studies suggest using an effective heat of combustion in the range of 6–12 MJ/kg for smoldering ignition, compared to typical values of 16–30 MJ/kg for flaming combustion [45], [177]. As the previous study suggests the following heating values were used for smoldering ignition in calculations: 14.6 MJ/kg for excelsior, 8.42 MJ/kg for bromus, 8.13 MJ/kg for avena, and 7.62 MJ/kg for wheatgrass.

Figure 6.10 presents the average heat release rate (HRR) for Excelsior, Avena, and Wheatgrass fuels under varying gust wind frequencies (0.03, 0.05, and 0.07 Hz) at two wind speeds (1 m/s and 2 m/s). Across all fuel types and ignition modes, increasing gust frequency results in a consistent rise in HRR, indicating that stronger gusts significantly intensify ignition process.

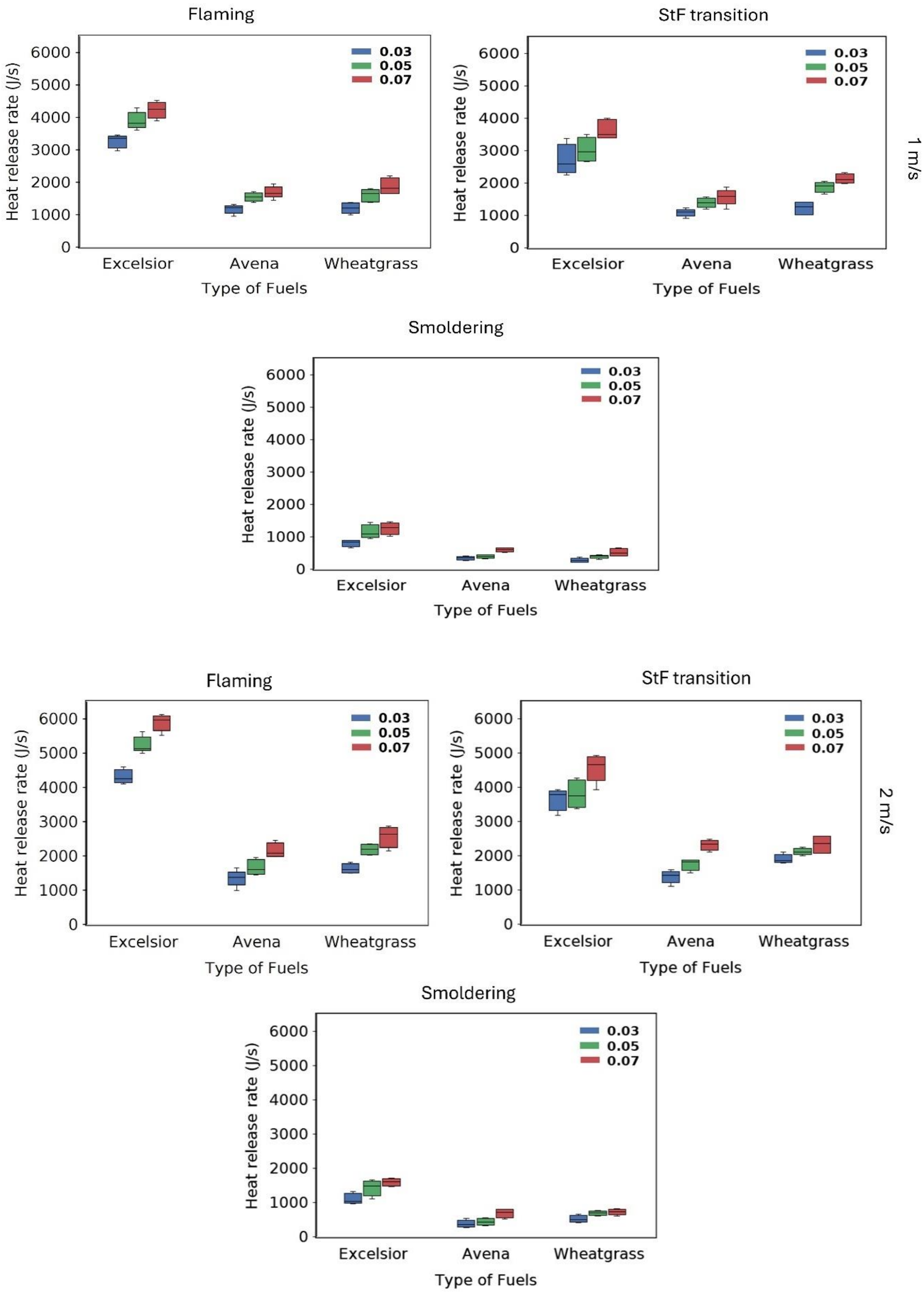
Flaming
StF transition
Smoldering
Heat release rate (J/s)
0
1000
2000
3000
4000
5000
6000
0.03
0.05
0.07
Excelsior
Avena
Wheatgrass
Type of Fuels
1 m/s
2 m/s

Figure 6.10 Average calculated Heat release rate for various fuels at different wind gusts at 1m/s and 2 m/s wind condition.

For flaming ignition, the effect of gust frequency is especially pronounced. In Excelsior, HRR increases from ~4100 J/s at 0.03 Hz to over 5980 J/s at 0.07 Hz at 2 m/s wind speed, highlighting the role of high-frequency gusts in driving rapid fuel consumption and flame propagation. Avena and Wheatgrass show similar trends, with HRR rising from ~1420J/s to ~2360 J/s and ~1650 J/s to ~2450 J/s, respectively, between 0.03 and 0.07 Hz at 2 m/s. These results confirm that higher gust frequencies deliver more frequent oxygen bursts, intensifying the flame and increasing the combustion rate.

In StF transitions, Excelsior again shows HRR increase from ~3900 J/s at 0.03 Hz to ~4860 J/s at 0.07 Hz at 2 m/s, demonstrating that stronger gusts facilitate stronger and forceful combustion during the transition phase. Avena and Wheatgrass follow similar patterns, with HRR increasing from ~1200 J/s to ~2100 J/s and ~1805 J/s to ~2105 J/s, respectively. These observations suggest that a threshold level of HRR, influenced by gust frequency, is essential for successful transition from smoldering to flaming combustion.

Smoldering ignition exhibits lower HRR values overall, but even here, gust frequency influences combustion strength. In Excelsior, HRR increases from ~1100 J/s at 0.03 Hz to nearly 1850 J/s at 0.07 Hz. For Avena and Wheatgrass, HRR remains similar increases with gust frequency, reaching ~880 J/s and ~998 J/s respectively at 0.07 Hz. These trends indicate that stronger gusts enhance heat feedback and oxygen delivery even during the low intensity smoldering phase. This trend aligns with previous studies, which indicate that higher wind speeds increase local flame-fuel contact frequency and enhance intermittent convective heating of the fuel bed surface [158], [164]. Stronger winds push flames forward, increasing the rate of heat transfer to unburned fuel, which accelerates ignition and promotes faster fuel consumption. Consequently, this leads to higher HRR values, as the effects of more rapid ignition also enhance mass loss [70], [71], [164].

6.3 Summery

This study makes a novel contribution to experimental combustion research, offering new insights that extend beyond those presented in previous literature [37], [53], [75], [167], [168]. The study demonstrates that wind gusts significantly facilitate the smoldering-to-flaming (StF) transition by enabling a two-phase mechanism: initially, gusts enhance smoldering through elevated oxygen supply, intensifying pyrolysis. Subsequently, when the wind subsides, the reduction in convective cooling and dilution allows pyrolyzates to accumulate and reach higher temperatures, thereby increasing their flammability. If the pyrolyzate concentration becomes sufficient during this pause, the StF transition occurs. If not, the next gust cycle reinforces the smoldering phase until ignition is achieved. Importantly, the stag-nation period between gusts does not hinder combustion instead, it sustains it by decreasing heat losses and promoting fuel-rich conditions. This process enables a more rapid and stable transition to flaming combustion and introduces a transition pathway not previously reported in the literature [37], [53], [75], [167], [168]. This mechanism is particularly relevant in wildfire scenarios, where rapidly shifting environmental wind conditions often dictate ignition potential and fire spread dynamics.

By using a bench-scale wind tunnel capable of generating controlled gust frequencies (0.03, 0.05, and 0.07 Hz) at wind speeds of 1.0 and 2.0 m/s, the research successfully replicates the transient airflow conditions observed in real fire environments. The results demonstrate that increasing gust frequency consistently reduces ignition delay and burnout duration while raising ignition temperatures and heat release rates (HRR) across all tested fuels: excelsior, avena, and wheatgrass.

The most notable findings include significantly shortened smoldering-to-flaming (StF) transition times and increased peak ignition temperatures with higher gust frequencies. For instance, in avena fuels, StF transition time dropped from 58 to 42 seconds and flaming ignition temperatures rose from ~415 °C to ~498 °C as gust frequency increased from 0.03 Hz to 0.07 Hz at 2.0 m/s wind speed. Such trends are attributed to enhanced convective heat transfer and more frequent oxygen delivery during gust events, which accelerate thermal feedback and combustion reactions. Furthermore, burnout time analysis revealed that higher gust frequencies result in faster fuel consumption and more intense, yet shorter, combustion durations. However, this trend also introduces increased variability at high wind speed (2.0 m/s) and high-frequency (0.07 Hz) conditions, likely due to intermittent flameouts followed by gust-induced reignition. This nuance highlights the complex interplay between turbulent flow and combustion stability in realistic fire scenarios. The HRR measurements further reinforce these findings, showing a marked increase in energy release with rising gust frequency. Excelsior, for example, reached an average HRR of ~5980 J/s under high gust conditions during flaming ignition, while smoldering and transition modes also showed notable gains across all fuels.

Collectively, this study underscores the inadequacy of steady-wind fire models in capturing the ignition risks posed by dynamic wind patterns. By integrating transient gust behavior into fire science, the findings support the development of more accurate ignition prediction models and risk mitigation strategies for wildland–urban interface (WUI) zones. The work also offers actionable insights for land management and firefighting policy highlighting the need for targeted vegetation treatments in gust-prone areas and improved planning for conditions conducive to rapid fire escalation. Ultimately, this research bridges a critical gap between field-scale fire observations and laboratory scale validation, enhancing our understanding of how gusty winds shape wildfire initiation and progression.

Acknowledgement

I thank Cobian-Iñiguez Fire Lab for their support in the research work. My special thanks go to the undergraduate students – Juan Hernandez, Jason Estevez, and Gen Duenas for their invaluable assistance and contribution in conducting experiments. This research is supported through startup funding from the University of California, Merced, School of Engineering.

Chapter 7
Future Work

While this research has provided critical insights into ignition behavior under various fuel types, structures, and wind conditions, there remain several important aspects for future investigation to further advance laboratory scales. One key limitation of this work is that only a narrow range of wind speeds and gust frequencies was examined specifically, 0.5 to 2.0 m/s wind speeds and gust frequencies of 0.03 to 0.07 Hz. Although these ranges allowed us to simulate realistic low to moderate wind conditions, they do not capture the full spectrum of wind dynamics encountered in actual wildfire events, particularly in high wind or gust prone regions.

Future studies should therefore focus on expanding both the range and resolution of wind speeds and gust frequencies. By testing higher wind velocities (e.g., 5-10 m/s) and a broader set of gust frequencies, researchers can better identify the thresholds at which wind begins to exhibit dual behavior, enhancing ignition through oxygen enrichment and convective heat transfer, while also potentially suppressing ignition through cooling effects. This trade-off is particularly relevant for smoldering-to-flaming (StF) transitions, which are sensitive to the delicate balance between heat accumulation and heat loss.

Additionally, a promising direction for future research is to systematically determine critical wind speed and gust frequency thresholds that either facilitate or hinder ignition in different fuel types. Identifying these thresholds will be crucial for predictive fire models and risk assessment tools, particularly in Wildland - Urban Interface (WUI) zones, where fuel diversity and wind exposure can vary significantly over short distances.

Another major opportunity lies in the integration of numerical modeling to complement and extend our experimental findings. Although this work was conducted entirely through laboratory scale experiments, future efforts should include simulations using tools such as the Fire Dynamics Simulator (FDS). These models can be used to replicate the complex interactions between wind flow, heat transfer, and fuel characteristics under various controlled conditions. Simulations will not only validate and extend experimental observations but also allow researchers to explore parameter spaces that are impractical or unsafe to test physically.

Moreover, future studies should consider fuel moisture content, ambient temperature fluctuations, and more diverse wildland fuels and different vegetation types, which are known to influence ignition behavior but were held constant in the present work. Incorporating these variables will result in a more comprehensive understanding of wildfire ignition and better inform both fire prevention strategies and emergency response planning.

Reference

[1] M. Boboulos and M. R. I. Purvis, "Wind and slope effects on ROS during the fire propagation in East-Mediterranean pine forest litter," *Fire Saf. J.*, vol. 44, no. 5, pp. 764–769, 2009, doi: 10.1016/j.firesaf.2009.03.006.

[2] S. J. Baker, "Fossil evidence that increased wildfire activity occurs in tandem with periods of global warming in Earth's past," *Earth-Science Rev.*, vol. 224, no. November 2021, p. 103871, 2022, doi: 10.1016/j.earscirev.2021.103871.

[3] M. D. Flannigan, M. A. Krawchuk, W. J. De Groot, B. M. Wotton, and L. M. Gowman, "Implications of changing climate for global wildland fire," *Int. J. Wildl. Fire*, vol. 18, no. 5, pp. 483–507, 2009, doi: 10.1071/WF08187.

[4] P. T. Brown *et al.*, "Climate warming increases extreme daily wildfire growth risk in California," *Nature*, vol. 621, no. 7980, pp. 760–766, 2023, doi: 10.1038/s41586-023-06444-3.

[5] Y. Liu, J. Stanturf, and S. Goodrick, "Trends in global wildfire potential in a changing climate," *For. Ecol. Manage.*, vol. 259, no. 4, pp. 685–697, 2010, doi: 10.1016/j.foreco.2009.09.002.

[6] M. D. Flannigan, Y. Bergeron, O. Engelmark, and B. M. Wotton, "Future wildfire in circumboreal forests in relation to global warming," *J. Veg. Sci.*, vol. 9, no. 4, pp. 469–476, 1998, doi: 10.2307/3237261.

[7] A. S. Nur, Y. J. Kim, and C. W. Lee, "Creation of Wildfire Susceptibility Maps in Plumas National Forest Using InSAR Coherence, Deep Learning, and Metaheuristic Optimization Approaches," *Remote Sens.*, vol. 14, no. 17, 2022, doi: 10.3390/rs14174416.

[8] G. Chown, "The impact of a residential fire on occupational engagement and performance: A reflexive narrative approach," *Burn. Open*, vol. 8, no. 3, pp. 165–168, 2024, doi: 10.1016/j.burnso.2024.04.001.

[9] K. D. Bladon, "Agricultural policy can reduce wildfires Rethinking wildfires and forest watersheds," *Science (80-.).*, no. March, pp. 5–7, 2018.

[10] J. T. Abatzoglou and A. P. Williams, "Impact of anthropogenic climate change on wildfire across western US forests," *Proc. Natl. Acad. Sci.*, vol. 113, no. 42, pp. 11770–11775, 2016, doi: 10.1073/pnas.1607171113.

[11] J. K. Balch, B. A. Bradley, J. T. Abatzoglou, R. Chelsea Nagy, E. J. Fusco, and A. L. Mahood, "Human-started wildfires expand the fire niche across the United States," *Proc. Natl. Acad. Sci. U. S. A.*, vol. 114,

no. 11, pp. 2946–2951, 2017, doi: 10.1073/pnas.1617394114.

[12] C. A. Alves *et al.*, “Smoke emissions from biomass burning in a Mediterranean shrubland,” *Atmos. Environ.*, vol. 44, no. 25, pp. 3024–3033, 2010, doi: 10.1016/j.atmosenv.2010.05.010.

[13] P. S. Rickly *et al.*, “Emission factors and evolution of SO2 measured from biomass burning in wildfires and agricultural fires,” *Atmos. Chem. Phys.*, vol. 22, no. 23, pp. 15603–15620, 2022, doi: 10.5194/acp-22-15603-2022.

[14] H. D. Nguyen *et al.*, “The summer 2019–2020 wildfires in east coast australia and their impacts on air quality and health in new south wales, australia,” *Int. J. Environ. Res. Public Health*, vol. 18, no. 7, 2021, doi: 10.3390/ijerph18073538.

[15] L. Hein *et al.*, “The health impacts of Indonesian peatland fires,” *Environ. Heal. A Glob. Access Sci. Source*, vol. 21, no. 1, pp. 1–17, 2022, doi: 10.1186/s12940-022-00872-w.

[16] A. A. Mamuji and J. L. Rozdilsky, “Wildfire as an increasingly common natural disaster facing Canada: understanding the 2016 Fort McMurray wildfire,” *Nat. Hazards*, vol. 98, no. 1, pp. 163–180, 2019, doi: 10.1007/s11069-018-3488-4.

[17] L. M. Ribeiro, A. Rodrigues, D. Lucas, and D. X. Viegas, “The impact on structures of the pedrógão grande fire complex in June 2017 (Portugal),” *Fire*, vol. 3, no. 4, pp. 1–22, 2020, doi: 10.3390/fire3040057.

[18] A. C. Fernandez-Pello, “Wildland fire spot ignition by sparks and firebrands,” *Fire Saf. J.*, vol. 91, no. May, pp. 2–10, 2017, doi: 10.1016/j.firesaf.2017.04.040.

[19] S. Suzuki and S. L. Manzello, “Role of accumulation for ignition of fuel beds by firebrands,” *Appl. Energy Combust. Sci.*, vol. 1–4, no. February, p. 100002, 2020, doi: 10.1016/j.jaecs.2020.100002.

[20] S. Saha, E. Ameri, J. Avalos, and J. Cobian-Iñiguez, “Experimental Study on the Ignition Behavior of Wildland Fuels Ignited by Heated Stainless-Steel Particles,” *Combust. Sci. Technol.*, vol. 00, no. 00, pp. 1–18, 2024, doi: 10.1080/00102202.2024.2379493.

[21] C. D. Zak, J. L. Urban, and C. Fernandez-Pello, “Characterizing the flaming ignition of cellulose fuel beds by hot steel spheres,” *Combust. Sci. Technol.*, vol. 186, no. 10–11, pp. 1618–1631, 2014, doi: 10.1080/00102202.2014.935612.

[22] S. Wang, X. Huang, H. Chen, and N. Liu, “Interaction between flaming

and smouldering in hot-particle ignition of forest fuels and effects of moisture and wind," *Int. J. Wildl. Fire*, vol. 26, no. 1, pp. 71–81, 2017, doi: 10.1071/WF16096.

[23] R. M. Hadden, S. Scott, C. Lautenberger, and C. C. Fernandez-Pello, "Ignition of Combustible Fuel Beds by Hot Particles: An Experimental and Theoretical Study," *Fire Technol.*, vol. 47, no. 2, pp. 341–355, 2011, doi: 10.1007/s10694-010-0181-x.

[24] J. L. Urban, C. D. Zak, and C. Fernandez-Pello, "Spot Fire Ignition of Natural Fuels by Hot Aluminum Particles," *Fire Technol.*, vol. 54, no. 3, pp. 797–808, 2018, doi: 10.1007/s10694-018-0712-4.

[25] A. Ganteaume *et al.*, "Laboratory characterization of firebrands involved in spot fires," *Ann. For. Sci.*, vol. 68, no. 3, pp. 531–541, 2011, doi: 10.1007/s13595-011-0056-4.

[26] K. Mikkelsen, "An Experimental Investigation of Ignition Propensity of Hot Work Processes in the Nuclear Industry," pp. 1–196, 2014.

[27] J. P. Prestemon *et al.*, "Wildfire ignitions : A review of the science and recommendations for empirical modeling," no. March 2016, p. 20, 2013.

[28] M. Bénichou, N.; Adelzadeh, M.; Singh, J.; Gomaa, I; Elsagan, N.; Kinateder M.; Ma, C.; Gaur, A.; Bwalya, A.; Sultan, *National Guide for Wildland-Urban*. 2021.

[29] E. Claridge and M. Spearpoint, "New Zealand fire service response times to structure fires," *Procedia Eng.*, vol. 62, pp. 1063–1072, 2013, doi: 10.1016/j.proeng.2013.08.162.

[30] M. Whitman and S. Holmgren, "Representations of wildfires in academia," *J. Environ. Plan. Manag.*, vol. 67, no. 9, pp. 1952–1976, 2024, doi: 10.1080/09640568.2022.2150155.

[31] Standards Association of Australia., Standards Association of Australia., and C. of B. in B.-P. A. Standards Association of Australia. Committee FP-020, "Construction of buildings in bushfire-prone areas.," p. 108, 2009.

[32] V. Babrauskas, "Firebrands and Embers," *Encycl. Wildfires Wildland-Urban Interface Fires*, pp. 431–444, 2020, doi: 10.1007/978-3-319-52090-2_3.

[33] M. A. Finney, S. S. McAllister, T. B. Maynard, and I. J. Grob, "A Study of Wildfire Ignition by Rifle Bullets," *Fire Technol.*, vol. 52, no. 3, pp. 931–954, 2016, doi: 10.1007/s10694-015-0518-6.

[34] J. L. Urban, C. D. Zak, J. Song, and C. Fernandez-Pello, "Smoldering

spot ignition of natural fuels by a hot metal particle," *Proc. Combust. Inst.*, vol. 36, no. 2, pp. 3211–3218, 2017, doi: 10.1016/j.proci.2016.09.014.

[35] R. Hadden *et al.*, "Smouldering Combustion Phenomena in Science and Technology," *Int. Rev. Chem. Eng.*, vol. 1, no. 3, pp. 3–18, 2009, doi: 10.1016/S0010-2180(98)00095-9.

[36] Q. Xie, Z. Zhang, S. Lin, Y. Qu, and X. Huang, "Smoldering Fire of High-Density Cotton Bale Under Concurrent Wind," *Fire Technol.*, vol. 56, no. 5, pp. 2241–2256, 2020, doi: 10.1007/s10694-020-00975-1.

[37] L. Carmignani *et al.*, "Smoldering of Wood: Effects of Wind and Fuel Geometry," *Fire Technol.*, vol. 60, no. 3, pp. 1667–1683, 2024, doi: 10.1007/s10694-024-01542-8.

[38] Y. Chen, Z. Liang, S. Lin, and X. Huang, "Limits of sustaining a flame above smoldering woody biomass," *Combust. Sci. Technol.*, vol. 195, no. 12, pp. 2801–2819, 2023, doi: 10.1080/00102202.2022.2041000.

[39] M. A. Santoso, E. G. Christensen, J. Yang, and G. Rein, "Review of the Transition From Smouldering to Flaming Combustion in Wildfires," *Front. Mech. Eng.*, vol. 5, no. September, 2019, doi: 10.3389/fmech.2019.00049.

[40] S. Saha and J. Cobian-Iñiguez, "Effect of Fuel Structure and Species on Grassy Fuel Ignition: Insights From Bench Scale Experiments and Thermogravimetric Analysis," *Fire Mater.*, pp. 1–19, 2025, doi: 10.1002/fam.3281.

[41] R. Hadden *et al.*, "Radiant Ignition of Polyurethane Foam: The Effect of Sample Size," *Combust. Flame*, vol. 50, no. 3, pp. 673–691, 2014, doi: 10.1016/S0010-2180(98)00095-9.

[42] V. Babrauskas and J. F. Krasny, "Fire Behavior of Upholstered Furniture.," *NBS Monogr. (United States)*, no. October 1985, 1985.

[43] D. Thomas, D. Butry, S. Gilbert, D. Webb, and J. Fung, "The Costs and Losses of Wildfires: A Literature Survey (NIST Special Publication 1215)," no. November, 2017, [Online]. Available: https://doi.org/10.6028/NIST.SP.1215.

[44] G. Rein and X. Huang, "Smouldering wildfires in peatlands, forests and the arctic: Challenges and perspectives," *Curr. Opin. Environ. Sci. Heal.*, vol. 24, p. 100296, 2021, doi: 10.1016/j.coesh.2021.100296.

[45] G. Rein, "Smouldering Fires and Natural Fuels," *Fire Phenom. Earth Syst. An Interdiscip. Guid. to Fire Sci.*, no. 1984, pp. 15–33, 2013, doi:

10.1002/9781118529539.ch2.

[46] E. Koo, P. J. Pagni, D. R. Weise, and J. P. Woycheese, “Firebrands and spotting ignition in large-scale fires,” *Int. J. Wildl. Fire*, vol. 19, no. 7, pp. 818–843, 2010, doi: 10.1071/WF07119.

[47] A. C. Fernandez-Pello *et al.*, “Spot fire ignition of natural fuel beds by hot metal particles, embers, and sparks,” *Combust. Sci. Technol.*, vol. 187, no. 1–2, pp. 269–295, 2015, doi: 10.1080/00102202.2014.973953.

[48] J. L. Urban, C. D. Zak, and C. Fernandez-Pello, “Cellulose spot fire ignition by hot metal particles,” *Proc. Combust. Inst.*, vol. 35, no. 3, pp. 2707–2714, 2015, doi: 10.1016/j.proci.2014.05.081.

[49] S. D. Tse and A. C. Fernandez-Pello, “On the Flight Paths of Metal Particles and Embers Generated by Power Lines in High Winds - A Potential Source of Wildland Fires,” *Fire Saf. J.*, vol. 30, no. 4, pp. 333–356, 1998, doi: 10.1016/S0379-7112(97)00050-7.

[50] D. Coldham, A. Czerwinski, and T. Marxsen, “Probability of Bushfire Ignition from Electric Arc Faults Final Report,” *Powerline Bushfire Saf. Taskforce*, no. December, p. 122, 2011, doi: 10.13140/RG.2.1.2991.3049.

[51] I. Ramljak, M. Majstrović, and E. Sutlović, “Statistical analysis of particles of conductor clashing,” *ENERGYCON 2014 - IEEE Int. Energy Conf.*, pp. 638–643, 2014, doi: 10.1109/ENERGYCON.2014.6850494.

[52] O. A. Ivchenko, A. V. Tiutin, G. P. Nadejkina, A. V. Kirichenko, and K. E. Pankin, “An approach to estimating the range of wild fire firebrands transportation by wind,” *IOP Conf. Ser. Earth Environ. Sci.*, vol. 979, no. 1, 2022, doi: 10.1088/1755-1315/979/1/012158.

[53] K. Himoto and Y. Hayashi, “Hierarchical Bayesian approach to developing probabilistic models for generation and transport of firebrands in large outdoor fires under limited data availability,” *Fire Saf. J.*, vol. 134, no. September, p. 103679, 2022, doi: 10.1016/j.firesaf.2022.103679.

[54] P. D. Wragg, T. Mielke, and D. Tilman, “Forbs, grasses, and grassland fire behaviour,” *J. Ecol.*, vol. 106, no. 5, pp. 1983–2001, 2018, doi: 10.1111/1365-2745.12980.

[55] S. L. Manzello, A. Maranghides, and W. E. Mell, “Firebrand generation from burning vegetation,” *Int. J. Wildl. Fire*, vol. 16, no. 4, pp. 458–462, 2007, doi: 10.1071/WF06079.

[56] S. Suzuki and S. L. Manzello, “Characteristics of Firebrands Collected from Actual Urban Fires,” *Fire Technol.*, vol. 54, no. 6, pp. 1533–1546,

2018, doi: 10.1007/s10694-018-0751-x.

[57] C. D. Zak, D. C. Murphy, and A. C. Fernandez-Pello, "Understanding ignition of natural fuels by heated particles," *WIT Trans. Built Environ.*, vol. 134, pp. 607–614, 2013, doi: 10.2495/SAFE130541.

[58] C. Zak, J. Urban, V. Tran, and C. Fernandez-Pello, "Flaming ignition behavior of hot steel and aluminum spheres landing in cellulose fuel beds," *Fire Saf. Sci.*, vol. 11, pp. 1368–1378, 2014, doi: 10.3801/IAFSS.FSS.11-1368.

[59] J. A. Cardille, S. J. Ventura, and M. G. Turner, "Environmental and social factors influencing wildfires in the Upper Midwest, United States," *Ecol. Appl.*, vol. 11, no. 1, pp. 111–127, 2001, doi: 10.1890/1051-0761(2001)011[0111:EASFIW]2.0.CO;2.

[60] J. E. Keeley and A. D. Syphard, "Twenty-first century California , USA , wildfires : fuel-dominated vs . wind- dominated fires," 2019.

[61] J. G. Pausas and J. E. Keeley, "Wildfires and global change," *Front. Ecol. Environ.*, vol. 19, no. 7, pp. 387–395, 2021, doi: 10.1002/fee.2359.

[62] J. J. Sharples, R. H. D. McRae, and S. R. Wilkes, "Wind-terrain effects on the propagation of wildfires in rugged terrain: Fire channelling," *Int. J. Wildl. Fire*, vol. 21, no. 3, pp. 282–296, 2012, doi: 10.1071/WF10055.

[63] J. Lecina-Diaz, A. Alvarez, and J. Retana, "Extreme fire severity patterns in topographic, convective and wind-driven historical wildfires of mediterranean pine forests," *PLoS One*, vol. 9, no. 1, 2014, doi: 10.1371/journal.pone.0085127.

[64] J. J. Whicker, J. E. Pinder, and D. D. Breshears, "Increased Wind Erosion from Forest Wildfire: Implications for Contaminant-Related Risks," *J. Environ. Qual.*, vol. 35, no. 2, pp. 468–478, 2006, doi: 10.2134/jeq2005.0112.

[65] Y. He, K. C. S. Kwok, G. B. Douglas, and I. M. Razali, "Numerical investigation of bushfire-wind interaction and its impact on building structure," *Fire Saf. Sci.*, no. January 2011, pp. 1449–1462, 2011, doi: 10.3801/IAFSS.FSS.10-1449.

[66] P. L. Andrews, M. G. Cruz, and R. C. Rothermel, "Examination of the wind speed limit function in the Rothermel surface fire spread model," *Int. J. Wildl. Fire*, vol. 22, no. 7, pp. 959–969, 2013, doi: 10.1071/WF12122.

[67] B. Butler *et al.*, "Exploring fire response to high wind speeds: Fire rate of spread, energy release and flame residence time from fires burned in

pine needle beds under winds up to 27 m s-1," *Int. J. Wildl. Fire*, vol. 29, no. 1, pp. 81–92, 2019, doi: 10.1071/WF18216.

[68] M. G. Cruz and M. E. Alexander, "The 10% wind speed rule of thumb for estimating a wildfire's forward rate of spread in forests and shrublands," *Ann. For. Sci.*, vol. 76, no. 2, 2019, doi: 10.1007/s13595-019-0829-8.

[69] R. M. Nelson, "An effective wind speed for models of fire spread," *Int. J. Wildl. Fire*, vol. 11, no. 2, pp. 153–161, 2002, doi: 10.1071/WF02031.

[70] R. C. Rothmell, "A Mathematical Model for Predicting Fire Spread," *United States Dep. Agric. For. Serv. Res. Pap.*, p. 46, 1972.

[71] J. Madrigal, M. Guijarro, C. Hernando, C. Díez, and E. Marino, "Estimation of peak heat release rate of a forest fuel bed in outdoor laboratory conditions," *J. Fire Sci.*, vol. 29, no. 1, pp. 53–70, 2011, doi: 10.1177/0734904110373890.

[72] J. T. Abatzoglou, C. A. Kolden, A. P. Williams, M. Sadegh, J. K. Balch, and A. Hall, "Downslope Wind-Driven Fires in the Western United States," *Earth's Futur.*, vol. 11, no. 5, pp. 1–16, 2023, doi: 10.1029/2022EF003471.

[73] F. Morandini, X. Silvani, J. L. Dupuy, and A. Susset, "Fire spread across a sloping fuel bed: Flame dynamics and heat transfers," *Combust. Flame*, vol. 190, pp. 158–170, 2018, doi: 10.1016/j.combustflame.2017.11.025.

[74] N. Liu, J. Lei, W. Gao, H. Chen, and X. Xie, "Combustion dynamics of large-scale wildfires," *Proc. Combust. Inst.*, vol. 38, no. 1, pp. 157–198, 2021, doi: 10.1016/j.proci.2020.11.006.

[75] J. Li, S. Mahalingam, and D. R. Weise, "Experimental investigation of fire propagation in single live shrubs," *Int. J. Wildl. Fire*, vol. 26, no. 1, pp. 58–70, 2017, doi: 10.1071/WF16042.

[76] N. V. Baranovskiy and A. V. Zakharevich, "Experimental investigation of processes of typical forest fuel ignition by a high-temperature steel particle," *Heat Transf. Res.*, vol. 47, no. 7, pp. 681–689, 2016, doi: 10.1615/HeatTransRes.2016010609.

[77] R. M. Ziazi, A. Singh, A. O. Said, and W. Gong, "Experimental investigation of fire spread across a vegetative fuel bed incorporating the effect of wind velocity," *12th Natl. Combust. Meet.*, no. July, pp. 1–10, 2021, doi: 10.31223/X56G9H.

[78] K. Zhang, S. Verma, A. Trouvé, and A. Lamorlette, "A study of the

canopy effect on fire regime transition using an objectively defined Byram convective number," *Fire Saf. J.*, vol. 112, no. January, 2020, doi: 10.1016/j.firesaf.2020.102950.

[79] D. Morvan and N. Frangieh, "Wildland fire behaviour : wind kW meffect versus Byram ' s convective number and consequences on the regime of propagation," 2015.

[80] A. C. dos Santos, S. da R. Montenegro, M. C. Ferreira, A. C. S. Barradas, and I. B. Schmidt, "Managing fires in a changing world: Fuel and weather determine fire behavior and safety in the neotropical savannas," *J. Environ. Manage.*, vol. 289, no. November 2020, p. 112508, 2021, doi: 10.1016/j.jenvman.2021.112508.

[81] A. L. Atchley *et al.*, "Effects of fuel spatial distribution on wildland fire behaviour," *Int. J. Wildl. Fire*, vol. 30, no. 3, pp. 179–189, 2021, doi: 10.1071/WF20096.

[82] J. R. Gallacher, "The influence of season, heating mode and slope angle on wildland fire behavior," p. 256, 2012.

[83] J. Matthew W., S. Adam J. P., B. Richard, C. Josep G., P. I. Colin, and L. Q. Corinne, "Climate change increases the risk of wildfires confirms new review," *Sci. Dly.*, vol. 14, no. January, pp. 2018–2020, 2020, [Online]. Available: https://www.sciencedaily.com/releases/2020/01/200114074046.htm%0Ainternal-pdf://0.0.18.150/200114074046.html.

[84] A. Long and C. K. Randall, "Wildfire Risk Assessment Guide for Homeowners in the Southern United States," pp. 1–16, 2004.

[85] M. A. Santoso, E. G. Christensen, and G. Rein, "The effects of pulsating wind on the transition from smouldering to flaming combustion," *Fire Saf. J.*, vol. 141, no. March, p. 103993, 2023, doi: 10.1016/j.firesaf.2023.103993.

[86] C. F. Mass and D. Ovens, "The northern California wildfires of 8–9 October 2017," *Bull. Am. Meteorol. Soc.*, vol. 100, no. 2, pp. 235–256, 2019, doi: 10.1175/BAMS-D-18-0037.1.

[87] P. Pinto, Á. P. Silva, D. X. Viegas, M. Almeida, J. Raposo, and L. M. Ribeiro, "Influence of Convectively Driven Flows in the Course of a Large Fire in Portugal: The Case of Pedrógão Grande," *Atmosphere (Basel).*, vol. 13, no. 3, pp. 1–34, 2022, doi: 10.3390/atmos13030414.

[88] S. G. Benjamin, E. P. James, E. J. Szoke, P. T. Schlatter, and J. M. Brown, "The 30 December 2021 Colorado Front Range Windstorm and Marshall Fire: Evolution of Surface and 3D Structure, NWP Guidance,

NWS Forecasts, and Decision Support," *Weather Forecast.*, vol. 38, no. 12, pp. 2551–2573, 2023, doi: 10.1175/WAF-D-23-0086.1.

[89] C. F. Mass and D. Ovens, "The Synoptic and Mesoscale Evolution Accompanying the 2018 Camp Fire of Northern California," *Bull. Am. Meteorol. Soc.*, vol. 102, no. 1, pp. E168–E192, 2021, doi: 10.1175/BAMS-D-20-0124.1.

[90] J. E. Keeley *et al.*, "Climate and weather drivers in southern California Santa Ana Wind and non-Santa Wind fires," *Int. J. Wildl. Fire*, vol. 33, no. 8, pp. 1–16, 2024, doi: 10.1071/WF23190.

[91] R. G. Fovell and Y. Cao, "The santa ana winds of southern California: Winds, gusts, and the 2007 witch fire," *Wind Struct. An Int. J.*, vol. 24, no. 6, pp. 529–564, 2017, doi: 10.12989/was.2017.24.6.529.

[92] J. E. Keeley *et al.*, "Ignitions explain more than temperature or precipitation in driving Santa Ana wind fires," *Sci. Adv.*, vol. 7, no. 30, 2021, doi: 10.1126/sciadv.abh2262.

[93] "Integrating earth observation data into the tri-environmental evaluation of the economic cost of natural disasters : a case study of 2025 LA wildfire," 2025.

[94] J. Trelles and P. Pagni, "Fire-induced Winds In The 20 October 1991 Oakland Hills Fire," *Fire Saf. Sci.*, vol. 5, no. October, pp. 911–922, 1997, doi: 10.3801/iafss.fss.5-911.

[95] R. G. Fovell and A. Gallagher, "Winds and gusts during the thomas fire," *Fire*, vol. 1, no. 3, pp. 1–22, 2018, doi: 10.3390/fire1030047.

[96] J. L. Urban, J. Song, S. Santamaria, and C. Fernandez-Pello, "Ignition of a spot smolder in a moist fuel bed by a firebrand," *Fire Saf. J.*, vol. 108, 2019, doi: 10.1016/j.firesaf.2019.102833.

[97] M. Shinohara, "Effects of wind speed and heat release rate on the vortex strength and size of fire whirls without an inner core of flame," *Fire Saf. J.*, vol. 120, no. May 2020, p. 103045, 2021, doi: 10.1016/j.firesaf.2020.103045.

[98] R. E. Keane, "Describing wildland surface fuel loading for fire management: A review of approaches, methods and systems," *Int. J. Wildl. Fire*, vol. 22, no. 1, pp. 51–62, 2013, doi: 10.1071/WF11139.

[99] M. G. Rollins, "LANDFIRE: A nationally consistent vegetation, wildland fire, and fuel assessment," *Int. J. Wildl. Fire*, vol. 18, no. 3, pp. 235–249, 2009, doi: 10.1071/WF08088.

[100] S. Wang, X. Huang, H. Chen, N. Liu, and G. Rein, "Ignition of low-

density expandable polystyrene foam by a hot particle," *Combust. Flame*, vol. 162, no. 11, pp. 4112–4118, 2015, doi: 10.1016/j.combustflame.2015.08.017.

[101] C. M. Belcher, "The influence of leaf morphology on litter flammability and its utility for interpreting palaeofire," *Philos. Trans. R. Soc. B Biol. Sci.*, vol. 371, no. 1696, 2016, doi: 10.1098/rstb.2015.0163.

[102] W. Cao, J. Li, T. Martí-Rosselló, and X. Zhang, "Experimental study on the ignition characteristics of cellulose, hemicellulose, lignin and their mixtures," *J. Energy Inst.*, vol. 92, no. 5, pp. 1303–1312, 2019, doi: 10.1016/j.joei.2018.10.004.

[103] V. Mendu *et al.*, "Identification and thermochemical analysis of high-lignin feedstocks for biofuel and biochemical production," *Biotechnol. Biofuels*, vol. 4, no. October, 2011, doi: 10.1186/1754-6834-4-43.

[104] L. Costes, F. Laoutid, S. Brohez, and P. Dubois, "Bio-based flame retardants: When nature meets fire protection," *Mater. Sci. Eng. R Reports*, vol. 117, pp. 1–25, 2017, doi: 10.1016/j.mser.2017.04.001.

[105] S. Liodakis, D. Bakirtzis, and A. P. Dimitrakopoulos, "Autoignition and thermogravimetric analysis of forest species treated with fire retardants," *Thermochim. Acta*, vol. 399, no. 1–2, pp. 31–42, 2003, doi: 10.1016/S0040-6031(02)00400-8.

[106] E. C. Okoroigwe, S. O. Enibe, and S. O. Onyegegbu, "Determination of oxidation characteristics and decomposition kinetics of some Nigerian biomass," *J. Energy South. Africa*, vol. 27, no. 3, pp. 39–49, 2016, doi: 10.17159/2413-3051/2016/v27i3a1554.

[107] Y. Yan *et al.*, "Ignition and Kinetic Studies: The Influence of Lignin on Biomass Combustion," *Energy and Fuels*, vol. 33, no. 7, pp. 6463–6472, 2019, doi: 10.1021/acs.energyfuels.9b01089.

[108] M. J. Peet, H. S. Hasan, and H. K. D. H. Bhadeshia, "Prediction of thermal conductivity of steel," *Int. J. Heat Mass Transf.*, vol. 54, no. 11–12, pp. 2602–2608, 2011, doi: 10.1016/j.ijheatmasstransfer.2011.01.025.

[109] N. Fernandez-Anez and J. Garcia-Torrent, "Influence of Particle Size and Density on the Hot Surface Ignition of Solid Fuel Layers," *Fire Technol.*, vol. 55, no. 1, pp. 175–191, 2019, doi: 10.1007/s10694-018-0782-3.

[110] C. Ryu, Y. Bin Yang, A. Khor, N. E. Yates, V. N. Sharifi, and J. Swithenbank, "Effect of fuel properties on biomass combustion: Part I. Experiments - Fuel type, equivalence ratio and particle size," *Fuel*, vol. 85, no. 7–8, pp. 1039–1046, 2006, doi: 10.1016/j.fuel.2005.09.019.

[111] Y. Bin Yang, C. Ryu, A. Khor, V. N. Sharifi, and J. Swithenbank, "Fuel size effect on pinewood combustion in a packed bed," *Fuel*, vol. 84, no. 16, pp. 2026–2038, 2005, doi: 10.1016/j.fuel.2005.04.022.

[112] S. Donghoon and C. Sangmin, "The combustion of simulated waste particles in a fixed bed," *Combust. Flame*, vol. 121, pp. 167--180, 2000.

[113] J. J. Saastamoinen, R. Taipale, M. Horttanainen, and P. Sarkomaa, "Propagation of the ignition front in beds of wood particles," *Combust. Flame*, vol. 123, no. 1–2, pp. 214–226, 2000, doi: 10.1016/S0010-2180(00)00144-9.

[114] J. L. Urban, C. D. Zak, and C. Fernandez-Pello, "Cellulose spot fire ignition by hot metal particles," *Proc. Combust. Inst.*, vol. 35, no. 3, pp. 2707–2714, 2015, doi: 10.1016/j.proci.2014.05.081.

[115] N. V. Baranovskiy, A. V. Zakharevich, and D. S. Osotova, "Experimental study of pine forest fuel layer ignition by the steel heated particle," *EPJ Web Conf.*, vol. 82, 2015, doi: 10.1051/epjconf/20158201020.

[116] W. Fang, Z. Peng, and H. Chen, "Ignition of pine needle fuel bed by the coupled effects of a hot metal particle and thermal radiation," *Proc. Combust. Inst.*, vol. 38, no. 3, pp. 5101–5108, 2021, doi: 10.1016/j.proci.2020.05.032.

[117] X. Shi *et al.*, "On the influence of material and shape of the hot particles on the ignition characteristics of coal dust," *Energy*, vol. 281, no. June, p. 128192, 2023, doi: 10.1016/j.energy.2023.128192.

[118] F. A. Alblni, "Response of Free-Burning Fires to Nonsteady Wind," *Combust. Sci. Technol.*, vol. 29, no. 3–6, pp. 225–241, 1982, doi: 10.1080/00102208208923599.

[119] C. Darwin, "This is a reproduction of a library book that was digitized by Google as part of an ongoing effort to preserve the information in books and make it universally accessible. https://books.google.com," *Oxford Univ.*, vol. XXX, p. 60, 1895.

[120] R. R. Linn and P. Cunningham, "Numerical simulations of grass fires using a coupled atmosphere-fire model: Basic fire behavior and dependence on wind speed," *J. Geophys. Res. Atmos.*, vol. 110, no. 13, pp. 1–19, 2005, doi: 10.1029/2004JD005597.

[121] S. K. Park, *Haines Index*. 2020.

[122] J. Cobian-Iñiguez, A. H. Aminfar, S. Saha, K. Awayan, D. R. Weise, and M. Princevac, "The Transition and Spread of a Chaparral Crown Fire:

Insights from Laboratory Scale Wind Tunnel Experiments," *J. Combust.*, vol. 2022, 2022, doi: 10.1155/2022/5630594.

[123] W. T. Sommers, R. A. Loehman, and C. C. Hardy, "Wildland fire emissions, carbon, and climate: Science overview and knowledge needs," *For. Ecol. Manage.*, vol. 317, pp. 1–8, 2014, doi: 10.1016/j.foreco.2013.12.014.

[124] A. Heather and L. Simpson, "Research Online - University of Wollongong," 2022, [Online]. Available: https://ro.uow.edu.au/.

[125] S. D. Wong, J. C. Broader, S. A. Shaheen, and E. Org, *Review of California Wildfire Evacuations Permalink https://escholarship.org/uc/item/5w85z07g*. 2020.

[126] W. H. Chen *et al.*, "Thermal degradation of carbohydrates, proteins and lipids in microalgae analyzed by evolutionary computation," *J. Anal. Appl. Pyrolysis*, vol. 107, no. November 2017, pp. 4112–4118, 2015, doi: 10.1016/j.jaap.2014.03.017.

[127] S. Wang *et al.*, "Effects of hemicellulose, cellulose and lignin on the ignition behaviors of biomass in a drop tube furnace," *Bioresour. Technol.*, vol. 310, no. April, p. 123456, 2020, doi: 10.1016/j.biortech.2020.123456.

[128] L. Burhenne, J. Messmer, T. Aicher, and M. P. Laborie, "The effect of the biomass components lignin, cellulose and hemicellulose on TGA and fixed bed pyrolysis," *J. Anal. Appl. Pyrolysis*, vol. 101, pp. 177–184, 2013, doi: 10.1016/j.jaap.2013.01.012.

[129] G. Dorez, L. Ferry, R. Sonnier, A. Taguet, and J. M. Lopez-Cuesta, "Effect of cellulose, hemicellulose and lignin contents on pyrolysis and combustion of natural fibers," *J. Anal. Appl. Pyrolysis*, vol. 107, pp. 323–331, 2014, doi: 10.1016/j.jaap.2014.03.017.

[130] A. Àgueda, E. Pastor, Y. Pérez, and E. Planas, "Experimental study of the emissivity of flames resulting from the combustion of forest fuels," *Int. J. Therm. Sci.*, vol. 49, no. 3, pp. 543–554, 2010, doi: 10.1016/j.ijthermalsci.2009.09.006.

[131] D. Sagel, K. Speer, S. Pokswinski, and B. Quaife, "Fine-scale fire spread in pine straw," *Fire*, vol. 4, no. 4, pp. 1–21, 2021, doi: 10.3390/fire4040069.

[132] G. Rein, "Smouldering Fires and Natural Fuels," *Fire Phenom. Earth Syst. An Interdiscip. Guid. to Fire Sci.*, pp. 15–33, 2013, doi: 10.1002/9781118529539.ch2.

[133] W. Cao, J. Li, and L. Lue, “Study on the ignition behavior and kinetics of combustion of biomass,” *Energy Procedia*, vol. 142, pp. 136–141, 2017, doi: 10.1016/j.egypro.2017.12.022.

[134] X. G. Li, B. G. Ma, L. Xu, Z. W. Hu, and X. G. Wang, “Thermogravimetric analysis of the co-combustion of the blends with high ash coal and waste tyres,” *Thermochim. Acta*, vol. 441, no. 1, pp. 79–83, 2006, doi: 10.1016/j.tca.2005.11.044.

[135] C. Wang, F. Wang, Q. Yang, and R. Liang, “Thermogravimetric studies of the behavior of wheat straw with added coal during combustion,” *Biomass and Bioenergy*, vol. 33, no. 1, pp. 50–56, 2009, doi: 10.1016/j.biombioe.2008.04.013.

[136] J. J. Lu and W. H. Chen, “Investigation on the ignition and burnout temperatures of bamboo and sugarcane bagasse by thermogravimetric analysis,” *Appl. Energy*, vol. 160, no. 2015, pp. 49–57, 2015, doi: 10.1016/j.apenergy.2015.09.026.

[137] J. M. Jones *et al.*, “Low temperature ignition of biomass,” *Fuel Process. Technol.*, vol. 134, pp. 372–377, 2015, doi: 10.1016/j.fuproc.2015.02.019.

[138] B. Li *et al.*, “Effects of particle size on the self-ignition behaviour of a coal dust layer on a hot plate,” *Fuel*, vol. 260, no. July 2019, 2020, doi: 10.1016/j.fuel.2019.116269.

[139] C. Shen and T. H. Fletcher, “Fuel element combustion properties for live wildland Utah shrubs,” *Combust. Sci. Technol.*, vol. 187, no. 3, pp. 428–444, 2015, doi: 10.1080/00102202.2014.950372.

[140] M. Thomsen, A. C. Fernandez-Pello, and F. A. Williams, “On the Growth of Wildland Fires from a Small Ignition Source,” *Combust. Sci. Technol.*, vol. 195, no. 14, pp. 3542–3556, 2023, doi: 10.1080/00102202.2023.2239461.

[141] S. Liodakis, D. Bakirtzis, and A. Dimitrakopoulos, “Ignition characteristics of forest species in relation to thermal analysis data,” *Thermochim. Acta*, vol. 390, no. 1–2, pp. 83–91, 2002, doi: 10.1016/S0040-6031(02)00077-1.

[142] C. J. Rallis and B. M. Mangaya, “Ignition of veld grass by hot aluminium particles ejected from clashing overhead transmission lines,” *Fire Technol.*, vol. 38, no. 1, pp. 81–92, 2002, doi: 10.1023/A:1013484932749.

[143] A. W. Cardoso *et al.*, “Grass Species Flammability, Not Biomass, Drives Changes in Fire Behavior at Tropical Forest-Savanna Transitions,” *Front. For. Glob. Chang.*, vol. 1, no. November, pp. 1–14, 2018, doi:

10.3389/ffgc.2018.00006.

[144] D. Glushkov, A. Zhuikov, N. Zemlyansky, A. Pleshko, O. Fetisova, and P. Kuznetsov, “Influence of the Composition and Particle Sizes of the Fuel Mixture of Coal and Biomass on the Ignition and Combustion Characteristics,” *Appl. Sci.*, vol. 13, no. 19, 2023, doi: 10.3390/app131911060.

[145] A. Skreiberg, O. Skreiberg, J. Sandquist, and L. Sørum, “TGA and macro-TGA characterisation of biomass fuels and fuel mixtures,” *Fuel*, vol. 90, no. 6, pp. 2182–2197, 2011, doi: 10.1016/j.fuel.2011.02.012.

[146] Z. Liu, A. Quek, S. Kent Hoekman, M. P. Srinivasan, and R. Balasubramanian, “Thermogravimetric investigation of hydrochar-lignite co-combustion,” *Bioresour. Technol.*, vol. 123, pp. 646–652, 2012, doi: 10.1016/j.biortech.2012.06.063.

[147] N. A. Liu, W. Fan, R. Dobashi, and L. Huang, “Kinetic modeling of thermal decomposition of natural cellulosic materials in air atmosphere,” *J. Anal. Appl. Pyrolysis*, vol. 63, no. 2, pp. 303–325, 2002, doi: 10.1016/S0165-2370(01)00161-9.

[148] W. H. Chen and P. C. Kuo, “A study on torrefaction of various biomass materials and its impact on lignocellulosic structure simulated by a thermogravimetry,” *Energy*, vol. 35, no. 6, pp. 2580–2586, 2010, doi: 10.1016/j.energy.2010.02.054.

[149] M. V. Gil, D. Casal, C. Pevida, J. J. Pis, and F. Rubiera, “Thermal behaviour and kinetics of coal/biomass blends during co-combustion,” *Bioresour. Technol.*, vol. 101, no. 14, pp. 5601–5608, 2010, doi: 10.1016/j.biortech.2010.02.008.

[150] H. H. Sait, A. Hussain, A. A. Salema, and F. N. Ani, “Pyrolysis and combustion kinetics of date palm biomass using thermogravimetric analysis,” *Bioresour. Technol.*, vol. 118, pp. 382–389, 2012, doi: 10.1016/j.biortech.2012.04.081.

[151] N. Fernandez-Anez, A. K. Meyer, J. Elio, G. Kleppe, B. C. Hagen, and V. Frette, “Behaviour of smoldering fires during periodic refilling of wood pellets into silos,” *J. Loss Prev. Process Ind.*, vol. 72, no. May, p. 104565, 2021, doi: 10.1016/j.jlp.2021.104565.

[152] V. S. Borovkova *et al.*, “Composition and Structure of Aspen (Pópulus trémula) Hemicelluloses Obtained by Oxidative Delignification,” *Polymers (Basel).*, vol. 14, no. 21, 2022, doi: 10.3390/polym14214521.

[153] R. W. Bovey, D. Le Tourneau, and L. C. Erickson, “The Chemical Composition of Medusahead and Downy Brome,” *Weeds*, vol. 9, no. 2, p.

307, 1961, doi: 10.2307/4040420.

[154] F. W. Sosulski and K. Sosulski, "Processing and composition of wild oat groats (Avena fatua L.)," *J. Food Eng.*, vol. 4, no. 3, pp. 189–203, 1985, doi: 10.1016/0260-8774(85)90003-2.

[155] C. B. Devi, K. Bains, and H. Kaur, "Effect of drying procedures on nutritional composition, bioactive compounds and antioxidant activity of wheatgrass (Triticum aestivum L)," *J. Food Sci. Technol.*, vol. 56, no. 1, pp. 491–496, 2019, doi: 10.1007/s13197-018-3473-7.

[156] F. Morandini *et al.*, "Fire spread experiment across Mediterranean shrub: Influence of wind on flame front properties," *Fire Saf. J.*, vol. 41, no. 3, pp. 229–235, 2006, doi: 10.1016/j.firesaf.2006.01.006.

[157] D. P. Kasymov, M. V Agafontsev, V. V Perminov, A. Y. Chechekov, and V. A. Tarakanova, "Laboratory Investigation of the Ignition of Wood Structural Materials Under the Influence of Spot Fires," no. 5, 2019.

[158] Q. He *et al.*, "Experimental study on fire spread over discrete fuel bed-Part II: Combined effects of wind and packing ratio," *Fire Saf. J.*, vol. 128, no. December 2021, pp. 1–8, 2022, doi: 10.1016/j.firesaf.2021.103520.

[159] W. Tachajapong, J. Lozano, S. Mahalingam, X. Zhou, and D. R. Weise, "Experimental and numerical modeling of shrub crown fire initiation," *Combust. Sci. Technol.*, vol. 181, no. 4, pp. 618–640, 2009, doi: 10.1080/00102200802693617.

[160] J. G. Quintiere, *Fundamentals of Fire Phenomena*. 2006.

[161] X. Sánchez-Monroy, W. Mell, J. Torres-Arenas, and B. W. Butler, "Fire spread upslope: Numerical simulation of laboratory experiments," *Fire Saf. J.*, vol. 108, no. July, 2019, doi: 10.1016/j.firesaf.2019.102844.

[162] F. Morandini, A. Simeoni, P. A. Santoni, and J. H. Balbi, "A model for the spread of fire across a fuel bed incorporating the effects of wind and slope," *Combust. Sci. Technol.*, vol. 177, no. 7, pp. 1381–1418, 2005, doi: 10.1080/00102200590950520.

[163] J. Cobian-Iñiguez *et al.*, "Wind Effects on Smoldering Behavior of Simulated Wildland Fuels," *Combust. Sci. Technol.*, vol. 195, no. 13, pp. 3212–3229, 2023, doi: 10.1080/00102202.2021.2019239.

[164] L. Malangone, P. Russo, and S. Vaccaro, "Effects of Wind and Terrain Slope on Flames Propagation in a Vegetative Fuel Bed," *XXXIV Meet. Ital. Sect. Combust. Inst.*, pp. 1–6, 2011, [Online]. Available: http://www.combustion-institute.it/proceedings/XXXIV-

ASICI/papers/34proci2011.III22.pdf.

[165] T. Catchpole and N. D. de Mestre, “Physical models for a spreading line fire,” *Aust. For.*, vol. 49, no. 2, pp. 102–111, 1986, doi: 10.1080/00049158.1986.10674471.

[166] J. M. C. Mendes-Lopes, J. M. P. Ventura, and J. M. P. Amaral, “Flame characteristics, temperature-time curves, and rate of spread in fires propagating in a bed of Pinus pinaster needles,” *Int. J. Wildl. Fire*, vol. 12, no. 1, pp. 67–84, 2003, doi: 10.1071/WF02063.

[167] H. Guo, D. Xiang, P. Zhang, Y. Gao, Y. Zhang, and L. Kong, “Effects of Wind on Heat Transfer and Spread of Different Fire Lines Across a Pine Needle Fuel Bed,” *Combust. Sci. Technol.*, vol. 197, no. 4, pp. 782–802, 2023, doi: 10.1080/00102202.2023.2273329.

[168] A. Simeoni, P. A. Santoni, M. Larini, and J. H. Balbi, “On the wind advection influence on the fire spread across a fuel bed: Modelling by a semi-physical approach and testing with experiments,” *Fire Saf. J.*, vol. 36, no. 5, pp. 491–513, 2001, doi: 10.1016/S0379-7112(00)00063-1.

[169] D. Morvan and J. L. Dupuy, “Modeling the propagation of a wildfire through a Mediterranean shrub using a multiphase formulation,” *Combust. Flame*, vol. 138, no. 3, pp. 199–210, 2004, doi: 10.1016/j.combustflame.2004.05.001.

[170] A. L. Sullivan, “Wildland surface fire spread modelling, 1990 - 2007. 3: Simulation and mathematical analogue models,” *Int. J. Wildl. Fire*, vol. 18, no. 4, p. 387, 2009, doi: 10.1071/wf06144.

[171] C. F. Schemel, A. Simeoni, H. Biteau, J. D. Rivera, and J. L. Torero, “A calorimetric study of wildland fuels,” *Exp. Therm. Fluid Sci.*, vol. 32, no. 7, pp. 1381–1389, 2008, doi: 10.1016/j.expthermflusci.2007.11.011.

[172] E. Pastor, L. Zárate, E. Planas, and J. Arnaldos, “Mathematical models and calculation systems for the study of wildland fire behaviour,” *Prog. Energy Combust. Sci.*, vol. 29, no. 2, pp. 139–153, 2003, doi: 10.1016/S0360-1285(03)00017-0.

[173] B. Waliszewska, M. Grzelak, E. Gaweł, A. Spek-Dźwigała, A. Sieradzka, and W. Czekała, “Chemical characteristics of selected grass species from polish meadows and their potential utilization for energy generation purposes,” *Energies*, vol. 14, no. 6, 2021, doi: 10.3390/en14061669.

[174] R. Tobiasz-Salach, B. Stadnik, and M. Bajcar, “Oat as a Potential Source of Energy,” *Energies*, vol. 16, no. 16, pp. 1–19, 2023, doi: 10.3390/en16166019.

[175] D. Martyniak, G. Żurek, and K. Prokopiuk, "Biomass yield and quality of wild populations of tall wheatgrass [Elymus elongatus (Host.) Runemark]," *Biomass and Bioenergy*, vol. 101, pp. 21–29, 2017, doi: 10.1016/j.biombioe.2017.03.025.

[176] R. Sussot, "Characterization of the Thermal Propieties of Forest Fuels by Combustible Gas Analysis," *For. Sci.*, vol. 2, no. 2, pp. 404–420, 1982.

[177] R. R. Blank, R. H. White, and L. H. Ziska, "Combustion properties of Bromus tectorum L.: Influence of ecotype and growth under four CO2 concentrations," *Int. J. Wildl. Fire*, vol. 15, no. 2, pp. 227–236, 2006, doi: 10.1071/WF05055.

[178] Y. Zhou, F. Yang, S. Lan, and L. Yi, "Effect of ambient wind on horizontal flame spread over discrete multi-column fuel arrays," *Therm. Sci. Eng. Prog.*, vol. 54, no. July, p. 102782, 2024, doi: 10.1016/j.tsep.2024.102782.

[179] V. B. Apte, A. R. Green, and J. H. Kent, "Pool fire plume flow in a large-scale wind tunnel," *Fire Saf. Sci. Proc. Third Int. Symp.*, pp. 425–434, 2006, doi: 10.4324/9780203973493.

[180] S. Kerber and D. Madrzykowski, "NIST Technical Note 1629, Fire Fighting Tactics Under Wind Driven Fire Conditions: 7-Story Building Experiments," *Tech. Note 1629*, vol. 1629, no. January, 2009.

[181] Y. Lai, X. Wang, T. B. O. Rockett, J. R. Willmott, and Y. Zhang, "Investigation into wind effects on fire spread on inclined wooden rods by multi-spectrum and schlieren imaging," *Fire Saf. J.*, vol. 127, no. November 2021, p. 103513, 2022, doi: 10.1016/j.firesaf.2021.103513.